이학박사학위논문

Effects of meteorological, hydrological, and biological factors on the eco-physiology of red tide organisms in Korean coastal waters

한국 연안에서 기상학적, 수리학적, 생물학적 요인들이 적조 유발 생물의 생태생리에 미치는 영향에 대한 연구

2017년 2월

서울대학교 대학원

지구환경과학부 해양학전공

이 경 하

Effects of meteorological, hydrological, and biological factors on the eco-physiology of red tide organisms in Korean coastal waters

한국 연안에서 기상학적, 수리학적, 생물학적 요인들이 적조 유발 생물의 생태생리에 미치는 영향에 대한 연구

지도교수 정 해 진

이 논문을 이학박사 학위논문으로 제출함
2016년 11월

서울대학교 대학원
지구환경과학부 해양학전공
이 경 하

이경하의 박사 학위논문을 인준함
2016년 12월

위 원 장 _____ (인)

부위원장 _____ (인)

위 원 _____ (인)

위 원 _____ (인)

위 원 _____ (인)

Abstract

Effects of meteorological, hydrological, and biological factors on the eco-physiology of red tide organisms in Korean coastal waters

Lee, Kyung Ha
Oceanography
School of Earth and Environmental Sciences
College of Natural Sciences
Graduate School of Seoul National University

The eco-physiology of marine plankton is easily affected by two major meteorological factors, temperature and precipitation. These marine plankton are important components of the basic marine food web with numerous predator-prey pathways, which contribute to diverse and important material cycles (e.g. C, N, and P cycles) under the sea. Moreover, in last several decades, global warming and eutrophication have been thought to be the two most serious environmental problems against marine ecosystems. However, the effects of meteorological, hydrological, and biological factors on natural phytoplankton communities are poorly understood. Thus, in this study, I explored the effects of meteorological, hydrological, and biological factors on eco-physiology of red tide organisms by combining data from both the laboratory incubation experiments and the field works.

In chapter 2, to investigate relationships among precipitation, salinity, and nutrients and their effects on phytoplankton communities in Korean coastal waters, I took water samples from Gwangyang Bay in 4 seasons in 2011 to 2013 and from Shiwha Bay every months from 2009 to 2011. In Gwangyang Bay, salinity showed significant negative correlations with sum of 7 to 20 days precipitation ($p<0.05$). Furthermore, in the summer, salinity had significant negative correlations with nitrate plus nitrite (NO_3) in 2011 and 2012 ($p<0.001$). Under this circumstance, diatoms dominated phytoplankton assemblages. However, salinity did not have any correlation with nitrate ($p>0.05$) in 2013. Under this circumstance, dinoflagellates dominated. Therefore, when NO_3 increased due to high precipitation, diatoms dominated, but when NO_3 did not increased probably due to relatively low precipitation, dinoflagellates dominated. Similar patterns were observed in Shiwha Bay. From 2009 to 2011, salinity had negative correlations with sum of 7 to 20 days precipitation ($p<0.05$) and diatoms and small flagellates dominated, while in 2009 and 2010, salinity did not have any correlation with nitrate and dinoflagellates dominated. Therefore, dominant groups of blooms in both bays can be predicted by analyzing data on precipitation, salinity, and nutrient concentrations.

In chapter 3, to investigate fast growing strategy of a mixotrophic dinoflagellate feeding on other protists, I conducted diverse feeding experiments with the newly described mixotrophic dinoflagellate *Gymnodinium smaydae* isolated from Shiwha Bay. I explored the feeding mechanism and the kinds of prey species that *G. smaydae* is able to feed on. In addition, I measured the growth and

ingestion rates of *G. smaydae* on optimal and suboptimal algal prey *Heterocapsa rotundata* and *Heterocapsa triquetra* as a function of prey concentration. Among the 19 algal prey species offered, *G. smaydae* ingested only thecate dinoflagellates *Heterocapsa rotundata, Heterocapsa triquetra*, *Heterocapsa* sp., and *Scrippsiella trochoidea*. Among the peduncle-feeding dinoflagellates so far reported, *G. smaydae* fed on algal prey using a peduncle after anchoring the prey by a tow filament. All *Heterocapsa* species supported high positive growth of *G. smaydae, S. trochoidea* only helped in merely maintaining the predator population. The maximum specific growth rates (i.e., mixotrophic growth) of *G. smaydae* on *H. rotundata* and *H. triquetra* were 2.226 d^{-1} and 1.053 d^{-1}, respectively, at 20 °C under a 14:10 h light-dark cycle of 20 μE m^{-2} s^{-1}, while the growth rates (i.e., phototrophic growth) under the same light conditions without added prey were 0.005 to −0.051 d^{-1}. The maximum ingestion rates of *G. smaydae* on *H. rotundata* and *H. triquetra* were 1.59 ng C $grazer^{-1}$ d^{-1} and 0.24 ng C $grazer^{-1}$ d^{-1}, respectively. The calculated grazing coefficients for *G. smaydae* on co-occurring *H. rotundata* or *H. triquetra* were up to 0.23 h^{-1} or 0.02 h^{-1}, respectively The results of this studysuggest that *G. smaydae* cannot survive only conducting photosynthesis but can survive by feeding other mixotrophic dinoflagellates and have pontential to occur red tides using mixotrophy.

In chapter 4, to investigate elevating growth and survival strategy of mixotrophic dinoflagellates by killing or feeding on other protists, I investigated the mixotrophic ability of the harmful

dinoflagellates *Alexandrium* spp. In the present study, whether each of three *Alexandrium* species (*A. andersonii*, *A. affine*, and *A. fraterculus*) isolated from Korean waters has or lacks mixotrophic ability, was investigated. When diets of diverse algal prey, cyanobacteria, and bacteria sized micro-beads were provided, *A. andersonii* was able to immobilized and feed on the prasinophyte *Pyramimonas* sp., the cryptophyte *Teleaulax* sp., and the dinoflagellate *Heterocapsa rotundata*, whereas neither *A. affine* nor *A. fraterculus* fed on any prey item. However, immobilization and/or lysis effects on other protistan prey species by *A. affine* and *A. fraterculus* were observed. Moreover, mixotrophy elevated the growth rate of *A. andersonii*. The maximum mixotrophic growth rates of *A. andersonii* on *Pyramimons* sp. under a 14:10 h light/dark cycle of 20 μE m^{-2} s^{-1} was 0.432 d^{-1}, while the autotrophic growth rate was 0.243 d^{-1}. The maximum ingestion rate by *A. andersonii* of *Pyramimons* sp. was 1.03 ng C $predator^{-1}d^{-1}$. Therefore, *A. andersonii* also donduct mixotrophy as a survival strategy of another nutrient uptake method by immoblzing and ingesting other protistan species and two other alexandrium species also have mechanisms of competition for their survival. Moreover, these evidence suggests that the mixotrophic ability of *A. andersonii* should be taken into consideration in predicting the outbreak, persistence, and decline of its harmful algal blooms.

In chapter 5, to investigate effects of heterotrophic protistan grazers on *Mesodinium rubrum*, a cosmopolitan ciliate that often causes red tides, I tested whether the 10 heterotrophic dinoflagellates and a ciliate preyed on *M. rubrum*. The heterotrophic

dinoflagellates *Gyrodinium dominans*, *Luciella masanensis*, *Oblea rotunda*, and *Polykrikos kofoidii* and the naked ciliate *Strombidium* sp. preyed on *M. rubrum*. However, only *G. dominans* had a positive growth feeding on *M. rubrum*. The maximum growth rate of *G. dominans* on *M. rubrum* was 0.48 d^{-1}, while the maximum ingestion rate was 0.55 ng C $predator^{-1}$ d^{-1}. The grazing coefficients by *G. dominans* on populations of *M. rubrum* were up to 0.236 h^{-1}. Thus, *G. dominans* may sometimes have a considerable grazing impact on populations of *M. rubrum*.

In chapter 6, to explore combined effects of warming and eutrophication on the phytoplankton production in the future, biomass of phytoplankton was monitored after establishing 64 different initial conditions formed by combining 4 different water temperatures (i.e., ambient, +2, +4, and +6 °C) and 2 different nutrient conditions (i.e., non-enriched and enriched) using natural water sampled 8 times at intervals of 1-2 months. Under non-enriched conditions, the effects of temperature elevation on phytoplankton production were inconsistent (i.e., positive, negative, or negligible) irrespective of temperature elevation, whereas under enriched conditions, the effects were all positive. The ratio of initial nitrate concentration to Chl-a concentration [NCCA, μM $(\mu g\ L^{-1})^{-1}$] mainly determined the directionality of the temperature effect. With a few exceptions, when the NCCA value in the ambient or nutrient-enriched waters was > 1.5, temperature elevation increased phytoplankton production. This study result suggests that the NCCA value is the critical factor affecting coastal phytoplankton production in periods of global warming.

Through the present study chages in phytoplankton community and dominant red-tide dynamics were approached from metrological, hydrological, biological perspectives. In addition, accelerated global warming and eutrophication were pointed out to be associated with the present day changes in phytoplankton production and protistan community composition. These environmental problems and the ecological responses by plankton communities are directly linked to fishery, aquaculture, and human food chains. Therefore this study results will be useful to better understand the current healthiness of marine ecosystem and also extend further to predict on the future marine ecosystems.

Keyword: coastal environment, eutrophication, global warming, harmful algal bloom, phytoplankton, protist, red tide

Student Number: 2012-30095

Table of Contents

Abstract i

Chapter 1. Overall introduction..... 1

Chapter 2. Precipitation select red tide caustative phytoplankton group: serial correlations of precipitation, salinity, nitrate, and dominant phytoplankton..... 13

Chapter 3. Elevating growth rate strategy of the newly described mixotrophic dinoflagellate *Gymnodinium smaydae* by acquiring nutrients from feeding.... 44

Chapter 4. Survival strategies of the toxic dinoflagellates *Alexandrium andersonii*, *A. affine*, and *A. fraterculus* by killing and/or feeding other protists 92

Chapter 5. Predation by common heterotrophic protists on the mixotrophic red−tide ciliate, *Mesodinium rubrum* 140

Chapter 6. Nutrient conditions altering effects of warming on phytoplankton production in coastal waters..... 168

Chapter 7. Overall discussion 197

Bibliography 207

Abstract in Korean 240

Chapter 1.
Overall introduction

Ocean covers ~70% of the earth and maintain homeostasis of the earth and our life. And phytoplankton in that waters contribute half of global primary production (Falkowski and Raven, 1997; Rogato et al., 2015). Among ca. 4,000 marine phytoplankton species has been reported, the dominant phytoplankton groups are dinoflagellates (40%) and diatoms (40%) (Sournia et al., 1991). The micro-units of these tiny phytoplankton are ubiquitous and divide fast using doublings. Phytoplankton is primary producer which synthesis organic compounds from inorganic compounds and transfer it to higher tropic level animals. However, if the water conditions are favorable for specific species, they can outgrow, occur red ride and/or harmful algal blooms (HABs), and cause massive economic losses (Jeong et al., 2015). We can monitor and control visible coastal type red-tide patches in near coastal fishery area, whereas we cannot control the thousands kilometers off-shore type of red tide patches coming from open oceans. Moreover, climate change is accelerating and changing structure and functions of marine ecosystems, thus climate change is expected to have influence on dominant phytoplankton group and red-tide dynamics. Therefore it is important of controlling and managing marine ecosystems by fully understanding structures and functions of marine ecosystems.

1.1. Coastal waters

Coastal waters which play the most important role of water exchange between river and oceanic waters (Fig 1.1). In addition, there are the main hotspot of phytoplankton production due to relatively high nutrient concentrations than off-shore waters, and thus most of fish harvest can occur there despite its relative small water bodies (Bianchi et al., 2013). Nutrients, especially inorganic nutrients, are the essential foods for phytoplankton to grow up. One of the main sources of nutrients in coastal waters are river flow originated from precipitations (Thompson et al., 2015a). Thus, the diverse components such as air pollutants in each area, utilization of land, and populations may decide the quality of runoff through rivers to coastal. Moreover, the frequency and amounts of precipitation in each coastal area may reflect temporal and seasonal characteristics there. Korea is situated in temperate middle latitude zone of the Northern Hemisphere, thus the precipitation is concentrate on summer (i.e., 50~60% of annual precipitations concentrate on summer). Therefore, to understand precipitation flowing through rivers to coastal waters effects on dominant phytoplankton groups, I investigated the correlation study among precipitation, salinity, nitrate concentrations, and dominant phytoplankton groups in inner Shiwha Bay in western Korea and Gwangyang Bay in southern Korean for Chapter 2 (Fig. 1.1).

1.2. Phytoplankton

Marine phytoplankton is the major primary producer and provide synthesized organic materials and energy to higher tropic level consumers, thus it is the most important basic components in marine ecosystem. They uptake carbon dioxide which causes greenhouse effects and ocean acidifications, and contribute to produce oxygen (Falkowski et al., 2004; McQuatters-Gollop et al., 2015). About 4,000 marine phytoplankton species have been reported and their physiology and ecology are totally different because it is affected by diverse biotic (preys, competitor, and grazer) and abiotic (temperature, salinity, light intensity, and available nutrients) factors (Sournia et al., 1991). Thus, to understand the taxonomy and physiology of dominant phytoplankton helps to understand marine food webs and marine ecosystem there. The basic physiology of the phytoplankton is growth rates. Phytoplankton are known as to grow conducting photosynthesis. However, recent studies have been revealed that the some of phytoplankton previously considered exclusively phototrophic is mixotrophic and the most active mixotrophic group in phytoplankton is dinoflagellates (Jeong et al., 2005a, 2005b, 2005c, 2010; Lee et al., 2014, 2016; Yoo et al., 2010b).

The growth of phytoplankton may define as following equation (1).

$$\frac{dP}{dt} = \mu P(N\ and/or\ F) - mP(g, c, El) \qquad \text{eq. (1)}$$

P is phytoplankton, μP is growth rate of phytoplankton from acquired nutrients(N) and/or mixotrophic feeding (F), mP is mortality of phytoplankton caused by grazers(g), killed by competitors (c), and energy loss (El) from swimming, anti-predation activities (i.e., producing toxins) and/or ingesting preys.

If the growth of phototrophic or mixotrophic plankton (μ) is higher than the death rates (mP, eaten by grazers or death by chemicals from competitors), red-tides or harmful algal blooms (HABs) can occur. However, μ is lower or comparable to mP, the red tides or HABs does not occur.

Therefore, I investigated the survival strategy of new mixotrophic dinoflagellate, *Gymnodinium smaydae*, by feeding other phototrophic protists in Chapter 3 and the other survival strategy of three toxic dinoflagellates, *Alexandrium* spp., by killing with allelopathical effects and/or ingesting other protists in Chapter 4.

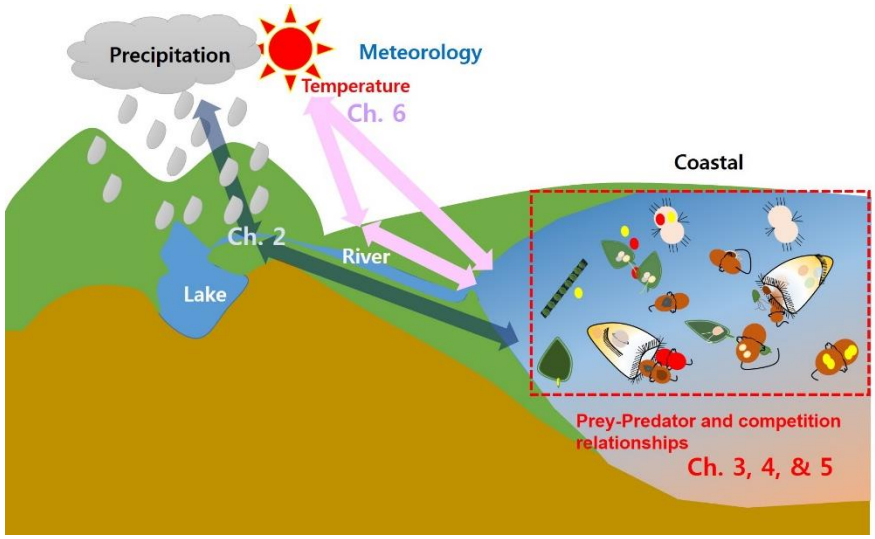

Fig. 1.1. Scheme of chapters in this study.

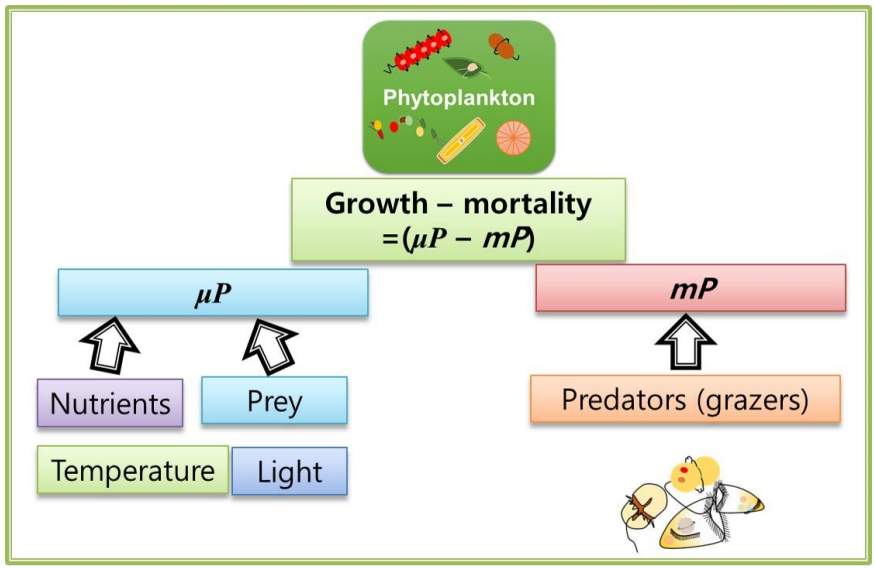

Fig. 1.2. Diagram of phytoplankton production and factors affecting phytoplankton biomass or abundances. Nutrient concentration, prey, temperature, and light affect growth rates of phytoplankton, while grazing by predators affects motality rates of phytoplankton.

1.3. Heterotrophic protists

Heterotrophic protists which is mainly composed of heterotrophic dinoflagellates and ciliates are dominant grazers of phytoplankton and play a role as a messenger to higher tropic level metazooplankton grazers (i.e., copepods, cladocerans, and benthos larvae). In addition, sometimes these heterotrophic protists play roles as preys for mixotrophic phytoplankton reversely (Bockstahler and Coats, 1993a, 1993b; Jacobson and Anderson, 1996; Jeong et al., 1997; Uchida et al., 1997; Smalley et al., 1999; Park et al., 2006; Berge et al., 2008; Nishitani et al., 2008a; Nagai et al., 2008; Blossom et al., 2012).

In previous mesocosm studies using environmental samples, the predators of phytoplankton was commonly considered as metazooplanktons such as copepods (Sommer and Lewandowska, 2011; Lewandowska et al., 2014). However, grazing impact by heterotrophic protistan grazers on phytoplankton is usually much greater than that by metazooplanktonic grazers because the abundances of heterotrophic protists are ca. 100−10,000 times higher than those of metazooplanktonic grazers, even though the ingestion rates of heterotrophic protists are ca. 10−100 times lower than those of metazooplanktonic grazers (Kim et al., 2013; Yoo et al., 2013a).

The growth of heterotrophic protists may define as following equation (2).

$$\frac{dHP}{dt} = \mu HP(F) - mHP(g, c, El) \qquad \text{eq. (2)}$$

HP is heterotrophic protists, μHP is growth rate of heterotrophic protists from feeding (F), mHP is mortality of heterotrophic protists caused by grazers(g), killed by competitors (c), and energy loss (El)from swimming and ingesting preys.

For these reasons, identifying heterotrophic protists and investigating their new food web pathway is important to understand better about the structures and functions of marine ecosystem. Therefore, I investigated the common heterotrophic protistan predators feeding on the red-tide causative mixotrophic ciliate, *Mesodinium rubrum* in Chapter 5.

1.4. Marine food web

These micro-units of planktons are co-exist whenever and wherever and make a balance to maintain micro-unit food webs (Fig. 1.3). These food web is the most fundamental converting processes from elements to one cell organisms and then the upper predators in micro food webs transfer energy to higher level food webs as preys. The repeated food chains finally form the whole marine food webs and interact with human life. Thus, exploring this basic micro-scale food webs response to global environmental problematic factor change is worthwhile work to better understand of the past and current of marine environmental status, and predict future and provide proper guidelines to maintain healthy marine ecosystems.

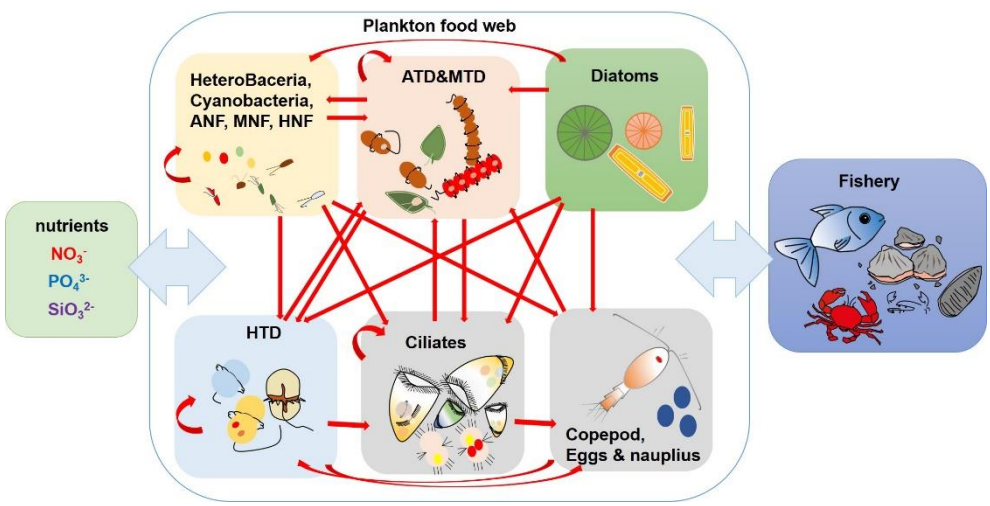

Fig. 1.3. Marine plankton foodwebs. Thinner line with an arrow head indicate feeding occurrences. Thicker line with two arrow heads indicate interactions.

1.5. Global warming and eutrophication

Global warming and eutrophication are serious global phenomena and they have been affected marine food webs (Nixon, 1995; McClain, 2009; Boyce et al., 2010; Canuel et al., 2012; Godhe et al., 2015). According to IPCC report (2013), the temperature may increase 2 to 6 ℃ in the worst case in the next 100 years and sea water temperature also expected to increase. Especially, coastal environment response faster than offshore waters, because it is shallow. The nutrient sources introduce through river by utilization of fertilizers or air pollution deposition to the sea waters (Kim et al. 2011). However, the nutrient concentrations in coastal waters in some countries are decreasing by reduction of nutrient loads in discharged freshwaters with well-equipped sewage treatment systems, while those in other countries are still increasing due to expansion of agriculture or hardness of water pollution control (Kim et al. 2011). Therefore, trends in nutrient concentrations in the future are dependent of efforts of each country. Increase or decrease in nutrient concentration cause a change in phytoplankton biomass and production and its dominant groups (Jeong et al. 2013b). An increase in nutrient concentrations usually cause increase in the biomass of fast-growing diatoms which in turn outgrow over relatively slow growing flagellates (Cloern et al., 1983; Cloern 2001). Thus, seawater temperature and nutrient concentrations are expected to change dynamically in the future, which may affect the production of marine organisms and eventually the structure and

functions of marine ecosystems (Boyce et al., 2010; Lee, 2012; Defriez et al., 2016). Therefore, I investigated temperature and nutrient concentration effects on phytoplankton productions using bottle incubation experiments containing environmental water samples for 8 months different initial conditions and combining 4 different water temperatures (T, T+2, T+4, and T+6 ℃) and 2 different nutrient conditions (natural nutrient conditions and enriched nutrient conditions) in each months in Chapter 6.

1.6. Outline of this thesis

This thesis focuses on two major physical and chemical factors, temperature and nutrients, effects on coastal environmental and the response by phytoplankton community and production dynamics. In addition, biological factors, prey, competitor, and grazing effects, were focused. Because prey, competitor, and grazing effects are strongly connected to nutritional strategy of phytoplankton and hetetrotrophic protists in marine food webs.

Therefore, this study was conducted following five sub-themes (Fig. 1.4). Inorganic nutrients are the most essential component for phytoplanktons to grow up. Also nutrients can be an indicating factor for plankton community composition. Thus, I investigated the most major inorganic nutrient, nitrate dynamics and related salinity and precipitations effect on dominant phytoplankton group in Chapter2 (Fig. 1.4, 1.5). In addition, I investigated nutritional strategy of phytoplankton and heterotrophic protists in marine food

webs in Chapter 3, 4, and 5 (Fig. 1.4, 1.5). In Chapter 3, I investigated the new food web pathway from new species, *Gymnodinium smaydae*, and the highest growth rate strategy by ingesting other protists (i.e., mixotrophy). In Chapter 4, I investigated another elevating growth strategy of *Alexandrium* species by ingesting (i.e., mixotrophy) and killing (i.e., allelopathy) other protists. Moreover, in chapter 5, I investigated how red-tide causative protists can be controlled by predators. In addition, how heterotrophic protistan species form new food web by ingesting red-tide species, inversely. Finally, base on diverse investigations of phytoplankton biomass or abundance dynamics from chapter 2, 3, 4, and 5, I investigated the response of phytoplankton production to different nutrient levels if water temperature elevates 2, 4, and 6°C by global warming using eight months environmental coastal waters to predict future marine ecosystem response in Chapter 6 (Fig. 1.4, 1.5). This study imply that contemporary important global environmental problems caused by anthropogenic activities global warming and eutrophication.

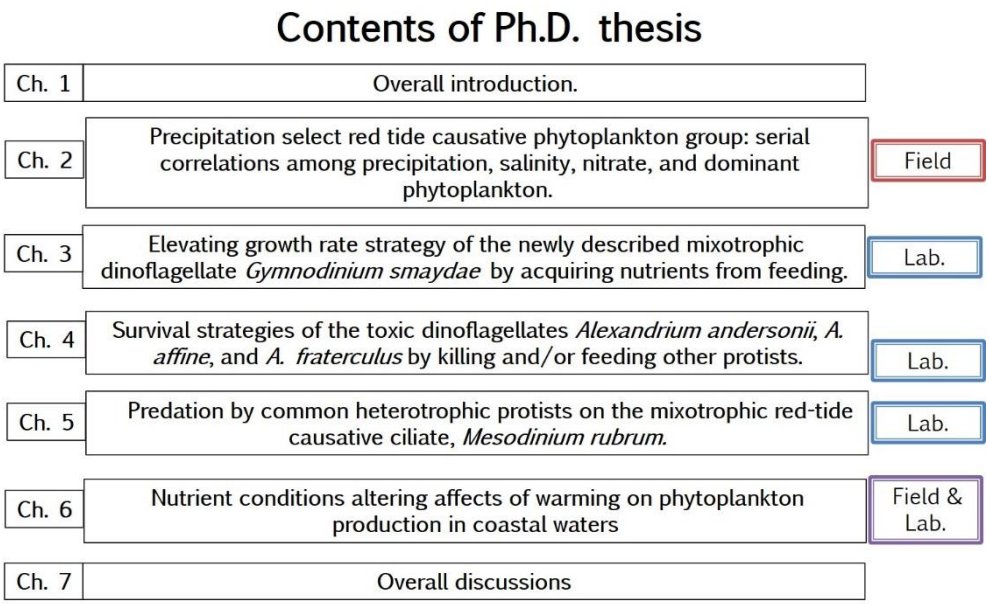

Fig. 1.4. Outline of Ph.D. thesis.

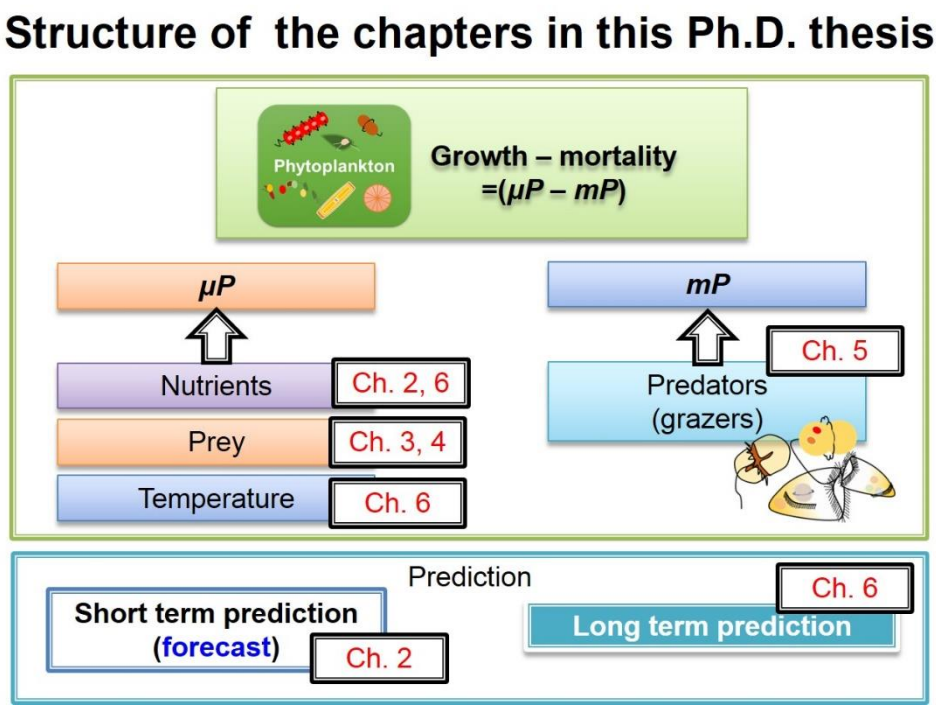

Fig. 1.5. Structure of the chapters in this Ph.D. thesis.

Chapter 2.
Precipitation select red tide causative phytoplankton group: serial correlations among precipitation, salinity, nitrate, and dominant phytoplankton

2.1 Abstract

Each components of precipitation, salinity and nitrate are have great influence on phytoplankton community and composition. However, how these components related each other and final dominant group are not well investigated yet. I investigated two major Korean coastal area, Gwangyang Bay in Southern Korea and Shiwha Bay in Western Korea to analysis the relationships among precipitation, salinity, nitrate, and dominant phytoplankton. In Gwangyang Bay, from 2011 2013 the correlations between salinity and 5 to 14 days precipitation sum (PS) were analyzed. Salinity showed significant negative correlations with 10 to 20 days PS ($p<0.001$). In each summer separate analysis salinity showed significant negative correlations with nitrate plus nitrite (NO_3^-) in 2011 and 2012 ($p<0.001$) biomass of diatoms were dominated. Moreover salinity and did not show any correlations with nitrate ($p>0.05$) and dinoflagellates was dominated up to 70% in July 2013. From 2009 to 2011 in Shiwha Bay, salinity showed negative

correlations with 7 to 20 days PS ($p<0.05$). In each year separate analysis, correlations results between salinity and precipitation sum was inconsistent unlike the results in Gwangyang Bay. However, in each year separate analysis salinity showed significant negative correlations with nitrate plus nitrite (NO_3^-) only in 2011 ($p<0.001$) and diatoms and small flagellates were dominated, while salinity did not show any correlations with nitrate in 2009 and 2010 ($p>0.05$) and dinoflagellates were dominated. Therefore, serial correlations in precipitation, salinity, and nitrate concentration were selected dominant phytoplankton groups. The results from this study may help to understand the basic coastal process, and provide guidelines of coastal management and proper nutrient levels to maintain healthy coastal area.

2.2. Introduction

Coastal waters which play the most important role of water exchange between river and open ocean waters are the main hotspot of phytoplankton production due to relatively high nutrient concentrations than off-shore waters, thus most of fish harvest can occur there despite its relative small water bodies (Odebrecht et al., 2015). Nutrients, especially inorganic nutrients, are the essential foods for phytoplankton productions. One of the main sources of nutrients in coastal waters are river flow originated from precipitations. Thus, the diverse components such as air pollutants in each area, utilization of land, and populations may decide the quality

of runoff through rivers to coastal. Moreover, the frequency and amounts of precipitation in each coastal area may reflect temporal and seasonal characteristics there.

Recently, meteorological events (i.e., temperature or precipitation) become more dynamic due to climate change and many studies has investigated the relationships between meteorological parameters and phytoplankton. Further trying to find its correlations out to predict phytoplankton production, composition, and/or community (Thompson et al., 2015b). In some regions, reduced precipitation events, the less phytoplankton has been observed from time series data and also expected similar trends in the future (Thompson et al., 2015a). Therefore, the temporal and seasonal precipitations may have direct influence on phytoplankton biomass and dominant phytoplankton group in coastal regions.

Phytoplankton is essential primary producers in aquatic environments. Phytoplankton synthesize inorganic carbon, nitrogen, phosphorus, and/or silicate into organic compound as its body (Kemp et al., 1997). The nutrient concentrations in each river, estuary, and coastal region is dynamic and it changes every day because of depending on uncertain input (i.e., precipitations, pollutants, runoffs) and uptake by phytoplankton. The dominant phytoplankton in coastal region is mainly decided by the nutrient concentrations in each region. The nutrient limitation and the ratio of N to P also can affect dominant phytoplankton or feeding choice of mixotrophic protists. Moreover, the dominant animal predators consuming plankton is decided by their favor phytoplankton species (Cloern et al., 1983) and the food chain

continue goes up. Therefore, the commercially important marine animal productions (i.e., fishery) may depend on dominant phytoplankton groups and this reflect fundamentally effects of nutrient concentrations in each area (Platt et al., 2003; Richardson and Schoeman, 2004; McQuatters-Gollop et al., 2015). However, there have been few studies investigating response by dominant phytoplankton group change to precipitation, salinity, and nitrate concentration series change.

In this chapter, I investigated two major Korean coastal area, Gwangyang Bay in Southern Korea and Shiwha Bay in Western Korea to analysis the relationships among precipitation, salinity, nitrate, and dominant phytoplankton. The results from this study may help to understand the basic coastal process, and provide guidelines of coastal management and proper nutrient levels to maintain healthy coastal area.

2.3. Methods

2.3.1. Study site

I selected two coastal sites for study area, Gwangyang Bay in Southern Korea (Fig. 2.1) and Shiwha Bay in Western Korea (Fig. 2.2). Gwangyang Bay (230 km^2 area) is one of the major Southern Korean coastal area and have the 5^{th} major Seomjin rivers flow running between Gwangyang and Hadong into this bay and the waters flow into the South Sea between Yeosu and Namhae city (Fig. 2.1).

Gwangyang Bay has been affected from many artificial human activities because steel industry and petrochemical complex have been working since 1980s, and cargo ships navigate from the harbor there. Due to these artificial reasons, Gwangyang bay is specially managed and the response of diverse coastal water environmental components such as T, S, nutrients, phytoplankton, and/or zooplankton has been reported by many environmental impact assessments (Jang et al., 2005; Lee et al., 2005; Baek et al., 2011; Kim et al., 2015). Sampling stations were selected considering freshwater input effects to coastal waters. At first, St. 1 where fresh waters from Seomjin River introduce was selected and St. 2 to St. 5 were selected because they are gradual flowing out points to the open South Sea.

Shiwha Bay (438 kim^2 area) is located in the western Korea, 12.7 km huge dike was constructed in 1996, and the world' s largest tidal power plant was also constructed in 2011 (Bae et al., 2010; Lee, 2012; Kang et al., 2013). The original purpose of dike construction in Shiwha Bay was to expend the land use of agriculture and freshwater supply for it. However, the water quality was getting worse after constructing the dike and the waster gate was constructed for water circulations, and finally the tidal power plant was constructed to use there (Kang et al., 2013). The sampling station in Shiwha Bay was also selected as close to river and land (Fig. 2.2).

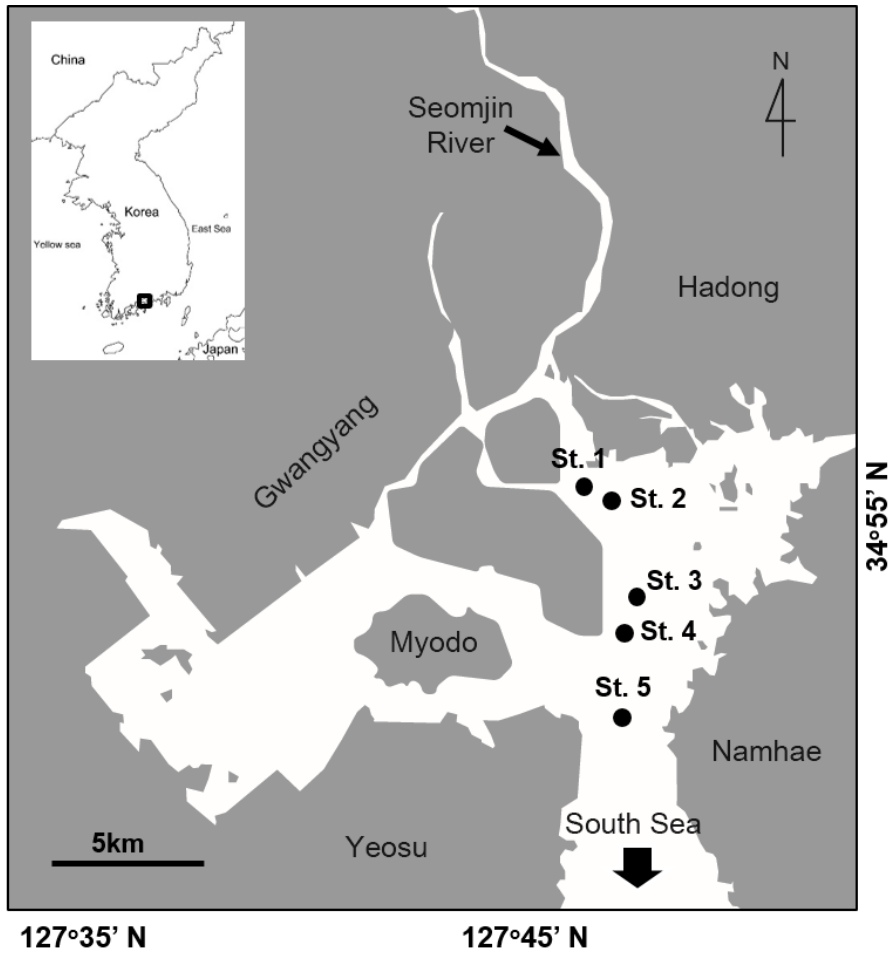

Fig. 2.1. The map of study sites (St. 1 to 5) in Gwangyang Bay.

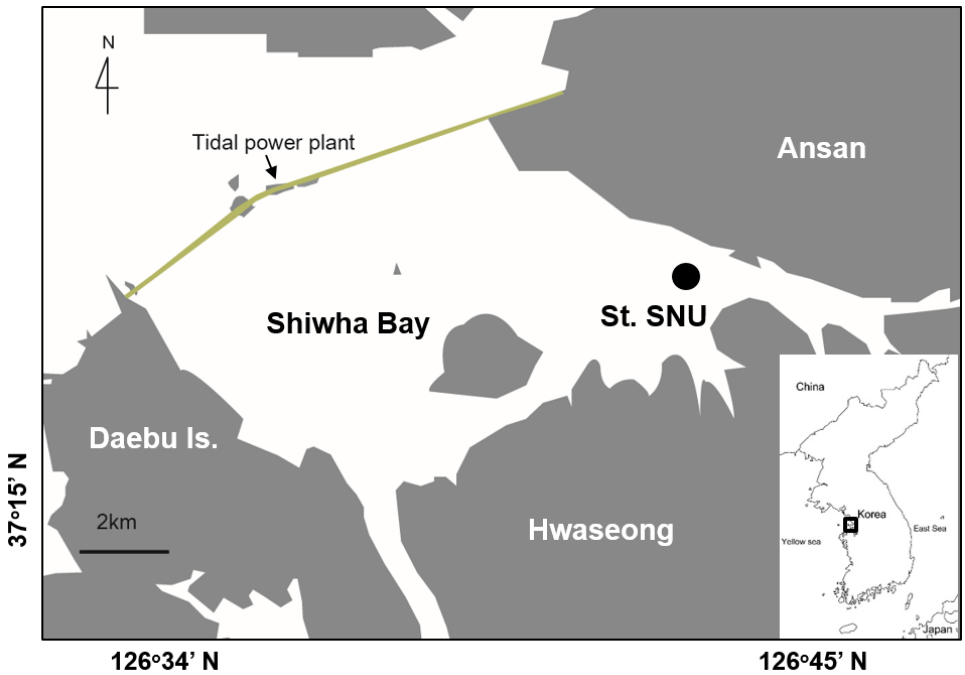

Fig. 2.2. The map of study sites (St. SNU) in Shiwha Bay.

3.2. Sampling and sample analysis

Water samples were taken at the surface at each station with water sampler for four seasons (February, April, July and December) from 2011 to 2013 in Gwangyang Bay. Water temperatures and salinities in surface waters were measured using a YSI 30 (YSI, LA, USA) and pH and dissolved oxygen (DO) was measured using pH-11 (Schott HandyLab, Mainz, Germany) and Oxi 197i (WTW, Weilheim, Germany), respectively. For inorganic nutrient analysis, the water samples were gently filtered through GF/F filter papers and moved to the laboratory and analyzed immediately. When the samples could not be analyzed immediately, they were preserved at −20 ° C in a freezer until analysis could take place. Ammonium (NH_4), nitrate plus nitrite

(NO_3 + NO_2, hereafter NO_3), phosphate (PO_4), and silicate (SiO_2) were detected using a nutrient auto-analyzer system (QuAAtro, Seal Analytical GmbH, Werkstrasse, Norderstedt, Germany). The nutrient data of St. 1 to 4 in February 2011 were unavailable, thus only St. 5 data was used.

Plankton samples for counting were poured into 500-ml polyethylene (PE) bottles and preserved with acidic Lugol's solution for protistan species counting. To determine the abundances of diatoms, phototrophic and mixotrophic dinoflagellates, heterotrophic protists, and diverse small flagellates (cryptophytes, raphidophytes, euglenophytes, etc.), samples preserved with acidic Lugol's solution were concentrated by 1/5-1/10 using settling and siphoning methods (Welch, 1948). After thorough mixing, all (or a minimum of 100) cells of each protist species in one to ten 1-ml Sedgwick-Rafter counting chambers were counted under a light microscope.

I calculated the carbon content for each of many protistan species from environmental sample counting applying previously measured with cultures in the laboratory using a CHN analyzer (Kang et al., 2013; Jeong et al., 2013b; Yoo et al., 2013c). For noncultured species or taxa, the length and width of cells preserved in 5% acidic Lugol's solution were measured using a light microscope and cell volume was then calculated according to geometry (Jeong et al., 2013b). The carbon content for each species of protists was calculated from the cell volume according to Menden-Deuer and Lessard (2000).

Water samples were taken at the surface at the station which with water sampler for every months from 2009 to 2011 in Shiwha Bay. December in 2009, January and February in 2010 and 2011, Sampling was not conducted due to frozen. The sampling and sample analyses procedure is same as described above.

2.3.3. Meteorological data

The precipitation used for correlation was based on the database of the Korea Meteorological Administration (KMA, http://web.kma.go/kr). The meteorological station of Gwangyang was selected for Gwangyang Bay and that of Incheon was selected for Shiwha Bay. In addition, to find out the best correlations between precipitation and salinity of each two coastal waters, the sum of precipitations from 5 to 20 days for Gwangyang and 2 to 20 days for Shiwha Bay were calculated and the strongly correlated days was selected.

2.3.4. Data analysis

Correlation coefficients between precipitation, salinity, nitrate plus nitrite, and dominant phytoplankton groups were calculated using the Pearson's correlation (Conover, 1980; Zar, 1999) and SPSS program (IBM SPSS statistcs 23, IBM, USA). In addition, all data were fitted using DelthGraph 4.0 (Red Rock Software, USA)

2.4. Results

2.4.1. Gwangyang Bay

Physical, chemical, and meteorological properties in Gwangyang Bay. From February 2011 to October 2013, the range of water temperature in Gwangyang Bay was 5.8 – 26.6 °C and that of salinity was 11.0 – 34.5 (Table 2.1, Fig. 2.3). The lowest salinity value was observed at St. 1 which is the most inner station. The range of ammonia, nitrate plus nitrite, phosphate, and silicate concentration was 0 – 6.1, 0 – 64.0, 0 – 5.8, and 0 – 121.3 μM, respectively. The highest concentrations of nitrate, phosphate, and silicate was also observed at St. 1 (Table 2.1, Fig. 2.3).

Correlations between precipitation and salinity in Gwangyang Bay. The maximum precipitations was occurred in every summer. The 14 days precipitation sum previous sampling day in summer were 455 mm in 2011, 296 mm in 2012, and 0.8 mm in 2013.

From February 2011 to October 2013 the correlations between salinity and 5 to 14 days precipitation sum (hereafter, PS) were analyzed. Salinity did not show any correlations with 5 days PS ($p>0.05$; Fig. 2.4A), showed weak negative correlations with 7 days PS ($p<0.05$; Fig. 2.4B), showed significant negative correlations with 10 to 20 days PS ($p<0.001$, linear regression, ANOVA; Fig. 2.4C–H; Table 2.2).

Table 2.1. The range of physical and chemical properties in Gwangyang Bay, Korea from February 2011 to October 2013. Temperature (T, °C), Salinity (S), and inorganic nutrients (μM).

	St. 1			St. 2			St. 3			St. 4			St. 5		
	AV	Min	Max	AV	Min	Max	AV	Min	Max	AV	Min	Max	AV	Min	Max
T	15.3	5.8	25.7	15.5	6.5	26.5	15.5	6.6	26.6	15.4	6.4	26.1	16.0	6.4	25.7
S	24.9	11.0	33.8	26.9	12.8	34.1	31.0	22.3	34.5	30.9	20.4	34.4	30.5	21.8	34.3
NH4	2.3	0.0	5.4	2.9	0.0	8.2	1.9	0.0	5.9	2.0	0.0	5.9	2.6	0.0	6.1
NO3	23.2	0.7	64.0	16.6	0.0	53.6	6.1	0.9	20.1	8.1	0.1	31.2	8.1	0.0	25.6
PO4	0.8	0.0	5.8	0.7	0.0	5.3	0.7	0.0	5.4	0.6	0.0	4.0	0.6	0.0	3.0
SiO3	39.4	2.9	121.3	27.9	0.9	114.8	11.0	0.0	36.5	15.5	0.7	69.1	13.8	0.0	60.6

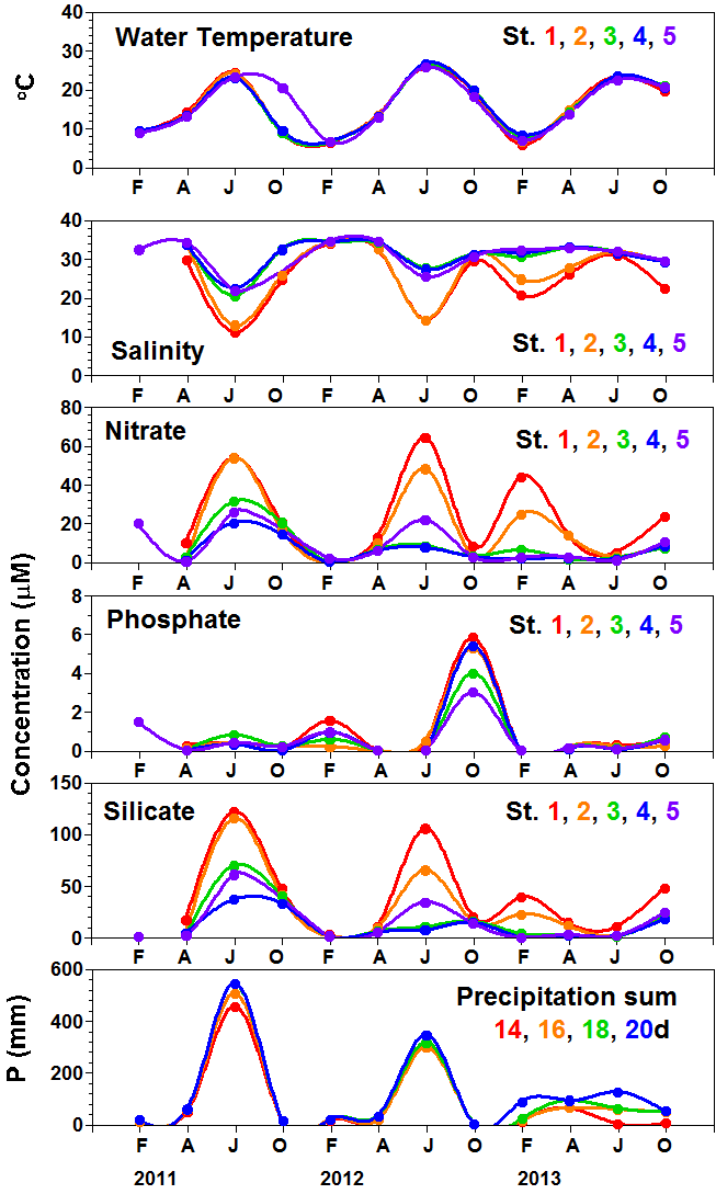

Fig. 2.3. The range of physical, chemical, and meteorological properties in Gwangyang Bay, Korea from February 2011 to October 2013.

From February 2011 to October 2013 in Gwangyang Bay, correlations between salinity and 5 to 14 days PS in each year were also analyzed. Salinity generally showed significant negative linear correlations with 5−14 days PS in 2011 and 2012, while did not show any significant correlations in 2013 (Table 2.3).

Correlations between salinity and nutrients in Gwangyang Bay. From 2011 to 2013, salinity showed significant negative correlations with nitrate plus nitrite (NO_3^-) and silicate (SiO_3^{2-}) ($p<0.001$, linear regression, ANOVA; Fig. 2.5, 2.6). However, salinity did not show any correlations with phosphates (PO_4^-) ($p>0.05$). In addition, each year separate analyses also showed same results.

However, in each summer separate analysis salinity showed significant negative correlations with nitrate plus nitrite (NO_3^-) in 2011 and 2012 ($p<0.001$, linear regression, ANOVA) and did not show any correlations in 2013 ($p>0.05$) (Fig. 2.7).

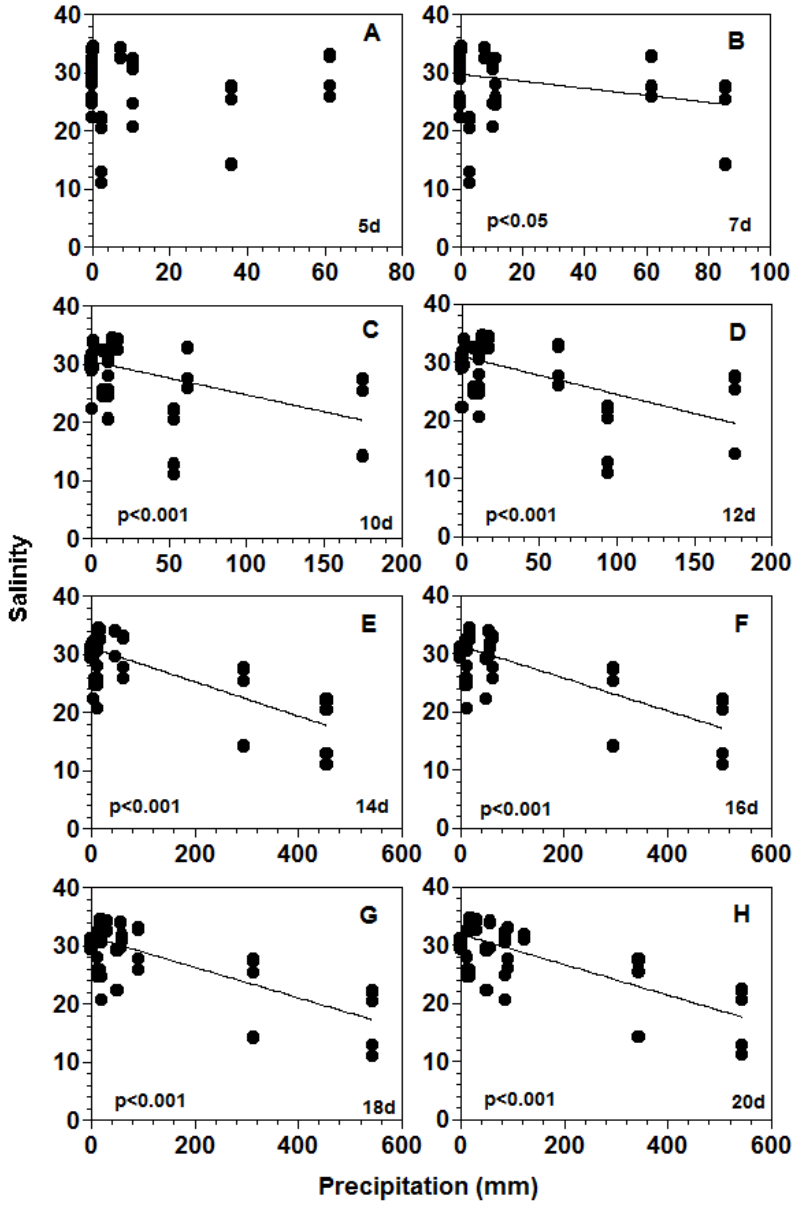

Fig. 2.4. Correlations between 5 to 20 days precipitation sum and salinity of coastal surface waters in Kwangyang Bay from February 2011 to October 2013.

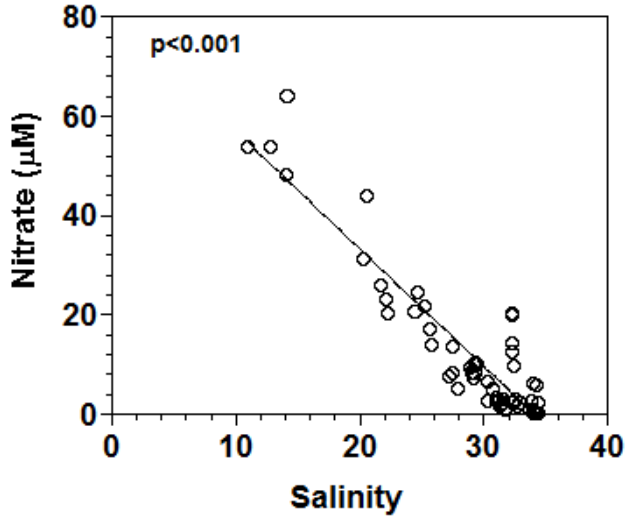

Fig. 2.5. Correlations between salinity of coastal surface waters and nitrate plus nitrite (NO_3^-) in Gwangyang Bay from February 2011 to October 2013.

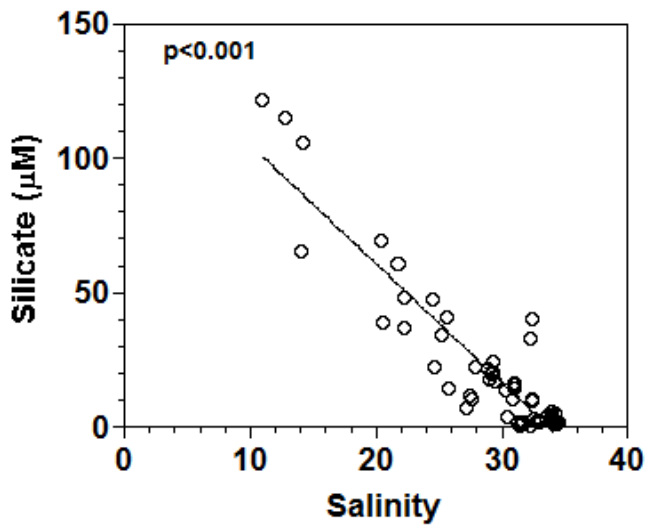

Fig. 2.6. Correlations between salinity of coastal surface waters and silicate (SiO_3^{2-}) in Gwangyang Bay from February 2011 to October 2013.

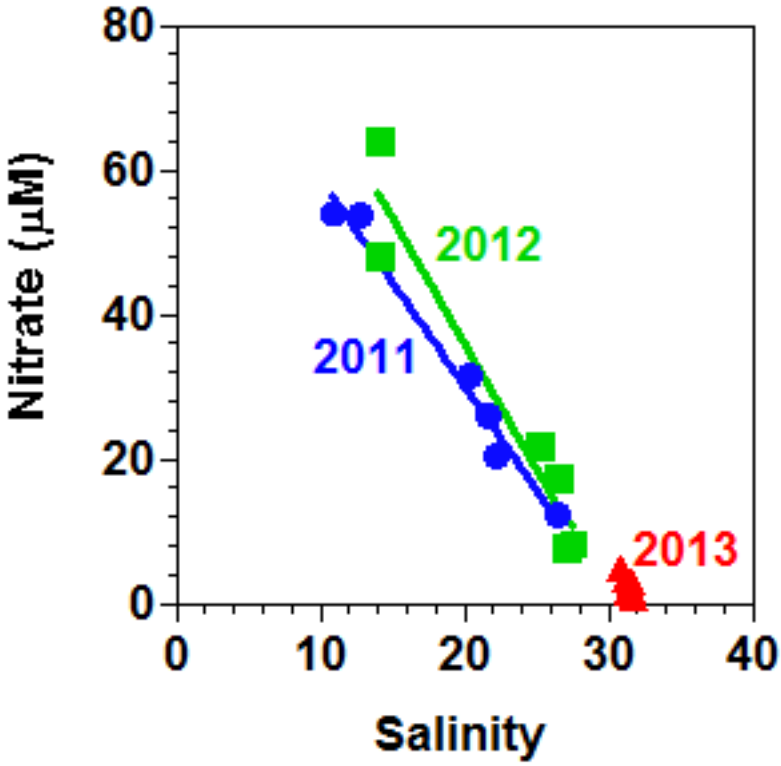

Fig. 2.7. Correlations between salinity of coastal surface waters and nitrate plus nitrite (NO_3^-) in Gwangyang Bay in July 2011 July 2012, and July 2013 ($p<0.001$ for 2011 and 2012).

Table 2.2. Results of correlations using linear regression between salinity and precipitation in Gwangyang Bay from February 2011 to October 2013. Gradients (a), Constants (b), and coefficient of determination (R^2) from equations.

PS	p-value	R^2	a	b
5 days	p>0.05	0.02	−0.04	29.24
7 days	p<0.05	0.08	−0.06	29.75
10 days	p<0.001	0.24	−0.06	30.55
12 days	p<0.001	0.35	−0.07	31.01
14 days	p<0.001	0.52	−0.03	31.11
16 days	p<0.001	0.52	−0.03	31.39
18 days	p<0.001	0.52	−0.03	31.49
20 days	p<0.001	0.53	−0.03	31.84

Table 2.3. Results of each year correlations between salinity and precipitation sums Gwangyang Bay from February 2011 to October 2013. Linear regression, ANOVA.

	Precipitation sum								
	5d	7d	10d	12d	14d	16d	18d	20d	n
2011	$p<0.001$	$p>0.05$	$p<0.001$	$p<0.001$	$p<0.001$	$p<0.001$	$p<0.001$	$p<0.001$	21
2012	$p<0.001$	$p<0.001$	$p<0.001$	$p<0.001$	$p<0.001$	$p<0.001$	$p<0.001$	$p<0.001$	20
2013	$p>0.05$	$p>0.05$	$p>0.05$	$p>0.05$	$p>0.05$	$p>0.05$	$p>0.05$	$p>0.05$	21

Dominant phytoplankton. From February 2011 to October 2013, the biomass of total phytoplankton was highest in July 2012 at station 3 and 4 (352–395 ng C ml^{-1}) and diatoms followed as a dominant group the similar trends (350–382 ng C ml^{-1}). The biomass of diatoms were dominated each season except July 2013. The biomass of dinoflagellates was highest and dominated up to 70% (i.e., 116 ng C ml^{-1} at St. 5) of total phytoplankton biomass in July 2013 (Fig. 2.8).

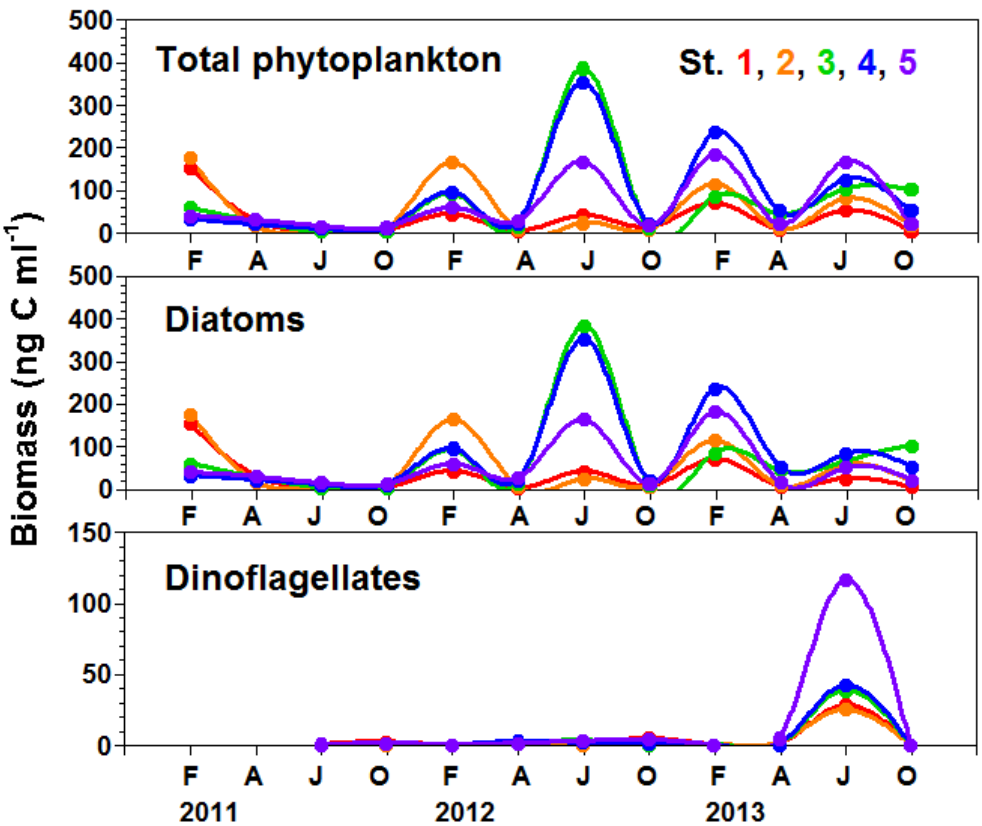

Fig. 2.8. The biomass of total phytoplankton, diatoms, and dinoflagellates in Gwangyang Bay from February 2011 to October 2013.

2.4.2. Shiwha Bay

Physical, chemical, and meteorological properties in Shiwha Bay. From January 2009 to December 2011, the range of water temperature in Shiwha Bay was 1.5 – 28.4 ℃ and that of salinity was 3.4 – 29.2 (Table 2.4, Fig. 2.9). The lowest salinity value was observed in August 2011. The range of ammonia, nitrate plus nitrite, phosphate, and silicate concentration was 0 to 0.4–81, 0 to 134, 0 to 1.4, and 0.8 to 68 μM, respectively. The highest concentrations of nitrate was also observed in August 2011 (Table 2.1, Fig. 2.8).

Correlations between precipitation and salinity in Shiwha Bay. The maximum precipitations was occurred in every summer. The 5, 7, and 10 day precipitation sum previous sampling day were highest (90, 169, and 235 mm, respectively) in July 2011.

From January 2009 to December 2011, the correlations between salinity and 2 to 20 days precipitation sum (hereafter, PS) were analyzed. Salinity did not show any correlations with 2 to 5 days PS ($p>0.05$; Fig. 2.10A–B), showed weak negative correlations with 7 days PS ($p<0.05$; Fig. 2.10C), showed significant negative correlations with 10 to 20 days PS ($p<0.001$, linear regression, ANOVA; Fig. 2.10D–F; Table 2.5).

From January 2009 to December 2011 in Shiwha Bay, correlations between salinity and 2 to 20 days PS in each year were also analyzed. Correlations results between salinity and diverse PS was inconsistent. (Table 2.6).

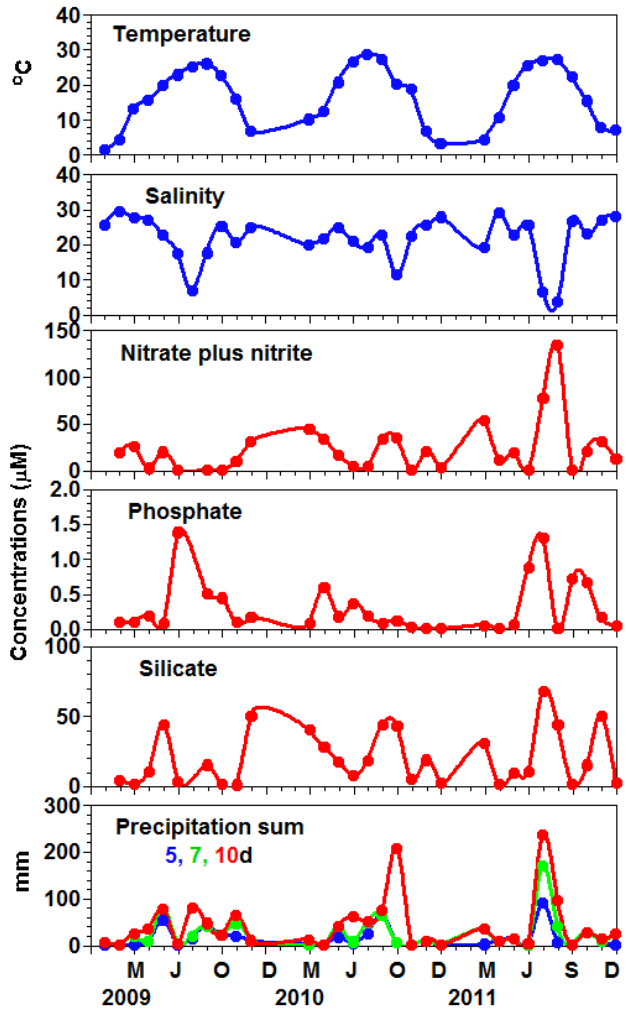

Fig. 2.9. The range of physical, chemical, and meteorological properties in Shiwha Bay, Korea from January 2009 to December 2011.

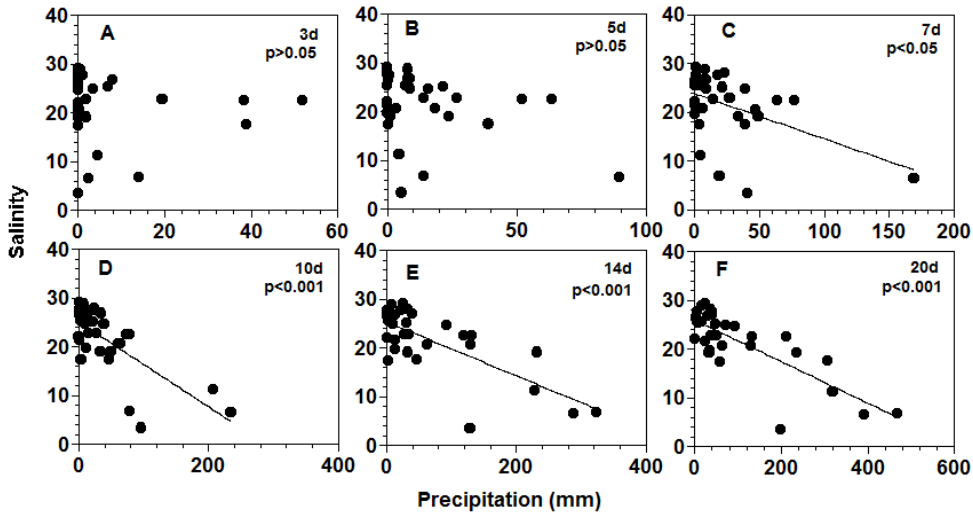

Fig. 2.10 Correlations between 3 to 20 days precipitation sum and salinity of coastal surface waters in Shiwha Bay, Korea from January 2009 to December 2011.

Table 2.4. The range of physical and chemical properties at the stations in Shiwha Bay, Korea from February 2011 to October 2013.

Component	average	min	max
T	16.5	1.5	28.4
S	21.6	3.4	29.2
NH_4	12.9	0.4	80.5
NO_3	22.7	0	133.9
PO_4	0.3	0	1.4
SiO_3	20	0.8	67.7

T: temperature (℃), P: precipitation (mm), S: salinity, inorganic nutrients (μM).

Table 2.5. Results of correlations using linear regression between salinity and sum of precipitation (PS) in Shiwha Bay, Korea from February 2011 to October 2013. Gradients (a), Constants (b), and coefficient of determination (R^2) from equations.

PS	P value	R^2	a	b
2 days	p>0.05	0.01	−0.06	21.79
3 days	p>0.05	0.01	−0.05	21.87
5 days	p>0.05	0.12	−0.11	23.11
7 days	p<0.05	0.22	−0.09	23.79
10 days	p<0.001	0.53	−0.09	25.12
14 days	p<0.001	0.55	−0.06	25.33
20 days	p<0.001	0.63	−0.04	25.87

Table 2.6. Results of each year correlations between salinity and precipitation sums in Shiwha Bay, Korea from January 2009 to December 2011. Linear regression, ANOVA.

	Precipitation sum							
	2d	3d	5d	7d	10d	14d	20d	n
2009	$p>0.05$	$p>0.05$	$p>0.05$	$p>0.05$	$p>0.05$	$p<0.001$	$p<0.001$	11
2010	$p>0.05$	$p>0.05$	$p>0.05$	$p>0.05$	$p<0.001$	$p<0.05$	$p<0.05$	10
2011	$p>0.05$	$p>0.05$	$p>0.05$	$p<0.05$	$p<0.001$	$p<0.001$	$p<0.001$	9

Correlations between salinity and nutrients in Shiwha Bay. From 2009 to 2011, salinity showed significant negative correlations with nitrate plus nitrite (NO_3^-) and silicate (SiO_3^{2-}) ($p<0.001$, linear regression, ANOVA; Fig. 2.11, 2.12). However, salinity did not show any correlations with phosphates (PO_4^-) ($p>0.05$).

However, in each year separate analysis salinity showed significant negative correlations with nitrate plus nitrite (NO_3^-) only in 2011 ($p<0.001$, linear regression, ANOVA) and did not show any correlations in 2009 and 2010 ($p>0.05$) (Fig. 2.13).

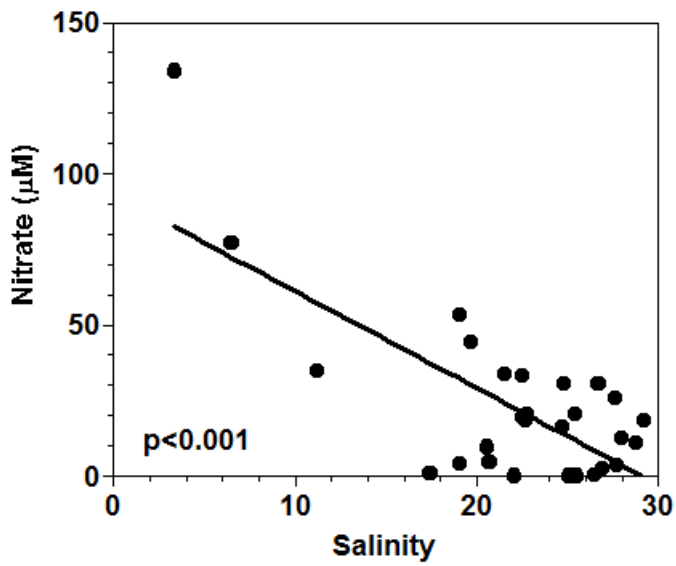

Fig. 2.11. Correlations between salinity of coastal surface waters and nitrate plus nitrite (NO_3^-) in Shiwha Bay from 2009 to 2011.

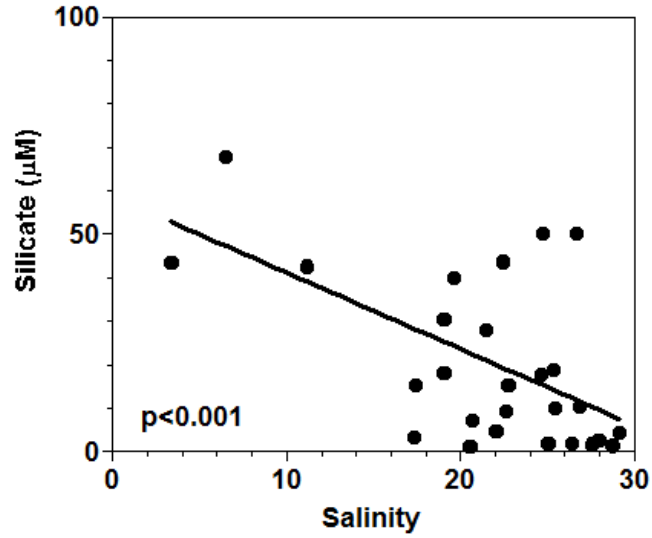

Fig. 2.12. Correlations between salinity of coastal surface waters and silicate (SiO_3^{2-}) in Shiwha Bay from 2009 to 2011.

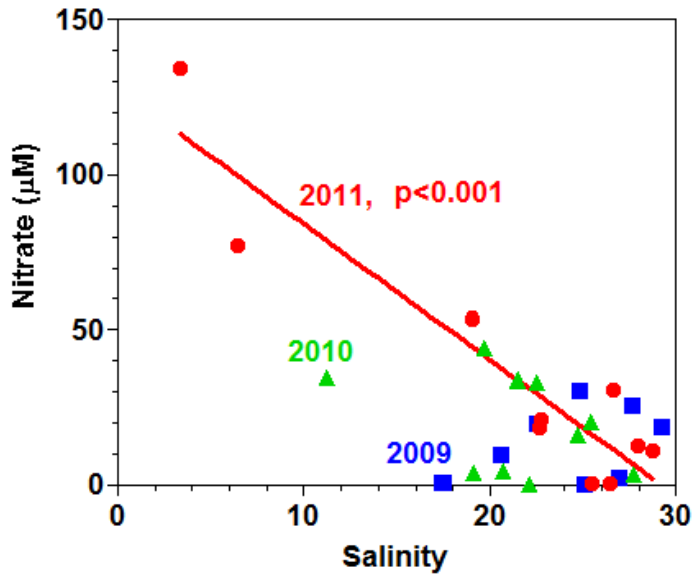

Fig. 2.13. Correlations between salinity of coastal surface waters and nitrate plus nitrite (NO_3^-) in Shiwha Bay from 2009 to 2011.

Dominant phytoplankton. From January 2009 to December 2011, the biomass of total phytoplankton was highest in May 2009, July 2010, and August 2011 (7,330–10,730 ng C ml^{-1}). The most dominant phytoplankton groups in Shiwha Bay in this study were diatoms, dinoflagellates, and crytophytes.

The dominant phytoplankton group when the highest biomass was reached in 2009 and 2010 was dinoflagelallates (10,710 ng C ml^{-1} and 3600 ng C ml^{-1}, respectively), while the dominant phytoplankton group when the highest biomass was reached in 2011 was diatom (7,330 ng C ml^{-1}) (Fig. 2.14).

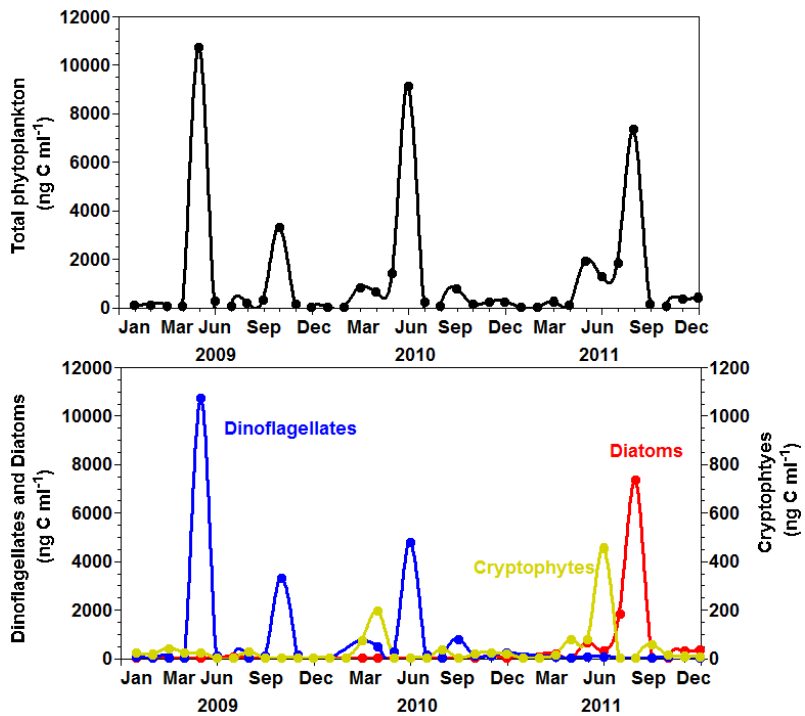

Fig. 2.14. The biomass of total phytoplankton, dinoflagellates, cryptophytes, and diatoms in Shiwha Bay from January 2009 to December 2011.

2.5. Discussion

2.5.1. Correlation between precipitation and salinity in two Korean coastal waters

In Gwangyang Bay, salinity during 2011 to 2013 showed significant negative correlation with 7–20 day accumulated precipitations. The waters from 5th largest Seomjin River directly flow into Gwangyang Bay and greatly contribute nitrogen input from precipitations (Baek et al., 2015; Kim et al., 2015). Similarly in Shiwha bay, salinity during 2009 to 2011 showed significant negative correlation with 7–20 day accumulated precipitations. The waters from 10 streams containing anthropogenic outputs of three major cities (i.e., Shiheong, Hwasung, and Ansan city) flow into Shiwha Bay inner parts (Kim et al., 2002). Therefore, both two coastal regions are highly affected by anthropogenic sources from land, and the generally more than 7 days of accumulated precipitation is expected to have an impact on salinity level in both Gwangyang Bay and Shiwha Bay.

2.5.2. Response by dominant phytoplankton group to precipitation, salinity, and nitrate concentrations

Strong relationships between salinity and nitrate concentration is also observed in other studies (Wong et al., 1998; Herbeck et al., 2011). In addition, nitrate concentration level can select dominant phytoplankton groups due to difference of their own physiological

response time (Smayda, 1997; Smayda and Reynolds, 2001; Jeong et al., 2015). The fast growing diatoms or small autotrophic flagellates have benefit to dominate high nutrient containing waters because they spend most of their energy only to grow, while slow growing mixotrophic dinoflagellates dominate low nutrient containing waters by acquiring energy from both ingesting other protists and photosynthesis (Burkholder et al., 2008; Jeong et al., 2015; Nielsen & Kiørboe, 2015). In addition, the salinity tolerance of diatoms are greater than dinoflagellates, thus diatoms may have more benefits when waters are diluted from fresh waters (Lim and Ogata, 2005; Balzano et al., 2010). In Gwangyang Bay, diatom (i.e., *Skeletonema* spp.) is general dominant phytoplankton group due to high nitrate concentrations (Baek et al., 2015). However, in July 2013 the dinoflagellates, *Ceratium* spp., outcompete in high salinity (30.8–31.8) and lower nitrate concentration (0.9–4.8 μM) conditions cause by lower 14 days precipitation sum (<1mm) (Fig. 2.3, 2.7). In Shiwha Bay, diverse dinoflagellates, small flagellates, and diatoms are known to dominate waters dynamically diatom (Lee, 2012; Kang et al., 2013). Dinoflagellates outcompeted in 2009 and 2010 when salinity did not correlated with nitrate concentrations, while the small flagelaltes, cryptophytes, and diatom were dominated 2011 when the salinity was significantly correlated with nitrate concentrations and the maximum 7 days precipitation sum was more than two times of maximum precipitations in 2009 and 2010 (Fig. 2.13, 2.14). Precipitation have great influence on phytoplankton community and composition because it is original drivers of nutrient deliver, retention time, dilution, declining salinity, and etc (Kim et al., 2014, 2015; Thompson et al., 2015a, b; Weisse et al., 2016). In addition,

the precipitation pattern was affected by spatial and seasonal variations and it becomes hard to predict due to climate change (Thompson et al., 2015a). In Gwangyang Bay, each year precipitation sum was consistent patters and summer dominant phytoplankton was exactly followed the trends. Thus, in Kwangyang Bay, precipitation may concentration in summer and summer precipitations may decide one year precipitation patterns. However, in Shiwha Bay, each year precipitation sum was inconsistent patterns and dominant phytoplankton was not exactly followed the trends. There have been reported diverse red tides in Shiwha Bay (Kang et al., 2013) since dike has established. In addition, diverse artificial construction has been occurred for long time there such as establishing dike, opening water gates to improve water quality, and establishing and operating tidal power plants (Kang et al., 2013). Therefore, the enclosed Shiwha bay may be affected not only meteorological effects but other artificial interactions. From this study results, dominant phytoplankton groups in two Korean coastal regions also have affected directly and indirectly by precipitation. Moreover metrological relationships and marine environments may have different from each coastal area. Therefore, prediction models for marine ecosystem to prepare future climate change must consider coastal structures and functions of past and present status in each specific area.

2.5.3. Implications for future climate change

Future climate change will shift the frequency and intensity of precipitation and regional variations of precipitation also will be changed (Reichwaldt and Ghaduani, 2012). However, shifts of frequency and intensity of precipitations have influenced on dominant phytoplankton and their ecology (Mallin et al., 1993; Phlips et al., 2007; Thompson et al., 2015a). And dominant animal predators consuming plankton is decided by their favor phytoplankton species (Cloern et al., 1983). Therefore, investigating response by dominant phytoplankton communities to temporal and spatial precipitation should be conducted in other coastal regions to establish and develop accurate models for future climate change.

Chapter 3.

Elevating growth rate strategy of the newly described mixotrophic dinoflagellate *Gymnodinium smaydae* by acquiring nutrients from feeding

3.1. Abstract

To investigate feeding by the newly described mixotrophic dinoflagellate *Gymnodinium smaydae*, I explored the feeding mechanism and the kinds of prey species that *G. smaydae* is able to feed on. In addition, I measured the growth and ingestion rates of *G. smaydae* on optimal and suboptimal algal prey *Heterocapsa rotundata* and *Heterocapsa triquetra* as a function of prey concentration. Among the 19 algal prey species offered, *G. smaydae* ingested only thecate dinoflagellates *Heterocapsa rotundata, Heterocapsa triquetra*, *Heterocapsa* sp., and *Scrippsiella trochoidea*. Among the peduncle-feeding dinoflagellates so far reported, *G. smaydae* is the only grazer that is able to feed on *S. trochoidea* and one of the two species that are able to feed on *H. triquetra*. However, *G. smaydae* did not feed on the raphidophyte *Heterosigma akashiwo,* the cryptophytes *Teleaulax* sp. and *Rhodomonas salina*, and the small dinoflagellate *Amphidinium carterae* which all the other peduncle-feeding dinoflagellates except *Stoeckeria algicida* are able to feed on. *G. smaydae* fed on algal prey using a peduncle after anchoring the prey by a tow filament. All *Heterocapsa* species supported high positive

growth of *G. smaydae, S. trochoidea* only helped in merely maintaining the predator population. With increasing mean prey concentration, the growth and ingestion rates for *G. smaydae* on *H. rotundata* increased rapidly, but became saturated at concentrations of 455 ng C ml^{-1} (3500 cells ml^{-1}), while that on *H. triquetra* increased rapidly, but slowly at concentrations of 293 ng C ml^{-1} (945 cells ml^{-1}). The maximum specific growth rates (i.e., mixotrophic growth) of *G. smaydae* on *H. rotundata* and *H. triquetra* were 2.226 d^{-1} and 1.053 d^{-1}, respectively, at 20 ℃ under a 14:10 h light−dark cycle of 20 μE m^{-2} s^{-1}, while the growth rates (i.e., phototrophic growth) under the same light conditions without added prey were 0.005 to −0.051 d^{-1}. The maximum ingestion rates of *G. smaydae* on *H. rotundata* and *H. triquetra* were 1.59 ng C $grazer^{-1}d^{-1}$ (12.3 cells $grazer^{-1}d^{-1}$) and 0.24 ng C $grazer^{-1}d^{-1}$ (0.8 cells $grazer^{-1}d^{-1}$), respectively. The calculated grazing coefficients for *G. smaydae* on co−occurring *H. rotundata* or *H. triquetra* were up to 0.23 h^{-1} or 0.02 h^{-1}, respectively (i.e., 21% or 2% of the population of *H. rotundata* or *H. triquetra* was removed by *G. smaydae* populations in 1 h). The results of the present study suggest that *G. smaydae* can sometimes have a considerable grazing impact on the population of *H. rotundata*.

3.2. Introduction

Phototrophic dinoflagellates are one of the major components in marine planktonic communities (Jeong et al., 2013; Park et al., 2013; Smayda, 1997). They live in diverse habitats, such as in the water column, on the surface of macroalgae, and inside sediments and organisms (Jeong et al., 2012, 2013b; Kang et al., 2013; Lee et al., 2013). In the last 2 decades, several phototrophic dinoflagellates have been revealed to be mixotrophic (Burkholder et al., 2008; Jeong et al., 2005b, 2010b, 2012; Kang et al., 2011; Stoecker, 1999; Turner, 2006). These mixotrophic dinoflagellates are known to feed on diverse prey, such as heterotrophic bacteria, cyanobacteria, small flagellates, other mixotrophic dinoflagellates, and ciliates (Berge et al., 2008; Glibert et al., 2009; Jeong et al., 1999, 2005a, 2005b, 2005c,2010a, 2012; Kang et al., 2011; Li et al., 2000; Park et al., 2006; Seong et al., 2006; Stoecker et al., 1997; Yoo et al., 2009). However, the number of phototrophic dinoflagellates of known mixotrophy is only ca. 50 species among ca. 1200 reported phototrophic dinoflagellates (i.e., 4–5%) (Gomez, 2012; Jeong et al., 2010b). Furthermore, the phototrophic dinoflagellates whose growth and ingestion rates have been quantified are less than 30 species. Therefore, to understand the eco–physiology of phototrophic dinoflagellates and their roles in planktonic food webs of the ecosystem, the kind of prey that a certain phototrophic dinoflagellate is able to feed on, optimal prey species, growth and ingestion rates, and grazing impact should be fully understood.

Recently, I found a new mixotrophic dinoflagellate *Gymnodinium*

smaydae in Shiwha Bay, Korea (Kang et al., 2014). This dinoflagellate possesses nuclear chambers, a nuclear fibrous connective, an apical groove running in a counterclockwise direction around the apex, and peridinin as major accessory pigment, which are 4 key features for the genus *Gymnodinium*. This dinoflagellate (6–11 μm long and 5–10 μm wide) is smaller than any other *Gymnodinium* species so far reported, with the exception of *Gymnodinium nanum*. Cells are covered with polygonal amphiesmal vesicles arranged in 11 horizontal rows (Kang et al., 2014). This dinoflagellate has a sharp and elongated ventral ridge reaching halfway down the hypocone, which is unlike other *Gymnodinium* species. The new species possesses a peduncle, permanent chloroplasts, pyrenoids, and trichocysts, which suggest that it is a mixotrophic dinoflagellate.

I established a clonal culture of *Gymnodinium smaydae* and observed its feeding behavior under high-resolution video-microscopy in order to explore the feeding mechanisms and determine the prey species when diverse algal species were provided. I also conducted experiments to determine the effects of prey concentration on the growth and ingestion rates of *G. smaydae* on the optimal and suboptimal algal prey species *Heterocapsa rotundata* and *Heterocapsa triquetra*, respectively, as a function of prey concentration. In addition, I estimated the grazing coefficients attributable to *G. smaydae* on *H. rotundata* and *H. triquetra* using the ingestion rate data obtained from the laboratory experiments and the abundances of predators and prey in the field. The abundance of *G. smaydae* was quantified using real-time polymerase chain reaction (PCR). The results of the present study provide a basis for

understanding the feeding mechanisms and ecological roles of *G. smaydae* in marine planktonic food webs.

3.3. Materials and Methods

3.3.1. Preparation of experimental organisms

The mixotrophic dinoflagellates *Cochlodinium polykrikoides* and *Lingulodinium polyedrum* were grown at 20 °C in enriched f/2 seawater media (Guillard and Ryther, 1962) under a continuous illumination of 50 μE $m^{-2}s^{-1}$ of cool white fluorescent light, while the other phytoplankton species were grown under an illumination of 20 μE $m^{-2}s^{-1}$ of cool white fluorescent light on a 14:10 h light–dark cycle (Table 3.1). *C. polykrikoides* and *L. polyedrum* did not grow well under an illumination on a light–dark cycle. The mean equivalent spherical diameter (ESD) ± standard deviation was measured by an electronic particle counter (Coulter Multisizer II, Coulter Corporation, Miami, Florida, USA). The size of the phototrophic dinoflagellate *Heterocapsa rotundata* strain used in the present study (HRSH1201; ESD=9.5 μm) was bigger than that of the *H. rotundata* strain previously used in our papers (ESD=5.8 μm; Jeong et al., 2006, 2007, 2010a, 2011b, 2012; Kang et al., 2011; Yoo et al., 2010b).

Plankton samples were collected with a water sampler from Shiwha Bay, Korea (37° 18' N, 126° 36' E), during May 2010, when the water temperature and salinity were 19 °C and 27.7, respectively (Kang et al., 2014). The samples were filtered gently through a 154–μm Nitex mesh and placed in 6–well tissue culture plates. A clonal

culture of *Gymnodinium smaydae* was established following two serial single-cell isolations. *Heterocapsa rotundata* was provided as prey for *G. smaydae* at concentrations of ca. 60,000-100,000 cells ml^{-1}. When the concentration of *G. smaydae* increased, cells were transferred to 32-, 270-, and 500-ml polycarbonate (PC) bottles containing fresh cultures of *H. rotundata*. The bottles were filled to capacity with filtered seawater, capped, and placed on a rotating wheel at 0.9 rpm at 20°C under an illumination of 20 μE m^{-2} s^{-1} cool-white fluorescent light in a 14:10 h light-dark cycle. Once dense cultures of *G. smaydae* were obtained, they were transferred daily to 500-ml PC bottles of fresh cultures of *H. rotundata* containing ca. 100,000 cells ml^{-1}.

The carbon contents of *Heterocapsa rotundata* (0.13 ng C per cell), *Heterocapsa* sp. CCMP 3244 (0.10), *Heterocapsa triquetra* (0.31), and *Scrippsiella trochoidea* (0.7) were measured using a CHN Analyzer (vario MICRO, Elementar, Germany) and those of the other phytoplankton species were obtained from our previous studies (Jeong et al., 2010a, 2011b, 2012; Kang et al., 2011; Yoo et al., 2010b).

3.3.2. Prey species

Experiment 1 was designed to investigate whether or not *Gymnodinium smaydae* was able to feed on each target algal species when unialgal diets of diverse algal species were provided (Table 3.1). The initial concentrations of each algal species offered were similar, in terms of carbon biomass. To confirm no ingestion by *G. smaydae* on some algal species, additional higher prey concentrations

were provided.

A dense culture (ca. 10,000 cells ml^{-1}) of *Gymnodinium smaydae* growing mixotrophically on *Heterocapsa rotundata* in f/2 media and under 14:10 h light−dark cycle of cool white fluorescent light at 20 μE $m^{-2}s^{-1}$ was transferred to one 1−L PC bottle containing f/2 medium when *H. rotundata* was undetectable. This culture was maintained in f/2 media for 2 d under 14:10 h light−dark cycle at 20 μE $m^{-2}s^{-1}$. Three 1−ml aliquots were then removed from the bottle and examined using a compound microscope to determine the *G. smaydae* concentration.

In this experiment, the initial concentrations of *Gymnodinium smaydae* and each target algal species were established by using an autopipette to deliver a predetermined volume of culture with a known cell density to the experimental bottles. Triplicate 80−ml PC bottles with mixtures of *G. smaydae* and the target prey and duplicate predator control bottles containing *G. smaydae* only were set up for each target algal species. The bottles were filled to capacity with freshly filtered seawater, capped, and then placed on a vertically rotating plate rotating at 0.9 rpm and incubated at 20 °C under a 14:10 h light−dark cycle of cool white fluorescent light at 20 μE $m^{-2}s^{-1}$. After 6, 12, 24, and 48 h, a 5−ml aliquot was removed from each bottle and transferred into a 20−ml bottle. Two 0.1 ml aliquots were placed on slides and then cover−glasses were added. Under these conditions, the *G. smaydae* cells were alive, but almost motionless. The protoplasms of >200 *G. smaydae* cells were carefully examined with a compound microscope and/or an epifluorescence microscope (Zeiss−Axiovert 200M, Carl Zeiss Ltd., Göttingen, Germany) at a magnification of 100−630 X to determine whether or not *G. smaydae*

was able to feed on the target prey species. Pictures showing the ingested cells of each target algal species inside a *G. smaydae* cell were taken using digital cameras on these microscopes at a magnification of 630−1000X.

3.3.3. Feeding mechanisms

Experiment 2 was designed to investigate the feeding behaviors of *Gymnodinium smaydae* when a unialgal diet of *Heterocapsa rotundata*, *H. triquetra*, and *Scrippsiella trochoidea* was provided as prey. Feeding by *G. smaydae* on these prey species had been observed in Experiment 1. The initial concentrations of predators and prey were the same as above.

The initial concentrations of *Gymnodinium smaydae* and the target algal species were established using an autopipette to deliver a predetermined volume of culture with a known cell density to the experimental bottles. One 80−ml PC bottle with a mixture of *G. smaydae* and the algal prey was set up for each target algal species. The bottle was filled to capacity with freshly filtered seawater, capped, and then well mixed. After 1−min incubation, a 1−ml aliquot was removed from the bottle and transferred into a 1−ml Sedgewick−Rafter Chamber (SRCs). By monitoring the behavior of > 60 unfed *G. smaydae* cells for each target prey species under a compound microscope and/or an epifluorescence microscope at a magnification of 100−630 X, all of the feeding processes were observed, from the time a prey cell was captured to the time that it was fed on by the predator with a peduncle. A series of pictures showing the feeding process for a *G. smaydae* cell was taken using a

video analyzing system (Sony DXC-C33, Sony Co., Tokyo, Japan) mounted on an epifluorescence microscope at a magnification of 200-630 X. After *Heterocapsa rotundata* was provided to *G. smaydae* as prey, the time lag (n = 5 for prey) between the deployment of tow filament and peduncle of *G. smaydae* and the time (n = 5 for prey) for a prey cell to be completely ingested by a *G. smaydae* cell after the predator had deployed its peduncle to the prey cell were measured.

3.3.4. Growth and ingestion rates

Experiment 3-5 was designed to investigate the growth and ingestion rates of *Gymnodinium smaydae*. I measured the growth, ingestion, and clearance rates of *G. smaydae* on unialgal diet of the optimal prey *Heterocapsa rotundata* and the suboptimal prey *Heterocapsa triquetra* as a function of prey concentration. In addition, I measured the growth and ingestion rates of *G. smaydae* when feeding on the dinoflagellate *Scrippsiella trochoidea* at single prey concentration where the growth and ingestion rates of *G. smaydae* on *H. rotundata* were saturated.

A dense culture (ca. 10,000 cells ml^{-1}) of *Gymnodinium smaydae* growing mixotrophically on *Heterocapsa rotundata* under a 14:10 h light-dark cycle of 20 μE m^{-2} s^{-1} in f/2 medium was transferred into a 1-L PC bottle containing freshly-filtered seawater. When the prey was undetectable, the culture was transferred into two 1-L PC bottles; one of these bottles had a low prey concentration of *H. rotundata* (ca. 50 cells ml^{-1} for 5 lower prey concentrations), and the other had a medium prey concentration (ca. 6000 cells ml^{-1}

for 4 medium and higher prey concentrations); After approximately 2-day incubation, when the prey was undetectable, the cultures were transferred into 1-L PC bottles. Three 1-ml aliquots from each of these two bottles were counted using a compound microscope to determine the cell concentrations of *G. smaydae* in each bottle, and the cultures were then used to conduct experiments. For the *Heterocapsa triquetra* prey, the procedure was similar to that of *H. rotundata* prey except that one of these bottles had a low prey concentration of *H. triquetra* (ca. 10 cells ml^{-1} for 4 lower prey concentrations), and the other had a medium prey concentration (ca. 500 cells ml^{-1} for 4 medium and higher prey concentrations).

The initial concentrations of *Gymnodinium smaydae* and *Heterocapsa rotundata* (or *Heterocapsa triquetra*) were established as described above. Triplicate 42-ml PC experimental bottles containing mixtures of predators and prey, triplicate prey control bottles containing prey only, and triplicate predator control bottles containing predators only were set up for each predator-prey combination. To make the water conditions similar, the same procedure was used as in Experiment 1. Five ml of f/2 medium were added to all bottles, which were then filled to capacity with freshly filtered seawater and capped. To determine the actual initial predator and prey densities (cells ml^{-1}) at the beginning of the experiment (*G. smaydae* and *H. rotundata* = 3/78, 4/171, 7/597, 7/2120, 13/7180, 31/9580, 41/17,870, 109/34,700, 252/66,720; *G. smaydae* and *H. triquetra* = 7/22, 11/54, 15/109, 21/215, 36/635, 64/1350, 129/2730, 200/5000) and after 2 d incubation, 5-ml aliquots were removed from each bottle and fixed with 5% Lugol's solution, and all *G. smaydae* cells and all or >300 prey cells in three 1-ml SRCs were

enumerated. Prior to taking the subsamples, the condition of *G. smaydae* and its prey was assessed under a dissecting microscope. The bottles were filled again to capacity with f/2 medium, capped, placed on a vertically rotating plate rotating at 0.9 rpm, and incubated at 20 °C under a 14:10 h light–dark cycle of 20 μE m^{-2} s^{-1} of cool white fluorescent light. The dilution of the cultures associated with refilling the bottles was considered in calculating the growth and ingestion rates.

The specific growth rate of *Gymnodinium smaydae* , μ (d^{-1}), was calculated as follows:

$$\mu = \frac{\mathrm{Ln}\,(P_t / P_0)}{t} \qquad (1)$$

where P_O is the initial concentration of *Gymnodinium smaydae* and P_t is the final concentration after time t. The time period was 2 d.

Data for *Gymnodinium smaydae* growth rate were fitted to the following equation:

$$\mu = \frac{\mu_{max}\ (x - x')}{K_{GR} + (x - x')} \qquad (2)$$

where μ_{max} = the maximum growth rate (d^{-1}); x = prey concentration (cells ml^{-1} or ng C ml^{-1}), x' = threshold prey concentration (the prey concentration where μ = 0), and K_{GR} = the prey concentration sustaining ½ μ_{max}. Data were iteratively fitted to the model using DeltaGraph® (SPSS Inc., Chicago, IL, USA).

Ingestion and clearance rates for 2 d were also calculated using the equations of Frost (1972) and Heinbokel (1978). The incubation

times for calculating the ingestion and clearance rates were the same as for estimating the growth rate.

Ingestion rate data were fitted to a Michaelis-Menten equation:

$$IR = \frac{I_{max}(x)}{K_{IR} + (x)} \quad (3)$$

where I_{max} = the maximum ingestion rate (cells predator^{-1}d^{-1} or ng C predator^{-1}d^{-1}); x = prey concentration (cells ml^{-1} or ng C ml^{-1}), and K_{IR} = the prey concentration sustaining ½ I_{max}.

Additionally, the growth and ingestion rates of *Gymnodinium smaydae* on *Hetereocapsa* sp. CCMP 3244 and *Scirppsiella trochoidea* prey at a single prey concentration at which both growth and ingestion rates of *G. smaydae* on *Heterocapsa rotundata* were saturated were measured as described above.

3.3.5. Cell volume of *G. smaydae*

After the 2-day incubation, the cell length and maximum width of *Gymnodinium smaydae* preserved in 5% acid Lugol' s solution (n=10-30 for each prey concentration) were measured using an image analysis system on images collected with a epifluorescence microscope (AxioVision 4.5, Carl Zeiss Ltd., Göttingen, Germany). The shape of *G. smaydae* was estimated to be an oval. The cell volume of the preserved *G. smaydae* was calculated according to the following equation: volume = 4/3 π [(cell length + cell width)/4]^3. The carbon content of *G. smaydae* was also estimated from cell volume according to Menden-Deuer and Lessard (2000).

3.3.6. Swimming speed

A dense culture (ca. 10,000 cells ml^{-1}) of *Gymnodinium smaydae* growing mixotrophically on *Heterocapsa rotundata* under a 14:10 h light-dark cycle of 20 μE m^{-2} s^{-1} in f/2 medium were transferred into 500-ml PC bottle. When prey was undetectable, *G. smaydae* cells were starved for 36 h. An aliquot from the bottle was added to a 50-ml cell culture flask and allowed to acclimate for 30 min. The video camera focused on one field seen as one circle in a cell culture flask under a dissecting microscope at 20 °C and swimming of *G. smaydae* cells was then recorded at a magnification of 40 X using a video analyzing system (Samsung, SV-C660, Seoul, Korea) and taken using a CCD camera (Hitachi, KP-D20BU, Tokyo, Japan). The mean and maximum swimming velocities were analyzed for all swimming cells seen for the first 10 min. The average swimming speed was calculated based on the linear displacement of cells in 1 sec. during single-frame playback. The swimming speeds of 30 cells were measured.

3.3.7. Measurement of photosynthetic rate

In Experiment 6, the photosynthetic rate of *Gymnodinium smaydae* was measured using the C^{14} method. For comparison, photosynthetic rates of the mixotrophic dinoflagellate preys *Heterocapsa rotundata* and *Heterocapsa* sp. CCMP 3244 were also measured using the same method.

A dense culture (ca. 20,000 cells ml^{-1}) of *Gymnodinium*

smaydae growing mixotrophically on *Heterocapsa rotundata* and *Heterocapsa* sp. CCMP 3244 respectively, under a 14:10 h light–dark cycle of 20 μE m^{-2} s^{-1} in f/2 medium was transferred into a 500–ml PC bottle. In addition, dense cultures of *H. rotundata* (ca. 200,000 cells ml^{-1}) and *Heterocapsa* sp. CCMP 3244 (ca. 160,000 cells ml^{-1}) growing photosynthetically under an illumination of 20 μE $m^{-2}s^{-1}$ of cool white fluorescent light on a 14:10 h light–dark cycle were transferred into 500–ml PC bottles.

The target concentration of each species was established by using an autopipette to deliver a predetermined volume of culture with a known cell density to 250–ml culture flasks. The final concentrations were 1,000 cells ml^{-1} for *Gymnodinium smaydae* and 20,000 cells ml^{-1} for *Heterocapsa* spp.. Triplicate 250–ml culture flasks were set up for each target species. Five tenth μCi of $NaH^{14}CO_3$ were added to each flask and then the flasks were incubated for 2 h under the same conditions as those used to maintain each species (Mateo et al., 2001). After incubation, all contents in the flask were filtered through glass membrane filters (GF/F, Whatman). The filter paper was placed to 20–ml HDPE Scintillation vial (Kartell, Noviglio, Italy) and 1ml of 0.5N HCl was added for acid fuming under dark conditions for 1 day. UltimaGold™ (PerkinElmer, USA) scintillation cocktail (10 mL) was added to the filters before analysis of the radioactivity. The radioactivity of the synthesized particulate carbon was measured using a liquid scintillation counter (Tri–Carb 2100 TR, Packard Instruments Co, Meriden, CT, USA). The photosynthetic rate per cell of each species was calculated using an equation derived by Strickland and Parsons (1972).

For the analysis of chlorophyll-*a* content per mixotrophic dinoflagellate cell, the same cultures were used as for the photosynthesis analysis. Triplicate 50ml aliquots were taken and each aliquot was filtered through glass membrane filters (GF/F, Whatman) and the filter paper was placed in 15-ml conical tubes. The extraction was performed by treating with 90% ethanol and sonication and kept overnight in cold (4° C) and dark conditions. Analyses were conducted using Turner fluorometer 10-AU (Turner Designs, Sunnyvale, CA, USA).

The cell volume of each species was measured with same method as described above in 2.5.

3.3.8. Potential grazing impact

By combining field data on the abundances of the predators and the target prey with the ingestion rates of the predator on the prey obtained in the present study, I estimated the grazing coefficients attributable to *Gymnodinium smaydae* on co-occurring *Heterocapsa* spp.. Data on the abundances of *G. smaydae* and the co-occurring *Heterocapsa* spp. used in this estimate were obtained by analyzing the water samples taken from the waters inside and outside Shiwha Bay, Korea in May 2008 and 2010 using real-time PCR for *G. smaydae* and cell counting for *Heterocapsa* spp. (Kang et al., unpublished observation).

The grazing coefficients (g, h^{-1}) were calculated as:

$$g = CR \times PC \qquad (4)$$

where CR (ml $predator^{-1}h^{-1}$) is the clearance rate of

Gymnodinium smaydae on a target prey at a prey concentration and PC is a predator concentration (cells ml^{-1}). The CR values were calculated as:

$$CR = IR/x \qquad (5)$$

where IR (cells eaten $predator^{-1}h^{-1}$) is the ingestion rate of *Gymnodinium smaydae* on the target prey and x (cells ml^{-1}) is the prey concentration. These CR values were corrected using Q_{10} = 2.8 (Hansen et al., 1997) because the in situ water temperature and the temperature used in the laboratory for this experiment (20 °C) were sometimes different.

3.4. Results

3.4.1. Prey species

Among the algal prey offered, *Gymnodinium smaydae* ingested the medium-sized thecate dinoflagellates *Heterocapsa rotundata, Heterocapsa triquetra*, *Heterocapsa* sp. (CCMP 3244), and *Scrippsiella trochoidea* (Fig. 3.1, 3.2; Table 3.1). However, it did not feed on the diatom *Skeletonema costatum*, cryptophytes (e.g., *Storeatula* sp., *Teleaulax* sp. and *Rhodomonas salina*), the raphidophyte *Heterosigma akashiwo*, the naked dinoflagellates (*Amphidinium carterae*, *Cochlodinium polykrikoides*, *Akashiwo sanguinea*), large thecate dinoflagellates (*Alexandrium tamarense*, *Prorocentrum micans*, and *Lingulodinium polyedrum*), and a small thecate dinoflagellate *Prorocentrum minimum* (Table 3.1). The

prymnesiophyte *Isochrysis galbana* was observed to be eaten by *G. smaydae* once, but it was not confirmed in additional trials.

3.4.2. Feeding mechanisms

Gymnodinium smaydae fed on its prey using a peduncle (Fig. 3-1). It was difficult to detect deployment of a tow filament, which is usually observed in the other peduncle-feeding dinoflagellates, because this process occurred very quickly. Predator cells deployed peduncles on the surface of the prey as soon as the predator cells attacked prey cells. The time (mean $\pm$ standard error, n = 5) for a prey cell to be completely fed on by a *G. smaydae* cell after the predator deployed its peduncle to the prey cell was 321 $\pm$ 27 sec for *Heterocapsa rotundata*. Up to 3 *G. smaydae* cells were observed deploying their peduncles simultaneously on a prey cell.

The other edible prey species tested in the present study were observed to be fed on by a *Gymnodinium smaydae* cell in the same manner as the *Heterocapsa rotundata* prey (data not shown).

Table 3.1. Taxa, sizes, and initial concentrations of prey species (IC, cells ml^{-1}) offered as food to *Gymnodinium smaydae* (GS) in Experiment 1.

Prey species	ESD (±SD)	IC	Feeding by GS	Attack
Diatom				
Skeletonema costatum	5.9 (1.1)	50,000	N	X
Prymnesiophyceae				
Isochrysis galbana	4.8 (0.2)	150,000	Y	O
Cryptophytes				
Teleaulax sp.	5.6 (1.5)	50,000	N	X
Storeatula major	6.0 (1.7)	50,000	N	X
Rhodomonas salina	8.8 (1.5)	50,000	N	X
Raphidophytes				
Heterosigma akashiwo	11.5 (1.9)	30,000	N	X
Chatonella ovata	40.0 (1.6)	2,000	N	X
Mixotrophic dinoflagellates				
Heterocapsa rotundata (T)	5.8 (0.4)	100,000	Y	O
Amphidinium carterae (NT)	9.7 (1.6)	30,000	N	X
Heterocapsa sp. (CCMP3244) (T)	10.5 (2.7)	100,000	Y	O
Prorocentrum minimum (T)	12.1 (2.5)	15,000	N	O
Prorocentrum donghaiense (T)	13.3 (2.0)	15,000	N	X

Prey species	ESD (±SD)	IC	Feeding by GS	Attack
Heterocapsa triquetra (T)	15.0 (4.3)	10,000	Y	O
Scrippsiella trochoidea (T)	22.8 (2.7)	10,000	Y	O
Cochlodinium polykrikoides (NT)	25.9 (2.9)	1,000	N	X
Prorocentrum micans (T)	26.6 (2.8)	3,000	N	O
Akashiwo sanguinea (NT)	30.8 (3.5)	1,000	N	O
Alexandrium tamarense (T)	32.6 (2.7)	1,000	N	X
Lingulodinium polyedrum (T)	38.2 (3.6)	1,000	N	O

ESD, Mean equivalent spherical diameter (μm); SD, Standard deviation; NT, Non-thecate; T, Thecate; Y, *G. smaydae* was observed to feed on a living prey; N, *G. smaydae* was observed not to feed on a living prey; O, *G. smaydae* was observed to attack a living prey; X, *G. smaydae* was observed not to attack a living prey. The abundances of the predator for each target prey were 2000-5000 cells ml^{-1}.

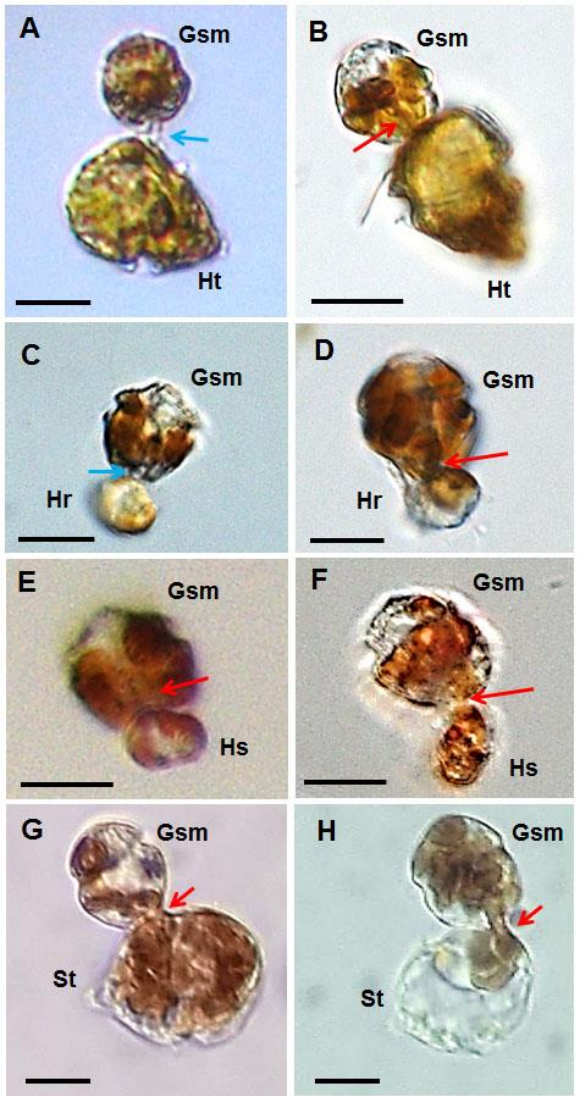

Fig. 3.1. Feeding by the mixotrophic dinoflagellate *Gymnodinium smaydae* on algal prey species. (A–B) *G. smaydae* (Gsm) feeding on *Heterocapsa triquetra* (Ht). (C–D) *G. smaydae* (Gsm) feeding on *Heterocapsa rotundata* (Hr). (E–F) *G. smaydae* (Gsm) feeding on *Heterocapsa* sp. CCMP 3244 (Hs). (G–H) *G. smaydae* (Gsm) feeding on *Scrippsiella trochoidea* (St). The blue arrow indicates the peduncle; the red arrow indicates the prey materials. Scale bars are 10μm.

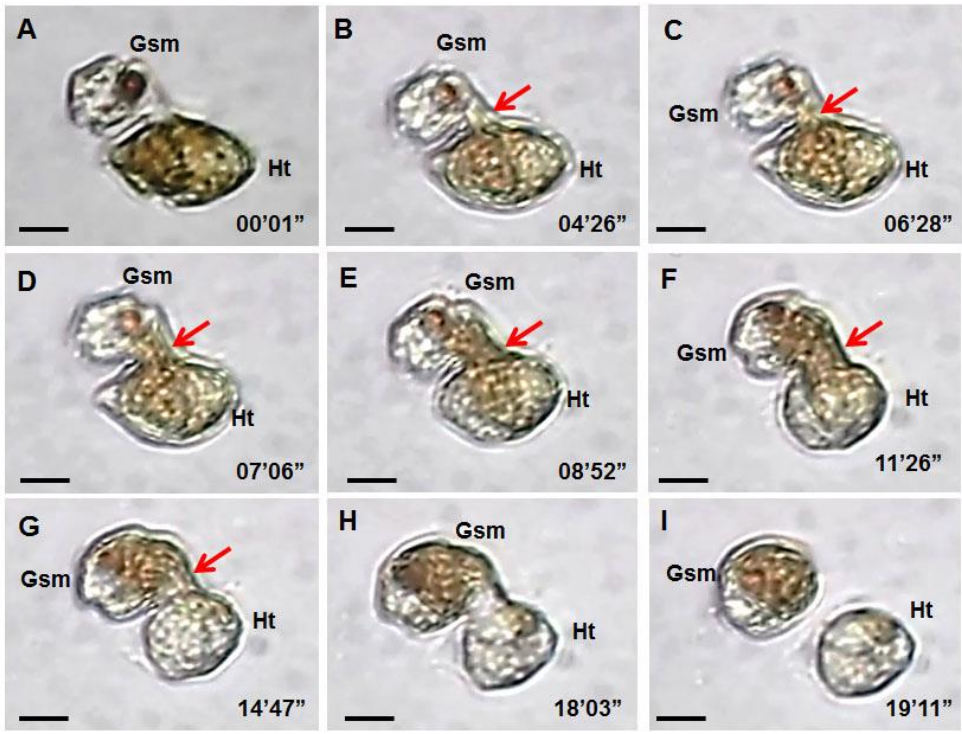

Fig. 3.2. Feeding process (A–I) of *Gymnodinium smaydae* (Gsm) on feeding on *Heterocapsa triquetra* (Ht). The red arrow indicates the prey materials. Scale bars are 10 μm.

3.4.3. Growth and ingestion rates

Heterocapsa rotundata, *Heterocapsa* sp. CCMP 3244, and *Heterocapsa triquetra* supported high positive growth of *G. smaydae*, but *Scrippsiella trochoidea* was only helpful in maintaining predator populations (Table 3.2).

With increasing mean prey concentration, the specific growth rates of *Gymnodinium smaydae* increased rapidly before saturating at a *Heterocapsa rotundata* concentration of 455 ng C ml^{-1} (3500 cells ml^{-1}) (Fig. 3.3A). When the data were fitted to Eq. (2), the maximum specific growth rate (i.e. mixotrophic growth) of *G. smaydae* on *H. rotundata* was 2.226 d^{-1}, at 20 ℃ under a 14:10 h light–dark cycle of 20 μE m^{-2} s^{-1}, while its growth rate (i.e. phototrophic growth) under the same light conditions without added prey was 0.005 d^{-1}. The K_{GR} (i.e. the prey concentration sustaining ½ μ_{max}.) was 119 ng C ml^{-1} (916 cells ml^{-1}).

With increasing mean prey concentration, the specific growth rates of *Gymnodinium smaydae* increased rapidly at a *Heterocapsa triquetra* concentration of 293 ng C ml^{-1} (945 cells ml^{-1}), but slowly at the higher prey concentrations (Fig. 3.3B). When the data were fitted to Eq. (2), the maximum specific growth rate (i.e. mixotrophic growth) of *G. smaydae* on *H. triquetra* was 1.053 d^{-1}, at 20 ℃ under a 14:10 h light–dark cycle of 20 μE m^{-2} s^{-1}, while its growth rate (i.e. phototrophic growth) under the same light conditions without added prey was −0.051 d^{-1}. The K_{GR} was 238 ng C ml^{-1} (768 cells ml^{-1}) and the threshold prey concentration (where net growth = 0) was 11 ng C ml^{-1} (36 cells ml^{-1}).

With increasing mean prey concentration, the ingestion rates of *Gymnodinium smaydae* increased rapidly before saturating at a *Heterocapsa rotundata* concentration of 455 ng C ml^{-1} (3500 cells ml^{-1}) (Fig. 3.4A). When the data were fitted to Eq. (3), the maximum ingestion rate of *G. smaydae* on *H. rotundata* was 1.59 ng C $grazer^{-1}d^{-1}$ (12.3 cells $grazer^{-1}d^{-1}$) and K_{IR} (the prey concentration sustaining ½ I_{max}) was 136.8 ng C ml^{-1} (1052 cells ml^{-1}). The maximum clearance rate of *G. smaydae* on *H. rotundata* was 0.7 μl $grazer^{-1}h^{-1}$.

With increasing mean prey concentration, the ingestion rates of *Gymnodinium smaydae* increased rapidly at a *Heterocapsa triquetra* concentration of 293 ng C ml^{-1} (945 cells ml^{-1}), but slowly at the higher prey concentrations (Fig. 4.4B). When the data were fitted to Eq. (3), the maximum ingestion rate of *G. smaydae* on *H. triquetra* was 0.237 ng C $grazer^{-1}d^{-1}$ (0.8 cells $grazer^{-1}d^{-1}$) and K_{IR} (the prey concentration sustaining ½ I_{max}) was 214.6 ng C ml^{-1} (692 cells ml^{-1}). The maximum clearance rate of *G. smaydae* on *H. triquetra* was 0.36 μl $grazer^{-1}h^{-1}$.

The growth rates of *Gymnodinium smaydae* on 4 thecated dinoflagellates (*Heterocapsa rotundata, Heterocapsa* sp. CCMP 3244, *Heterocapsa triquetra,* and *Scrippsiella trochoidea*) at single prey concentrations of 892–1218 ng C ml^{-1} was significantly correlated with the ESD of prey species ($p < 0.05$, linear regression ANOVA; Fig. 3.5).

Table 3.2. Comparison of the growth (GR, d^{-1}) and ingestion rates (IR, ng C $predator^{-1}$ d^{-1}) of *Gymnodinium smaydae* on 4 edible prey species at single mean prey concentrations (MPC, ng C ml^{-1}). Values are means (± standard errors), n=3.

Prey species	ESD	MPC	GR	IR
Heterocapsa rotundata	9.5	892	2.23 (0.06)	1.4 (0.1)
Heterocapsa sp. (CCMP3244)	10.5	1073	1.76 (0.02)	0.9 (0.1)
Heterocapsa triquetra	15.0	1218	0.85 (0.05)	0.2 (0.0)
Scrippsiella trochoidea	22.8	1091	0.06 (0.04)	2.1 (0.2)
Control (without added prey)		0	0.08 (0.09)	

ESD, equivalent spherical diameter (μm).

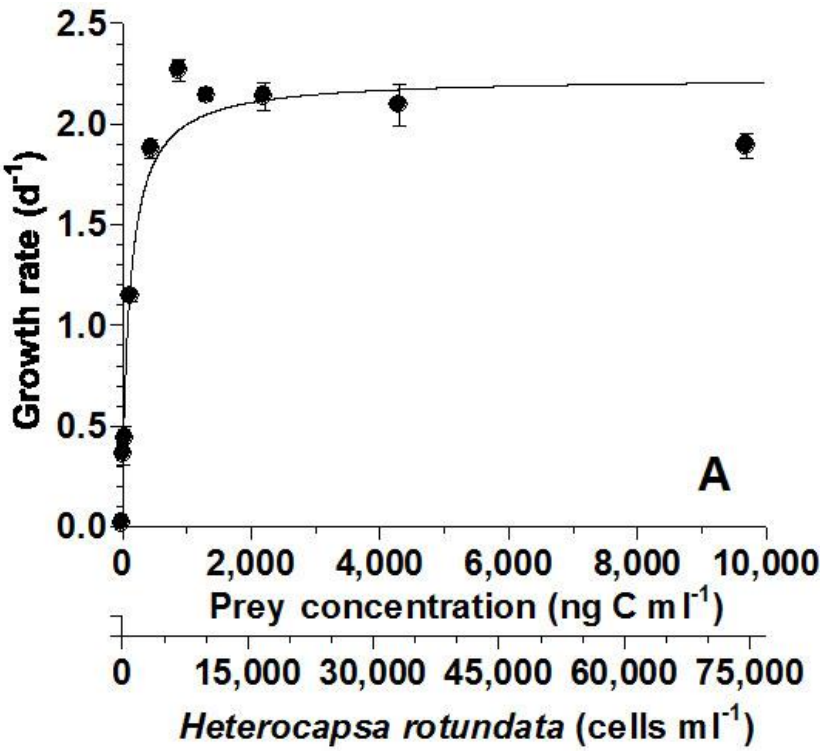

Fig. 3.3A. Specific growth rates of *Gymnodinium smaydae* on *Heterocapsa rotundata* as a function of mean prey concentration (x, ng C ml^{-1}). Symbols represent treatment means $\pm$ 1 SE. The curve is fitted by a Michaelis –Menten equation [Eq. (2)] using all treatmensts in the experiment. Growth rate (GR, d^{-1}) = 2.226 [(x+0.2567)/(118.5+(x+0.2567))], r^2 = 0.968.

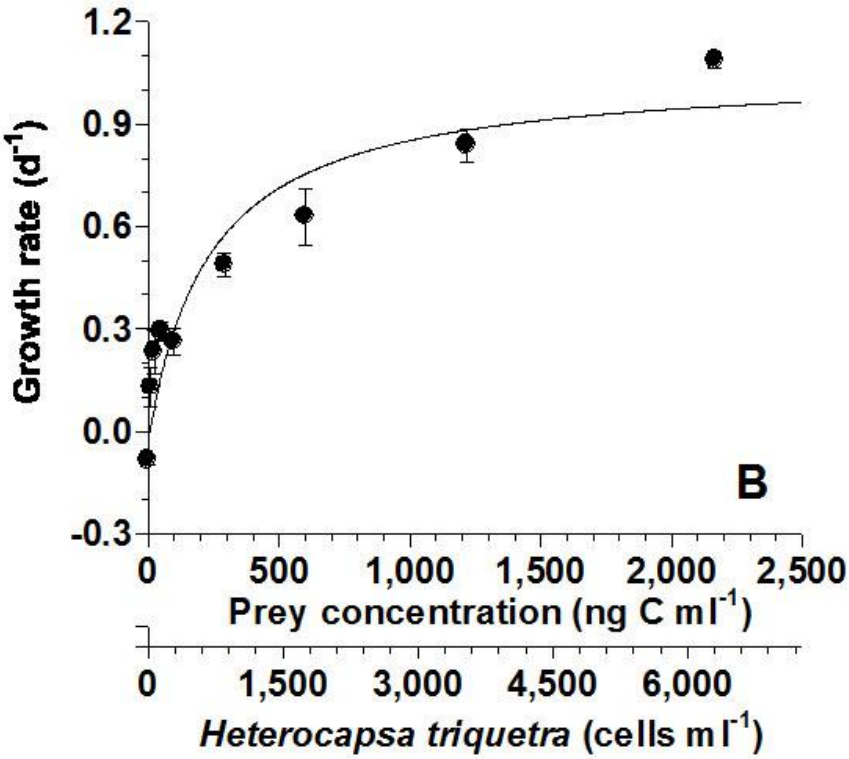

Fig. 3.3B. Specific growth rates of *Gymnodinium smaydae* on *Heterocapsa triquetra* as a function of mean prey concentration (x, ng C ml^{-1}). Symbols represent treatment means $\pm$ 1 SE. The curve is fitted by a Michaelis –Menten equation [Eq. (2)] using all treatmensts in the experiment. Growth rate (GR, d^{-1}) = 1.053 [(x+11.09)/(238.3+(x+11.09))], r^2 = 0.903.

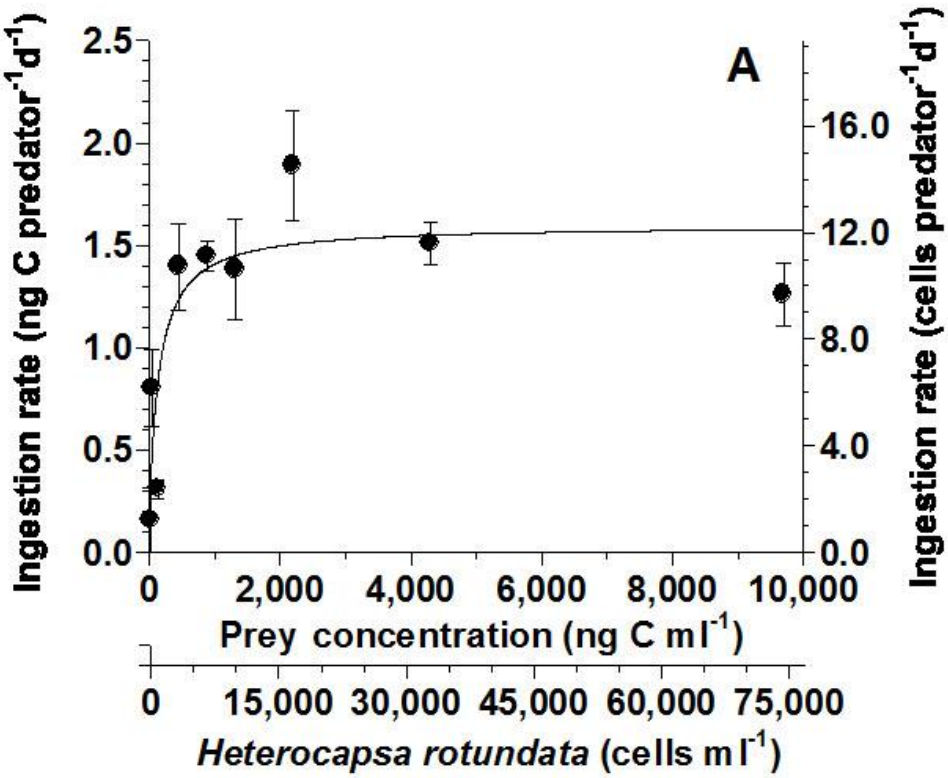

Fig. 3.4A. Ingestion rates of *Gymnodinium smaydae* on *Heterocapsa rotundata* as a function of mean prey concentration (x, ng C ml^{-1}). Symbols represent treatment means $\pm$ 1 SE. The curve is fitted by a Michaelis –Menten equation [Eq. (3)] using all treatmensts in the experiment. Ingestion rate (IR, d^{-1}) = 1.594 [$(x)/(13.68+x)$)], r^2 = 0.616.

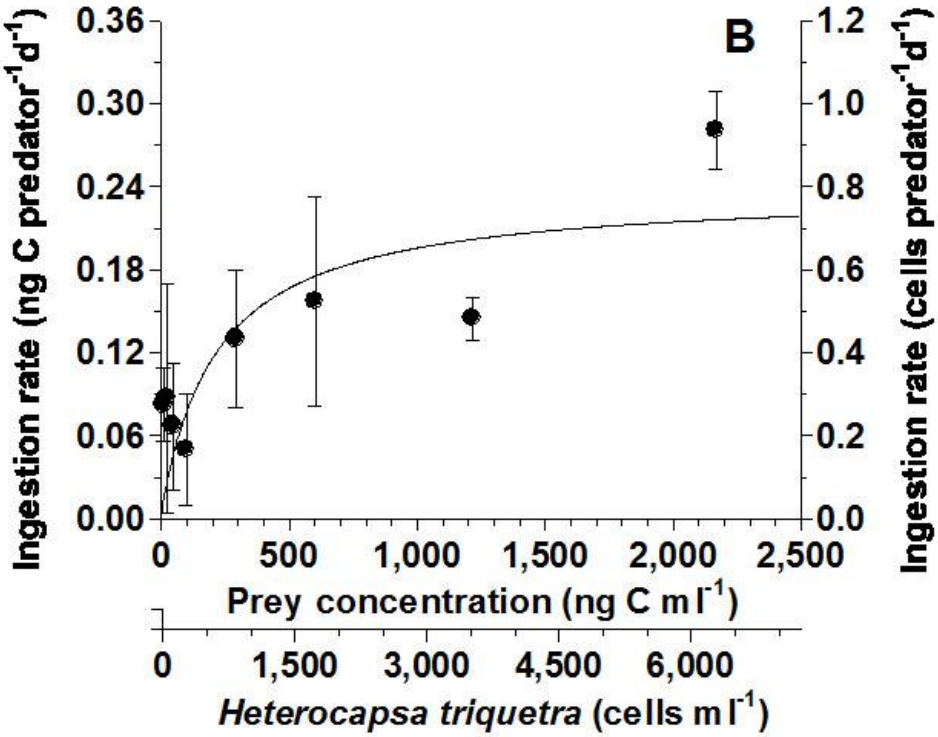

Fig. 3.4B. Ingestion rates of *Gymnodinium smaydae* on *Heterocapsa triquetra* as a function of mean prey concentration (x, ng C ml^{-1}). Symbols represent treatment means $\pm$ 1 SE. The curve is fitted by a Michaelis –Menten equation [Eq. (3)] using all treatmensts in the experiment. Ingestion rate (IR, d^{-1}) = 0.2366 [$(x)/(214.6+x)$)], r^2 = 0.307.

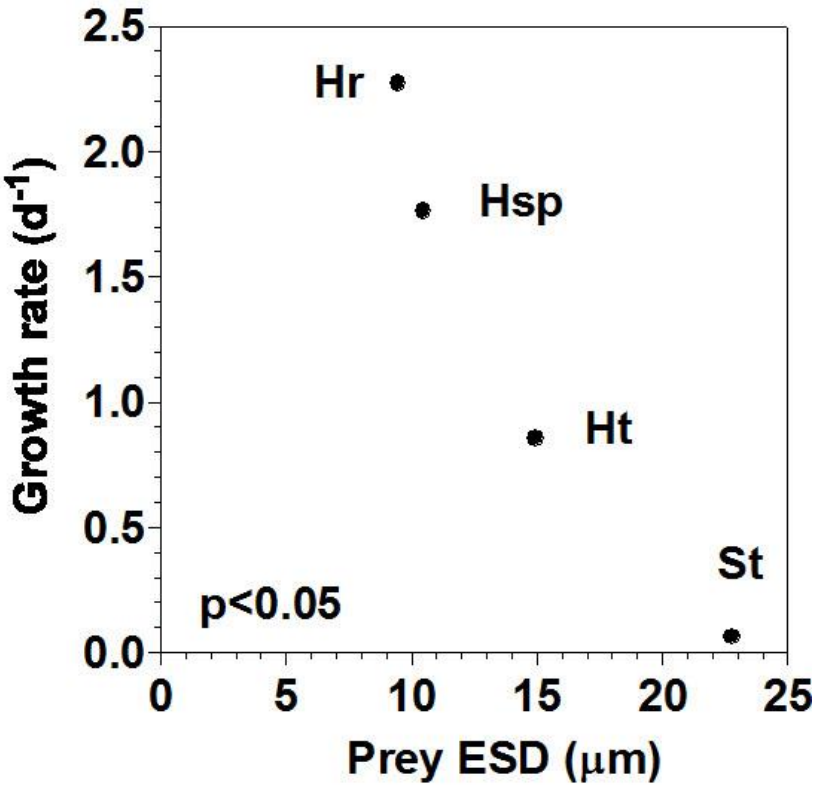

Fig. 3.5. Comparison of the growth rates of *Gymnodinium smaydae* feeding on the mixotrophic algal prey as a function of prey ESD (equivalent spherical diameter, μm). The p-values in panels were $p < 0.05$ (linear regression ANOVA).

3.4.4. Cell volume

After a 2-d incubation, the mean cell volumes of *Gymnodinium smaydae* feed on *Heterocapsa rotundata* at the lowest mean prey concentrations of 21.3 ng C ml^{-1} (305 μm^3) was comparable to that that were starved (340 μm^3) (Fig. 3.6A). The cell volume increased rapidly up to 1140 μm^3 at the mean prey concentration of 1319 ng C ml^{-1} and then slowly up to 1620 μm^3 at the mean prey concentration of 9698 ng C ml^{-1} (Fig. 3.6A).

After a 2-d incubation, the mean cell volumes of *Gymnodinium smaydae* feed on *Heterocapsa triquetra* at the 2 lowest mean prey concentrations of 49 ng C ml^{-1} (260 μm^3) was comparable to those of the cells that were starved (270 μm^3) (Fig. 3.6B). The cell volume increased continuously up to 595 μm^3 at the highest mean prey concentration of 2168 ng C ml^{-1} (Fig. 3.6B).

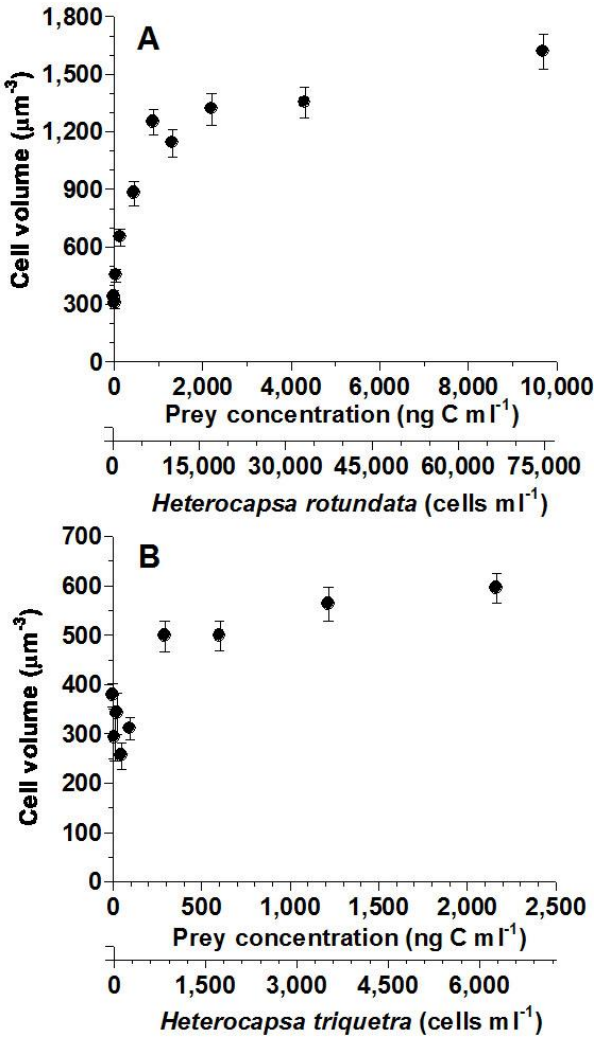

Fig. 3.6. The cell volume of *Gymnodinium smaydae* on *Heterocapsa rotundata* (A) and *Heterocapsa triquetra* (B) after a 48-h incubation as a function of mean prey concentration. Symbols represent treatment means ± 1 SE.

3.4.5. Swimming speed

The average (± SE, n=30) and maximum swimming speeds of *Gymnodinium smaydae* were 335 (± 32) and 707 μm s^{-1}, respectively.

3.4.6. Photosynthetic rate

When *Gymnodinium smaydae* maintained its abundance feeding on *Heterocapsa rotundata,* the average (± SE, n=3) of the chlorophyll-a content per cell of *G. smaydae* at the light intensity at 20 μE $m^{-2}s^{-1}$ was 1.9 pg chl-a $cell^{-1}$ (± 0.13) (Table 3.3). The average (± SE, n=3) of the photosynthetic rate per cell of *G. smaydae* was 1.5 pg C $cell^{-1}$ h^{-1} (± 0.16). The average (± SE, n=3) of the photosynthetic rate per chlorophyll-a of *G. smaydae* was 0.8 pg C $cell^{-1}$ h^{-1} (± 0.10). In addition, when *G. smaydae* maintained its abundance feeding on *Heterocapsa* sp., the average (± SE, n=3) of the chlorophyll-a content per cell of *G. smaydae* was 4.3 pg chl-a $cell^{-1}$ (± 0.18) (Table 3.3). The average (± SE, n=3) of the photosynthetic rate per cell of *G. smaydae* was 2.3 pg C $cell^{-1}$ h^{-1} (± 0.30). The average (± SE, n=3) of the photosynthetic rate per chlorophyll-a of *G. smaydae* was 0.5 pg C $cell^{-1}$ h^{-1} (± 0.08).

Table 3.3. Chlorophyll-a contents and photosynthetic rates of *Gymnodinium smaydae* on *Heterocapsa* spp., *Heterocapsa rotundata*, and *Heterocapsa* sp. CCMP 3244.

Predator	CV	L	Chl-a	SC	PT	PC
Gymnodinium smaydae on *Heterocapsa rotundata*	600	20	1.9 (0.13)	3.2 (0.21)	1.5 (0.16)	0.8 (0.10)
Gymnodinium smaydae on *Heterocapsa* sp. CCMP 3244	770	20	4.3 (0.18)	5.6 (0.24)	2.3 (0.30)	0.5 (0.08)
Heterocapsa rotundata	460	20	1.6 (0.06)	3.4 (0.13)	3.9 (0.14)	2.5 (0.02)
Heterocapsa sp. CCMP 3244	607	20	2.7 (0.41)	4.5 (0.67)	8.6 (0.79)	3.2 (0.43)

CV, cell volume (μm^3); L, light intensity ($\mu E\ m^{-2}\ s^{-1}$); Chl-a, chlorophyll-a content per cell (pg chl-a $cell^{-1}$); SC, specific chlorophyll-a (fg μm^{-3}); PT, photosynthetic rate per cell (pg C $cell^{-1}\ h^{-1}$); PC, photosynthetic rate per chlorophyll-a (ng C (ng chl-a)$^{-1}\ h^{-1}$); Values were means ($\pm$ SE); n=3 for chl-a and PT.

3.4.7. Potential grazing impact

The grazing coefficients attributable to *Gymnodinium smaydae* on co-occurring *Heterocapsa rotundata* in the water samples taken in the waters inside Shiwha Bay, Korea in 2008 and 2010, when the abundances of *H. rotundata* and *G. smaydae* were 117-717 cells ml^{-1} and 1-26 cells ml^{-1}, respectively, were 0.08-0.230 h^{-1} (Fig. 3.7A). The grazing coefficients attributable to *Gymnodinium smaydae* on co-occurring *Heterocapsa triquetra* in the same samples, when the abundances of *H. triquetra* and *G. smaydae* were 3-1,271 cells ml^{-1} and 1-26 cells ml^{-1}, respectively, were 0.002-0.019 h^{-1} (Fig. 3.7B).

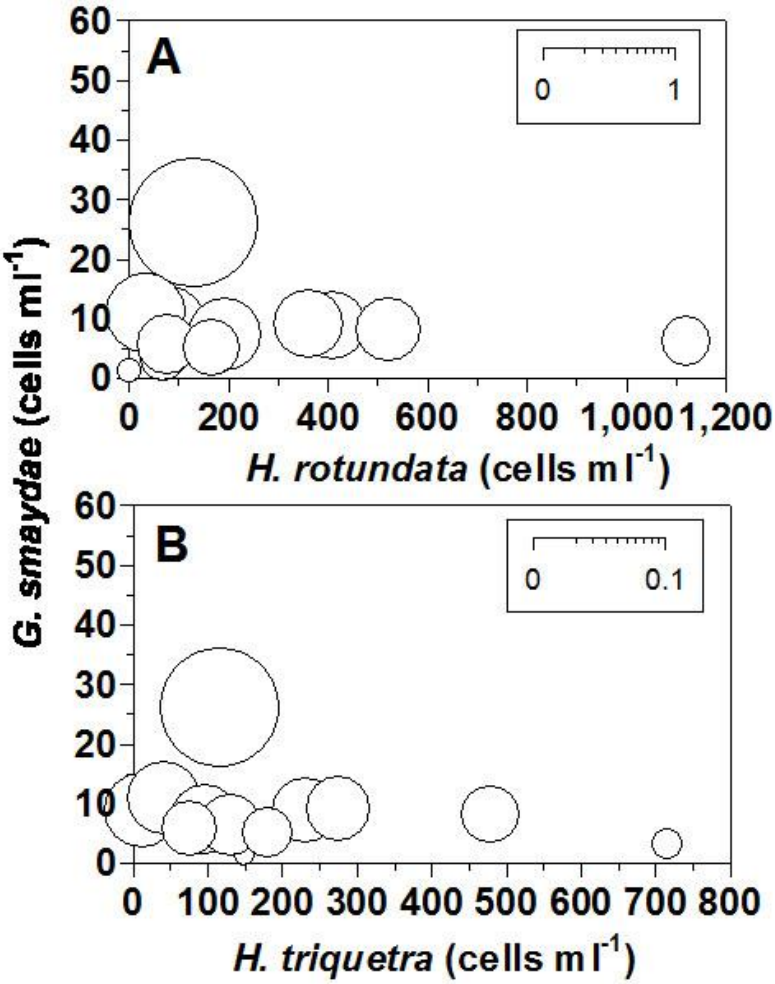

Fig. 3.7. Calculated grazing coefficients (g, h^{-1}) attributable to *Gymnodinium smaydae* on natural populations of *Heterocapsa rotundata* (A) and *Heterocapsa triquetra* (B) (see text for calculation). n=12

3.5. Discussion

3.5.1. Feeding mechanisms and prey species

The mixotrophic dinoflagellate *Gymnodinium smaydae* fed on algal prey using a peduncle. The similar-sized mixotrophic dinoflagellates *Biecheleria cincta* (previously *Woloszynskia cincta*), *Gymnodinium aureolum*, *Karlodinium armiger,* and *Paragymnodinium shiwhaense*, along with the heterotrophic dinoflagellates *Gyrodiniellum shiwhaense*, *Luciella masanensis, Pfiesteria piscicida,* and *Stoeckeria algicida* also feed on algal prey using a peduncle (Berge et al. 2008; Burkholder et al.1992; Harvey et al., 2013; Jeong et al. 2005a, 2010a, 2011b, 2006, 2007; Kang et al., 2011; Yoo et al., 2010b). However, the kind of prey that *G. smaydae* is able to feed on is different from that of the other peduncle-feeding dinoflagellates (Table 3.4); *G. smaydae* is able to feed on *Scrippsiella trochoidea* which the other peduncle-feeding dinoflagellates are not able to feed on. Thus, among the peduncle-feeding dinoflagellates so far reported, *G. smaydae* is the only species that is able to feed on *S. trochoidea*. In addition, *G. smaydae* is able to feed on *Heterocapsa triquetra*. Previously, *K. armiger* was the only peduncle-feeding dinoflagellate that was able to feed on *H. triquetra*. Therefore, *G. smaydae* is one of two species that are able to feed on *H. triquetra*. *G. smaydae* may have some enzymes to digest *S. trochoidea* and *H. triquetra*. On the contrary, *G. smaydae* does not feed on some prey items that all or most other peduncle-feeding dinoflagellates are able to feed on (Table 3.4); *G. smaydae* does not feed *Heterosigma akashiwo*, which all other peduncle-

feeding dinoflagellates are able to feed on. Furthermore, *G. smaydae* does not feed the cryptophytes *Teleaulax* sp. and *Rhodomonas salina* and the dinoflagellate *Amphidinium carterae* that the other peduncle-feeding dinoflagellates except *Stoeckeria algicida* are able to feed on. *S. algicida* is known to feed on only *H. akashiwo*. Thus, *G. smaydae* has an ecological niche different from the other peduncle-feeding dinoflagellates and may play roles different from the others.

3.5.2. Growth and ingestion rates

Heterocapsa rotundata supports the highest growth rate of *Gymnodinium smaydae*. *Heterocapsa* sp. CCMP 3244 (*H. rotundata*-like species) has also high growth rates. In addition, *Heterocapsa triquetra* is a suboptimal prey. The optimal (and suboptimal) prey for the other peduncle-feeding mixotrophic dinoflagellates are *Heterosigma akashiwo* for *Symbiodinium voratum*, *H. akashiwo* (*Rhodomonas salina*) for *Biecheleria cincta* (previously *Woloszynskia cinta*), *Rhodomonas baltica* (*R. salina*) for *Karlodinium armiger*, *Teleaulax* sp. (*Isochrysis galbana*) for *Gymnodinium aureolum* (Table 3.5). In addition, the optimal and suboptimal prey species for the peduncle-feeding heterotrophic dinoflagellates are perch blood cells (*R. salina*) for *Pfiesteria piscicida*, perch blood cells (*Amphidinium carterae*) for *Luciella masanensis*, *H. akashiwo* for *Stoeckeria algicida*, and *Teleaulax* sp. (*A. carterae*) for *Gyrodiniellum shiwhaense* (Table 3.5). Therefore, *G. smaydae* is the only peduncle-feeding heterotrophic dinoflagellate whose optimal and suboptimal prey are *Heterocapsa* spp.. The different optimal or

suboptimal prey species of peduncle-feeding heterotrophic dinoflagellates may reduce competition for prey and cause a different dominant grazer during blooms dominated by each optimal or suboptimal prey.

The maximum growth rate (i.e., mixotrophic growth) of *Gymnodinium smaydae* on the optimal prey obtained under a 14:10 h light-dark cycle of 20 μE m^{-2} s^{-1} (2.2 d^{-1}) is higher than that of any other mixotrophic dinoflagellates so far reported (0.20 – 1.1 d^{-1}) at diverse light intensities (Table 3.5). Furthermore, the maximum growth rate of *G. smaydae* on the optimal prey is also greater than that of *Pfiesteria piscicida*, *Luciella masanensis*, and *Stoeckeria algicida* which have 3 highest maximum growth rates among heterotrophic dinoflagellates (1.1-1.7 d^{-1}) (Table 3.5). Therefore, *G. smaydae* has the greatest maximum growth rate among the feeding dinoflagellates. With increasing predator size, the maximum growth rates of autotrophic, mixotrophic, or heterotrophic dinoflagellates inversely decreased (Jeong et al., 2010b). *G. smaydae* is one of the smallest dinoflagellates whose growth rates have been measured. The very small size of *G. smaydae* may cause its very high growth rate when feeding on the optimal prey. The maximum growth rate of *G. smaydae* suggests the fact that the maximum growth rates of peduncle-feeding dinoflagellates are greater than previously known engulfment-feeding dinoflagellates or pallium-feeding dinoflagellates (Table 3.5). Sucking and digesting materials in the protoplasms of prey cells through the peduncle may be effective for assimilation than digesting the surface layer (or theca) and materials in the protoplasms of prey cells after engulfing whole prey cells or using pallium and extra-cellular digestion.

Table 3.4. Comparison of the prey species and the maximum growth (MGR, d^{-1}) and ingestion rates (MIR, ng C $predator^{-1}$ d^{-1}) of the peduncle feeding mixotrophic (MTD) and heterotrophic dinoflagellates (HTD).

Trophic mode		MTD						HTD			
Prey species/predator	ESD	Gsm	Sm	Bc	Ga	Ps	Ka	Gsh	Lm	Sa	Pp
Prymnesiophytes											
Isochrysis galbana	4.8	Y	Y	Y	Y	Y	Y	Y	Y	**N**	Y
Diatoms											
Sksletonema costatum	5.9	N	N	N	N	N		N	**Y**	N	**Y**
Thalassiosira weissflogii	11.8						**Y**				
Thalassiosira rotula	29.3				N	N			Y	N	Y
Cryptophytes											
Teleaulax sp.	5.6	**N**	Y	Y	Y	Y		Y	Y	**N**	Y
Teleaulax amphioxeia	7.3						Y				
Rhodomonas salina	8.8	**N**	Y	Y	Y	Y	Y	Y	Y	**N**	Y
Rhaphidophytes											
Heterosigma akashiwo	11.5	**N**	Y	Y	Y	Y	Y	Y	Y	Y	Y
Chattonella ovata	40.0	N			N	N			Y	N	Y
Mixotrophic dinoflagellates											
Heterocapsa rotundata	5.8	Y	Y	Y	Y	Y	Y	Y	Y	**N**	Y
Amphidinium carterae	9.7	**N**	Y	Y	Y	Y		Y	Y	N	Y
Prorocentrum minimum	12.1	**N**	N	N	N	N	**Y**	Y	N	N	N
Heterocapsa triquetra	15.0	**Y**	N	N	N	N	**Y**	N	N	N	N
Scrippsiella trochoidea	22.8	**Y**	N	N	N	N		N	N	N	N

Cochlodinium polykrikoides	25.9	N	N	N	N	N		N	**Y**	N	**Y**
Prorocentrum micans	26.6	N	N	N	N	N	**Y**	N	N	N	N
Akashiwo sanguinea	30.8	N	N	N	N	N	**Y**	N	**Y**	N	**Y**
Gyrodinium instriatum	31.2						Y				
Gonyaulax polygramma	32.5		N	N	N	N		N	N	N	N
Alexandrium catenella	32.6					N			N	N	N
Gymnodinium catenatum	33.9					N			Y	N	Y
Lingulodinium polyedrum	38.2	N	N	N	N	N		N	N	N	N
MGR		2.23	0.47	0.50	0.17	1.10	0.65	1.05	1.46	1.63	1.74
MIR		1.6	0.1	0.5	0.1	0.4	1.0	0.5	2.6	0.8	4.3
Reference		(1)	(2)	(3)	(3, 4)	(5)	(6)	(7)	(5, 8)	(9)	(5, 10)

ESD, equivalent spherical diameter (㎛); Gsm, *Gymnodinium smaydae*; Sv, *Symbiodinium voratum*, Bc, *Biecheleria cincta*; Ga, *Gymnodinium aureolum*; Ps. *Paragymnodinium shiwhaense*; Ka, *Karlodinium armiger*; Gsh, *Gyrodiniellum shiwhaense*; Lm, *Luciella masanensis*; Sa, *Stoeckeria algicida*; Pp, *Pfiesteria piscicida*; (1), this study; (2), Jeong et al., 2012; (3), Kang et al., 2011; (4), Jeong et al., 2010a; (5), Yoo et al., 2010b; (6), Berge et al., 2008; (7), Jeong et al., 2011b; (8), Jeong et al., 2007; (9), Jeong et al., 2005d; (10), Jeong et al., 2006. Bold indicate different results from the other predators.

Table 3.5.

A. Optimal and sub-optimal(*) prey and maximum mixotrophic growth rates (MMG) of each mixotrophic dinoflagellate predator species at diverse light intensities.

Predator	ESD	Prey	Tx	ESD	T	L	MMG	AG	M-A	Ref.
Peduncle feeder										
Gymnodinium smaydae	10.5	*Heterocapsa rotundata*	DN	9.5	20	20	2.23	0.005	2.23	(1)
		Heterocapsa sp. 3244	DN	10.5	20	20	1.76	0.085	1.68	
		*Heterocapsa triquetra**	DN	15	20	20	1.05	-0.05	1.1	
Symbiodinium sp.	11.1	*Heterosigma akashiwo*	RA	11.5	20	20	0.47	0.3	0.17	(2)
Paragymnodinium shiwhaense	12.4	*Amphidinium carterae*	DN	9.7	20	20	1.1	-0.22	1.32	(3)
		Teleaulax sp.*	CR	5.6	20	20	0.64	-0.08	0.72	
Biecheleria cincta	13.4	*Heterosigma akashiwo*	RA	11.5	20	20	0.5	0.04	0.46	(4)
		*Rhodomonas salina**	CR	8.8	20	20	0.27	0.03	0.23	
*Karlodinium armiger**	16.7	*Rhodomonas baltica*	CR	10.7	15	180	0.65	0.06	0.59	(5)
		*Rhodomonas salina**	CR	9	15	180	0.55	0.06	0.49	

Gymnodinium aureolum	19.4	*Teleaulax* sp.	CR	5.6	20	20	0.17	0.12	0.05	(6)
		*Isochrysis galbana**	PR	4.8	20	20	0.16	0.1	0.05	
Karlodinium veneficum	11	*Storeatula major*	CR	6.6	20	250	0.75	0.55	0.2	(7)
Dinophysis acuminata	35	*Mesodinium rubrum*	NC	22	20	60	0.91	0.19	0.72	(8)
Engulfment feeder										
Prorocentrum donghaiense	13.2	*Teleaulax* sp.	CR	5.6	20	20	0.51	0.38	0.14	(9)
Heterocapsa triquetra	15	*Teleaulax* sp.	CR	5.6	20	20	0.28	0.18	0.1	(9)
Prorocentrum micans	26.6	*Teleaulax* sp.	CR	5.6	20	20	0.2	0.11	0.09	(9)
Fragilidium cf. *mexicanum*	54.5	*Lingulodinium polyedrum*	DN	37.9	22	20	0.36	−0.05	0.41	(10)
Amylax triacantha	30	*Mesodinium rubrum*	NC	22	15	20	0.68	−0.08	0.76	(11)

B. Optimal and sub-optimal prey and maximum growth rates of each heterotrophic dinoflagellate predator species.

Predator	ESD	Optimal Prey	Tx	ESD	T	MG	Ref.
Peduncle feeder							
Pfiesteria piscicida	13.5	Perch blood cell	BL	6.1	20	1.7	(12)
		*Rhodomonas salina**	CR	8.8	20	1.4	
Stoeckeria algicida	13.9	*Heterosigma akashiwo*	RA	11.5	20	1.6	(13)
Luciella masaensis	13.5	Perch blood cell	BL	6.1	20	1.5	(14)
		*Amphidinium carterae**	DN	9.7	20	0.6	
Gyrodiniellum shiwhaense	12.4	*Teleaulax* sp.	CR	5.6	20	1.1	(15)
		*Amphidinium carterae**	DN	9.7	20	0.8	
Engulfment feeder							
Gyrodinium moestrupii	18.4	*Alexandrium minutum*	DN	21.9	20	1.6	(16)
		*Scrippsiella trochoidea**	DN	22.8	20	1.5	
Oxyrrhis marina	15.6	*Heterosigma akashiwo*	RA	11.5	20	1.4	(17)
		*Phaeodactylum tricornutum**	DA	4.2	20	1.3	(18, 20)
Gyrodinium dominans	20.0	*Prorocentrum minimum*	DN	12.1		1.1	(19)
		*Eutreptiella gymnastica**	EU	12.6	20	1.1	(20)

Polykrikos kofoidii	43.5	*Gymnodinium catenatum*	DN	34	20	1.1	(21)
		*Scrippsiella trochoidea**	DN	25.1	20	1.0	
Pellium feeder							
Protoperidinium bipes	7.8	*Skeletonema costatum*	DA	5.9	20	1.4	(22)
		*Eutreptiella gymnastica**	EU	12.6	20	0.8	(20)
Protoperidinium hirobis	8.7	*Leptocylindrum danicus*	DA	19.7	20	1.2	(23)
Oblea rotunda	21.6	*Ditylum brightwellii*	DA	33	20	0.7	(24)

ESD, equivalent spherical diameter (μm); Tx, taxa; T, temperature (℃); L, light intensity (μE m^{-2} s^{-1}); MMG, maximum mixotrophic growth rate (d^{-1}); AG, autotrophic growth rate (d^{-1}); M−A, MMG−AG; MG, maximum growth rate; (1), this study; (2), Jeong et al., 2012; (3), Yoo et al., 2010b; (4), Kang et al., 2011; (5), Berge et al., 2008; (6), Jeong et al., 2010a; (7), Adolf et al., 2006; (8), Kim et al. 2008; (9), Jeong et al., 2005b; (10), Jeong et al., 1999; (11), Park et al., 2013; (12), Jeong et al., 2006; (13), Jeong et al., 2005d; (14), Jeong et al., 2007; (15), Jeong et al., 2011b; (16), Yoo et al. 2013; (17), Jeong et al., 2003; (18), Goldman et al., 1989; (19), Kim and Jeong 2004; (20), Jeong et al., 2011a; (21), Jeong et al., 2001; (22), Jeong et al. 2004; (23), Jacobson and Anderson, 1986; (24), Strom and Buskey, 1993.* indicates that *Karlodinium armiger* is able to both peduncle and engulfment feeding.

Gymnodinium smaydae did not grow without added algal prey like *Paragymnodinium shiwhaense*. The calculated daily carbon obtained from photosynthesis only by *G. smaydae* is 0.036 ng C, which is ca 30% of the body carbon of a *G. smaydae* cell. Thus, low photosynthetic rate per cell of *G. smaydae* may cause no phototrophic growth. Therefore, *G. smaydae* may be able to increase or maintain its population only when *Heterocapsa rotundata* and/or *Heterocapsa triquetra* is abundant in a natural environment. In Shiwha in 2008 and 2010, *G. smaydae* was abundant when the abundance of *H. rotundata* or *H. triquetra* was abundant. *G. smaydae* can maintain its population without added algal prey (0.005 to −0.051 d^{-1}) unlike *P. shiwhaense* whose population decreases (−0.22 d^{-1}). Thus, *G. smaydae* may have an advantage in maintaining its population when its prey cells are absent and then rapidly increase its population when its prey cells are abundant, while *P. shiwhaense* may have difficulty in maintaining its population when its prey cells are absent.

Both maximum growth and ingestion rates of *Gymnodinium smaydae* on *Heterocapsa rotundata* are greater than those of any other dinoflagellate grazer on the same prey so far reported (Table 3.6). Thus, *G. smaydae* is likely to be the most important dinoflagellate grazer during *H. rotundata* blooms and play an important role in population dynamics of *H. rotundata*. The maximum growth rate of *G. smaydae* on *H. triquetra* is greater than that of any other dinoflagellate grazer on the same prey so far reported, while its maximum ingestion rate is lower than that of the other dinoflagellate grazers, except *Karlodinium armiger* (Table 3.6). Therefore, *G. smaydae* is likely to be the most important dinoflagellate grazer during *H. triquetra* blooms.

The growth rates of *Gymnodinium smaydae* on *Heterocapsa* spp. and *Scrippsiella trochoidea* at similar mean prey concentrations are negatively correlated with the ESD of prey species. *G. smaydae* may spend less energy to capture, handle, and ingest smaller prey species (i.e., *Heterocapsa rotundata*) than bigger prey species (i.e., *S. trochoidea*) and deploying the peduncle to prey's surface.

4.5.3. Photosynthetic rate

Both chlorophyll-a content and photosynthetic rate per cell of *Gymnodinium smaydae* fed *Heterocapsa* sp. CCMP 3244 are greater than those fed *Heterocapsa rotundata*. Interestingly, the chlorophyll-a content and the photosynthetic rate per cell of *Heterocapsa* sp. CCMP 3244 are also greater than those of *H. rotundata*. Thus, chlorophyll-a content and the photosynthetic rate per cell of *G. smaydae* are likely to be affected by the kind of prey species. In addition, the photosynthetic rate per cell of *G. smaydae* fed *Heterocapsa* sp. CCMP 3244 is also greater than that fed *H. rotundata*, and the photosynthetic rate per cell of *Heterocapsa* sp. CCMP 3244 is also greater than that of *H rotundata*. Thus, *G. smaydae* may have a higher photosynthetic rate if it feeds on prey whose photosynthetic rate is higher. It is worthwhile to explore mechanisms of affecting an ability of host photosynthesis by prey photosynthesis.

Table 3.6. Comparision of the maximum growth (MG, d^{-1}) and ingestion (MIR, ng C $predator^{-1}$ d^{-1}) rates of *Gymnodinium smaydae* and other protists on *Heterocapsa rotundata* and *Heterocapsa triquetra*.

Prey species	Predator	ESD	Taxon	T	MG	MIR	References
Heterocapsa rotundata	*Gymnodinium smaydae*	10.6	MTD	20	2.23	1.59	This study
	Karlodinium armiger	16.7	MTD	15	0.35	0.02	Berge et al., 2008
	Gymnodinium aureolum	19.5	MTD	20	0.14	0.07	Jeong et al., 2010a
	Paragymnodinium shiwhaense	12.4	MTD	20	−0.16	0.09	Yoo et al., 2010b
	Pfiesteria piscicida	13.5	HTD	20	0.32	0.16	Jeong et al., 2006
Heterocapsa triquetra	*Gymnodinium smaydae*	10.6	MTD	20	1.05	0.24	This study
	Karlodinium armiger	16.7	MTD	15	0.48	0.22	Berge et al., 2008
	Gyrodinium spirale	31.8	HTD	20	1.08	7.5	Hansen, 1992 Kim and Jeong, 2004
	Gyrodinium dominans	20.0	HTD	20	0.54	2.3	Nakamura et al., 1995 Kim and Jeong, 2004
	Protoperidinium steinii	25.8	HTD	15	0.18		Naustvoll, 2000

ESD, equivalent spherical diameter (μm); MTD, mixotrophic dinoflagellate; HTD, heterotrophic dinoflagellate; T, temperature (°C).

3.5.4. Grazing impact

The grazing coefficients (g) attributable to *Gymnodinium smaydae* on co-occurring *Heterocapsa rotundata* obtained in the present study were up to 0.230 h^{-1} (i.e., up to 21 % of the *H. rotundata* populations were removed by a *G. smaydae* population in 1 h), while those on co-occurring *Heterocapsa triquetra* were up to 0.019 h^{-1} (i.e., up to 2 % of the *H. triquetra* populations were removed by a *G. smaydae* population in 1 h). Therefore, *G. smaydae* may have a considerable grazing impact on populations of co-occurring *H. rotundata,* but it may not have a high enough grazing impact to control populations of co-occurring *H. triquetra*.

Chapter 4.

Survival strategies of the toxic dinoflagellates *Alexandrium andersonii*, *A. affine*, *and A. fraterculus* by killing and/or feeding other protists

4.1. Abstract.

The dinoflagellate *Alexandrium* spp. have received much attention due to their harmful effects on diverse marine organisms, including commercially important species. For minimizing loss due to red tides or blooms of *Alexandrium* spp., it is very important to understand the eco-physiology of each *Alexandrium* species and to predict its population dynamics. Its trophic mode (i.e., exclusively autotrophic or mixotrophic) is one of the most critical parameters in establishing prediction models. However, among the 35 *Alexandrium* species so far described, only six *Alexandrium* species have been revealed to be mixotrophic. Thus, mixotrophic ability of the other *Alexandrium* species should be explored. In the present study, whether each of three *Alexandrium* species (*A. andersonii*, *A. affine*, and *A. fraterculus*) isolated from Korean waters has or lacks mixotrophic ability, was investigated. When diets of diverse algal prey, cyanobacteria, and bacteria sized micro-beads were provided, *A. andersonii* was able to feed on the prasinophyte *Pyramimonas* sp., the cryptophyte *Teleaulax* sp., and the dinoflagellate *Heterocapsa rotundata*, whereas neither *A. affine* nor *A. fraterculus* fed on any

prey item. Moreover, mixotrophy elevated the growth rate of *A. andersonii*. The maximum mixotrophic growth rates of *A. andersonii* on *Pyramimons* sp. under a 14:10 h light/dark cycle of 20 μE m^{-2} s^{-1} was 0.432 d^{-1}, while the autotrophic growth rate was 0.243 d^{-1}. With increasing mean prey concentration, the ingestion rate of *A. andersonii* increased rapidly at prey concentrations < 650 ng C ml^{-1} (ca. 16,240 cells ml^{-1}), but became saturated at the higher prey concentrations. The maximum ingestion rate by *A. andersonii* of *Pyramimons* sp. was 1.03 ng C $predator^{-1}d^{-1}$ (25.6 cells $predator^{-1}d^{-1}$). This evidence suggests that the mixotrophic ability of *A. andersonii* should be taken into consideration in predicting the outbreak, persistence, and decline of its harmful algal blooms.

4.2. Introduction

There are three major trophic modes in dinoflagellates: exclusively autotrophic, heterotrophic, and mixotrophic (i.e., capable of feeding and conducting photosynthesis) (Stoecker, 1998, 1999; Burkholder et al., 2008; Jeong et al., 2010b; Johnson, 2011; Mitra et al., 2016). In establishing models predicting the outbreak, persistence, and decline of a red tide or harmful algal bloom, the trophic mode of a red tide dinoflagellate is a critical factor (Jeong et al., 2015). In last three decades, many dinoflagellates that were believed to be exclusively autotrophic have been revealed to be mixotrophic organisms (Bockstahler and Coats, 1993a, 1993b; Jacobson and Anderson, 1996. Skovgaard, 1996; Stoecker, 1999; Jeong et al., 2005a, 2005b, 2005c, 2010a, 2012; Park et al., 2006;

Kang et al., 2011; Lee et al., 2015). Thus, models predicting their red tide dynamics have been modified to reflect their mixotrophy. Furthermore, mixotrophic organisms have recently been proposed as one of the major functional groups in ecosystem models (Mitra and Flynn, 2010; Mitra et al., 2016). However, among ca. 1200 phototrophic dinoflagellates so far reported, only ~50 species (i.e., 4–5%) have been revealed to be mixotrophic (Jeong et al., 2010b; Gómez, 2012; Lee et al., 2014a). Moreover, the potential for mixotrophy has not yet been explored for many toxic or harmful dinoflagellates. Thus, it is worthwhile to investigate whether each of the phototrophic dinoflagellates not yet determined, is mixotrophic or exclusively phototrophic.

The dinoflagellates *Alexandrium* spp. have received much attention due to their harmful effects on diverse marine organisms, including commercially important species (Anderson, 1995; Shumway et al., 2003; Samson et al., 2008). Of these, several species have been revealed to produce paralytic shellfish poisoning (PSP) toxins and often toxify shellfish (Anderson, 1995; Shumway et al., 2003). For minimizing loss due to red tides or blooms of *Alexandrium* spp., understanding the eco-physiology of each *Alexandrium* species and predicting its population dynamics are very important steps. Its trophic mode (i.e., exclusively autotrophic or mixotrophic) is one of the most critical parameters in establishing prediction models. However, among 42 described *Alexandrium* species, only six (*A. catenella, A. minutum, A. ostenfeldii, A. pohangense, A. pseudogonyaulax,* and *A. tamarense*) have been revealed to be mixotrophic (Jacobson and Anderson, 1996; Jeong et al., 2005b, 2005c; Yoo et al., 2009; Blossom et al., 2012; Lim et al., 2015). Of

the six mixotrophic *Alexandrium* species, the kind of prey that each *Alexandrium* sp. is able to feed on has been revealed for only *A. pohangense, A. pseudogonyaulax,* and *A. tamarense* (Jeong et al., 2005b; Blossom et al., 2012; Lim et al., 2015). The kind of prey utilized is important for understanding the eco-physiological and genetic characterizations of each *Alexandrium* sp. because detecting, capturing, and digesting prey cells can be related to enzymes. Moreover, the kind of prey utilized may provide clues to understanding speciation and evolution in the *Alexandrium* genus. To date, the mixotrophic growth and ingestion (or removal of prey) rates have been reported for only two *Alexandrium* species (Blossom et al., 2012; Lim et al., 2015): mixotrophic growth and ingestion rates by *A. pohangense* of *Cochlodinium polykrikoides;* and mixotrophic growth rates by *A. pseudogonyaulax* of *Heterocapsa rotundata*. Thus, there are limits to current understanding of the bloom dynamics of mixotrophic *Alexandrium* spp. due to lack of information on their mixotrophic growth and ingestion rates. Thus, it is worth exploring the functional and numerical responses of mixotrophic *Alexandrium* spp., to prey concentrations.

The non-chain forming species *A. andersonii* has been observed in China, Ireland, Korea, the Mediterranean Sea, and the USA (Balech, 1990; Ciminiello et al., 2000; Frangópulos et al., 2004; Wang et al., 2006; Touzet and Raine, 2007; Orr et al., 2011; Sampedro et al., 2013; this study). The presence or absence of saxitoxins (or other toxicity) of this species is strain-specific (Ciminiello et al., 2000; Frangópulos et al., 2004; Orr et al., 2011; Sampedro et al., 2013). Moreover, the chain-forming species *A. affine* has been reported in Hong Kong, Japan, Korea, Mexico, Spain,

and Vietnam (Fraga et al., 1989; Nakanishi et al., 1996; Band-Schmidt et al., 2003; Nguyen-Ngoc, 2004; Lee et al., 2009; Park et al., 2013). In addition, another chain-forming species *A. fraterculus* has been observed in Brazil, Korea, Japan, New Zealand, and Uruguay (Lagos, 2003; MacKenzie et al., 2004; Omachi et al., 2007; Nagai et al., 2009; Park et al., 2013). Interestingly, *A. andersonii* and *A. affine* were observed in the Mediterranean Sea, where *A. minutum*, *A. ostenfeldii*, *A. pseudogonyaulax*, *A. catenella*, and *A. tamarense* also occur, and which have been revealed to be both toxic and mixotrophic (Anderson et al., 2012). Thus, *A. andersonii* and *A. affine* are likely to compete with these other *Alexandrium* species. In competition among red tide species, relative growth rates are most important. The range of the growth rates of several strains of *A. andersonii* are 0.05–0.32 d^{-1}, lower than that of the other *Alexandrium* species described above (Jensen and Moestrup, 1997; Yamamoto and Tarutani, 1999; Frangópulos et al., 2004; Nguyen-Ngoc, 2004; Li et al., 2011). Thus, elevation of growth rate through mixotrophy by *A. andersonii* may be an important in such competition. The presence or absence of mixotrophic ability of *A. affine* and *A. fraterculus* is also important in understanding their competition with other species and their bloom dynamics.

The mixotrophic ability of *A. andersonii* (Equivalent Spherical Diameter, ESD = 14.9 μm), *A. affine*, and *A. fraterculus* (ESD = 31.4 and 32.3 μm, respectively), isolated from Korean coastal waters, was investigated by providing a unialgal diet of diverse algal prey, cyanobacteria, and bacterium-sized micro-beads. Of these potential prey items, at least one has been reported as prey of mixotrophic dinoflagellates (Jeong et al., 2010b). In addition, the kinds of prey

that each of the three target species (*A. andersonii*, *A. affine*, and *A. fraterculus*) was able to feed on (i.e., its feeding mechanism) were explored. Moreover, for the growth and ingestion rates by *A. andersonii* on the prasinophyte *Pyramimonas* sp., the optimal prey were measured and then compared with those of other mixotrophic dinoflagellate predators. Furthermore, chemicals produced by some *Alexadnrium* spp. are known to immobilize prey cells (e.g., Blossom et al., 2012). Thus, it is worthwhile to explore whether the chemicals for immobilization of potential prey cells are associated with saxitoxins which several *Alexadnrium* spp. have. The presence of saxitoxin genes in *A. andersonii*, *A. affine*, and *A. fraterculus* was investigated using DNA analysis. This study provides a basis for understanding mixotrophic ability, the interactions among *Alexandrium* species and with diverse phytoplankton of other taxa, and evolution in dinoflagellates.

4.3. Materials and Methods

4.3.1. Establishing clonal cultures and preparation of experimental organisms

Cells of *A. affine*, *A. andersonii*, and *A. fraterculus* were isolated from Korean coastal waters and then clonal cultures were established from two serial single isolations. *A. affine* was isolated from coastal waters off Taean (western Korea) in August 2013 when the water temperature and salinity was 21.5 ℃ and 32.2, respectively. *A. fraterculus* was isolated from Yeosu (southern Korea) when the water temperature and salinity was 23.4 ℃ and 32.8, respectively. *A. andersonii* was isolated from Jinhae Bay (southern Korea) in May 2015 when the water temperature and salinity was 15.3 ℃ and 27.4, respectively (Table 4.1).

When the concentrations of *A. affine*, *A. andersonii, and A. fraterculus* increased, cells were transferred to 50−, 250−, and 500−ml polycarbonate (PC) bottles containing f/2−Si (but L1−Si for *A. fraterculus*) medium (Guillard and Ryther, 1962), capped, and placed on the shelf at 20 ℃ under illumination of 20 μE m^{-2} s^{-1} cool−white fluorescent light in a 14:10 h light/dark cycle. Once a dense culture of each *Alexandrium* species was established, healthy cells were transferred to new 500 ml PC bottles containing fresh medium, where they reached maximum abundance (5000–10,000 cells ml^{-1}).

After establishing clonal cultures of the three *Alexandrium* species, all of these species were genetically confirmed to be *A. affine*, *A. andersonii, and A. fraterculus* using rDNA (small subunit, ITS1−5.8s−ITS2, and large subunit) analysis methods, as described

in Jeong et al. (2010a) and Lee et al. (2013).

The phototrophic and mixotrophic protistan species, and the cyanobacterium *Synechococcus* sp. provided as potential prey species, are listed in Table 4.2. All prey species except *Cochlodinium polykrikoides, Mesodinium rubrum,* and *Lingulodinium polyedrum* were grown at 20 ℃ in enriched f/2−Si seawater media under 20 μE $m^{-2}s^{-1}$ on a 14:10 h light–dark cycle. *C. polykrikoides* and *L. polyedrum* were grown under continuous illumination (50 μE $m^{-2}s^{-1}$) by cool white fluorescent light, because they did not grow well under lower illumination on a light/dark cycle (Lee et al., 2014a). *M. rubrum* was maintained by providing the cryptophyte *Teleaulax* sp. as prey (Lee et al., 2014b).

The cell size of the phototrophic dinoflagellate *Heterocapsa rotundata* strain used in the present study (HRSH1201; ESD = 9.5 μm; Lee et al., 2014a) was bigger than that of the *H. rotundata* strain previously used in our papers (ESD = 5.8 μm; Yoo et al., 2010b; Kang et al., 2011; Jeong et al., 2012). The other prey species tested in this study were the same strains used in Lee et al. (2014c).

The carbon content of *A. andersonii* (0.49−0.69 ng C per cell) was estimated from cell volume according to Menden−Deuer and Lessard (2000), while that of *Pyramimonas* sp. (0.04 ng C per cell) was measured using a CHN Analyzer (vario MICRO, Elementar, Germany). Furthermore, the carbon contents of the other phytoplankton species were obtained from our previous studies (Jeong et al. 2010a, 2011, 2012, Kang et al. 2011, Yoo et al. 2010).

4.3.2. Feeding occurrence, immobilization, and lytic effects

Experiment 1 was designed to investigate whether or not *A. affine, A. andersonii*, and *A. fraterculus* are able to feed on each target prey species or micro-bead when a diet of diverse prey items was provided (Table 4.2). The initial concentration of each algal species offered was similar in terms of carbon biomass.

A dense culture of *A. andersonii* (ca. 10,000 cells ml^{-1}) growing mixotrophically on *Pyramimonas* sp. in f/2-Si media, under 14:10 h light/dark cycle at 20 μE $m^{-2}s^{-1}$, was transferred to one 500 ml PC bottle containing f/2-Si medium when *Pyramimonas* sp. was undetectable. This culture was maintained in f/2-Si media for at least 5 d under a 14:10 h light/dark cycle at 20 μE $m^{-2}s^{-1}$. Three 1 ml aliquots were then removed from the bottle and examined using a compound microscope to determine the *A. andersonii* concentration.

In this experiment, the initial concentrations of *A. andersonii* and each target algal species were established by using an auto pipette to deliver a predetermined volume of culture with a known cell density to the experimental bottles. Duplicate 50 ml PC bottles with mixtures of *A. andersonii*, and the target prey and predator control bottles containing *A. andersonii* only, were set up for each target algal species. The bottles were filled to capacity with freshly filtered seawater, capped, and then placed on a vertically rotating plate rotating at 0.9 r/min and incubated at 20 ℃ under a 14:10 h light/dark cycle at 20 μE $m^{-2}s^{-1}$. After 6, 12, 24, and 48 h, a 5 ml aliquot was removed from each bottle and transferred into a culture plate. The bottles were filled again to capacity with f/2-Si medium, capped, placed on a rotating wheel again. Two 0.1-ml aliquots were

placed on a slide glass and the protoplasms of >200 cells slowly moving or becoming almost motionless were carefully examined with a compound microscope and/or an epifluorescence microscope (Axiovert 200M, Carl Zeiss, Germany) at a magnification of 100–630 × to determine whether or not *Alexandrium* spp. were able to feed on the target prey species. Pictures showing uningested prey cells outside, and ingested prey cells inside, *Alexandrium* cells were taken using digital cameras (Axio Cam HRC, Carl Zeiss, Germany) on the microscope, at magnifications of 400–1000×. Video of *Alexandrium* feeding were also taken using a video camera on the microscope at magnifications of 200–400×.

When observing feeding occurrence, prey immobilization and lytic effects were noted and micrographs were obtained using the method described above. The observation intervals were 0, 2, 6, 12, 24, and 48 h.

Transmission electron microscopy (TEM) was used to confirm the ingestion by *Alexandrium andersonii* of edible prey species after approximately 50,000–100,000 cells ml^{-1} of each target algal species were added to each of two 270−ml PC bottles, which contained *A. andersonii* at 8,000–10,000 cells ml^{-1}. One prey control bottle and one *A. andersonii* control bottle without added prey were set up for each experiment. The bottles were placed on a rotating wheel and incubated for two days and cells were concentrated at 1,610 g for 10 min using a centrifuge. Each concentrated pellet was carefully transferred into a 1.5−ml tube and fixed for 1.5 h in 4% (w/v, final concentration) glutaraldehyde. Next, the fixative was removed and the pellet was rinsed using 0.2 M cacodylate buffer, pH 7.4. After several rinses, the pellets were post−fixed in 1% (w/v, final

concentration) osmium tetroxide. The washed pellet was embedded in 1% (w/v) agar. Dehydration was accomplished using a graded ethanol series. The material was embedded in Spurr' s low-viscosity resin (Electron Microscopy Sciences, Fort Washington, PA, USA) (Spurr, 1969). Sections were prepared using an RMC MT-XL ultramicrotome (Boeckeler Instruments Inc., Tucson, AZ, USA) and stained with 3% aqueous uranyl acetate followed by lead citrate. The sections were viewed with a JEOL-1010 transmission electron microscope (JEOL Ltd., Tokyo, Japan).

4.3.3. Feeding behavior of *Alexandrium* spp.

Experiment 2 was designed to investigate the feeding behavior of each target species (*A. affine, A. andersonii*, and *A. fraterculus*) and possible immobilization and lysis of potential algal prey species when incubated with each *Alexandrium* species. The initial concentrations of predator and prey were the same as in Experiment 1.

The initial concentrations of *A. affine, A. andersonii*, *A. fraterculus*, and the target algal species, were established using an auto pipette to deliver a predetermined volume of culture with a known cell density to the experimental bottles. One 50 ml tissue culture flask with a mixture of *Alexandrium* spp. and the algal prey or micro beads was set up for each of the target concentrations. The flask was filled to capacity with freshly filtered seawater, capped, and then well mixed. After 1-min incubation, a 1 ml aliquot was removed from the bottle and transferred into a 1 ml Sedgwick-Rafter Chamber (SRC). By monitoring the behavior of > 50 unfed *Alexandrium* cells

for each target prey species under a compound microscope, and/or an epifluorescence microscope, at magnifications of 100–630×, all of the feeding processes were observed. A series of pictures showing the feeding process of *Alexandrium* cells was taken using a video analyzing system mounted on an inverted microscope at magnifications of 200–400×.

5.3.4. Growth and ingestion rates.

Experiment 3 was designed to investigate the growth and ingestion rates of *Alexandrium andersonii* feeding on *Pyramimonas* sp., the optimal prey, as a function of the *Pyramimonas* concentration.

A dense culture (ca. 15,000 cells ml^{-1}) of *A. andersonii* exponentially growing mixotrophically on *Pyramimonas* sp. under a 14:10 h light/dark cycle of 20 μE $m^{-2}s^{-1}$ in f/2−Si medium, was transferred to a 500 ml PC bottle containing freshly filtered seawater. When the prey was undetectable, the culture was transferred to two 500 ml PC bottles. After approximately 2−weeks incubation, when the prey was undetectable, the cultures were transferred into 500 ml PC bottles. Three 1 ml aliquots from each of these two bottles were counted using a compound microscope to determine the cell concentrations of *A. andersonii* in each bottle, and the cultures were then used to conduct experiments.

The initial concentration of *A. andersonii* and of *Pyramimonas* sp. was established as described above. Triplicate 50 ml PC experimental bottles containing mixtures of predator and prey, triplicate prey control bottles containing prey only, and triplicate predator control bottles containing predators only; were set up for

each predator–prey combination. To make the water conditions similar, the water of an *Alexandrium* predator culture was filtered through a 0.7 μm GF/F filter and then added to the prey control bottles in the same amount as the volume of the predator culture added to the predator control bottles and the experimental bottles, for each predator–prey combination. Furthermore, the water of a *Pyramimonas* prey culture was filtered in the same manner and then added to the predator control bottles in the same amount as the volume of the prey culture added to the prey control bottles and the experimental bottles. Five ml of f/2–Si medium was added to all the bottles, which were then filled to capacity with freshly filtered seawater and capped. To determine the actual initial predator and prey densities (cells ml^{-1}) at the beginning of the experiment (*A. andersonii* and *Pyramimonas* sp. = 20/193; 27/735; 54/2088; 81/4309; 214/7897; 231/20317; 444/46375; 1818/248,466; 245/0), and after 4 d incubation, 5 ml aliquots were removed from each bottle and fixed with 5% Lugol's solution. Then, all the *A. andersonii* cells and all or > 300 prey cells in three 1 ml SRCs were enumerated. Prior to taking the subsamples, the condition of *A. andersonii* and its prey was assessed under a dissecting microscope. The bottles were filled again to capacity with f/2–Si medium, capped, placed on a vertically rotating plate (at 0.9 r/min), and incubated at 20 ℃ under a 14:10 h light/dark cycle of 20 μE $m^{-2}s^{-1}$. The dilution of the cultures associated with refilling the bottles was considered in calculating the growth and ingestion rates.

The specific growth rate of *A. andersonii*, μ (d^{-1}), was calculated as follows:

$$\mu = \frac{\mathrm{Ln}\,(P_t / P_0)}{t} \qquad (1)$$

where P_O is the initial concentration of *A. andersonii* and P_t is the final concentration after time t. The time period was 4 d.

Data for *A. andersonii* growth rate were fitted to the following equation:

$$\mu = \frac{\mu_{max}\ (x - x')}{K_{GR} + (x - x')} \qquad (2)$$

where μ_{max} = the maximum growth rate (d^{-1}); x = prey concentration (cells ml^{-1} or ng C ml^{-1}), x′ = threshold prey concentration (the prey concentration where $\mu = 0$), and K_{GR} = the prey concentration sustaining ½ μ_{max}. Data were iteratively fitted to the model using DeltaGraph® (SPSS Inc., Chicago, IL, USA).

Ingestion and clearance rates were also calculated using the equations of Frost (1972) and Heinbokel (1978). The incubation times for calculating the ingestion and clearance rates were the same as for estimating the growth rate.

Ingestion rate data were fitted to a Michaelis–Menten equation:

$$IR = \frac{I_{max}\ (x)}{K_{IR} + (x)} \qquad (3)$$

where I_{max} = the maximum ingestion rate (cells $predator^{-1}d^{-1}$ or ng C $predator^{-1}d^{-1}$); x = prey concentration (cells ml^{-1} or ng C ml^{-1}), and K_{IR} = the prey concentration sustaining ½ I_{max}.

Table 4.1. Information on isolation and culturing of the *Alexandrium* species used in this study. WT, water temperature (℃); S, salinity; CLI, Culture maintenance light intensity (μE $m^{-2}s^{-1}$); CT Culture maintenance temperature (℃).

Species	Date	Area	WT	S	Prey or culture media	CLI	CT
Alexandrium affine	Aug, 2013	Yeosu, Korea	21.5	32.2	f/2−Si medium	20	20
Alexandrium fraterculus	Sep, 2013	Taean, Korea	23.4	32.8	L1−Si medium	20	20
Alexandrium andersonii	May, 2015	Jinhae, Korea	15.3	27.4	*Heterocapsa rotundata* or *Pyramimonas* sp.	20	20

Table 4.2. Taxa and equivalent spherical diameter (ESD, μm) of the three *Alexandrium* species, the potential prey provided, and their initial cell concentration (ICC, cells ml^{-1}) offered. Feeding occurrence of *Alexandrium affine*, *A. andersonii*, and *A. fraterculus*. Y−feeding was observed, N−feeding was not observed.

A. Predator species

Predator species	Strain name	Chain formation	ESD (±SE)	ICC
Alexandrium andersonii	AAJH1505	non−chain form	14.9 (0.5)	2000−5000
Alexandrium affine	AATA1308	chain form	31.4 (0.5)	2000−3000
Alexandrium fraterculus	AFYS1309	chain form	32.3 (0.7)	2000−3000

B. Prey species

Prey species/type	ESD (±SE)	ICC	*A. andersonii*	*A. affine*	*A. fraterculus*
Micro Bead					
micro bead A	1.9 (0.02)	1,000,000	N	N	N
micro bead B	5.3 (0.04)	100,000	N	N	N
Cyanobacteria					
Synechococcus	1.0 (0.2)	2,000,000	N	N	N
Diatom					
Skeletonema sp.	5.9 (1.1)	35,000–50,000	N	N	N
Prymnesiophyceae					
Isochrysis galbana	4.8 (0.2)	90,000–150,000	N	N	N
Prasinophytes					
Pyramimonas sp. (B)	5.6 (0.1)	150,000	**Y**	N	N
Cryptophytes					
Teleaulax sp.	5.6 (1.5)	50,000	**Y**	N	N
Storeatula major	6.0 (1.7)	50,000	N	N	N
Rhodomonas salina	8.8 (1.5)	50,000	N	N	N
Raphidophytes					
Heterosigma akashiwo	11.5 (1.9)	30,000	N	N	N
Chatonella ovata	40.0 (1.6)	2000	N	N	N
Dinoflagellates					
Heterocapsa rotundata (T, B)	9.5	50,000	**Y**	N	N
Amphidinium carterae (AT)	9.7 (1.6)	30,000	N	N	N

Prorocentrum minimum (T)	12.1 (2.5)	15,000	N	N	N
Prorocentrum donghaiense (T)	13.3 (2.0)	15,000	N	N	N
Heterocapsa triquetra (T, B)	15.0 (4.3)	10,000	N	N	N
Scrippsiella trochoidea (T)	22.8 (2.7)	7000	N	N	N
Cochlodinium polykrikoides (AT)	25.9 (2.9)	2000	N	N	N
Prorocentrum micans (T)	26.6 (2.8)	2000	N	N	N
Akashiwo sanguinea (AT)	30.8 (3.5)	2000	N	N	N
Alexandrium tamarense (T)	32.6 (2.7)	2000	N		
Lingulodinium polyedrum (T)	38.2 (3.6)	2000	N		
Naked ciliate					
Mesodinium rubrum	22 (0.04)	5500	N	N	N

T, thecate; AT, athecate (does not have thickened cellulose plates); B, body scales over the cell surface.

4.3.5. Cell volume of A. andersonii

After the 4-day incubation, the cell length and maximum width of *A. andersonii* preserved in 5% acid Lugol's solution (n = 10-30 for each prey concentration), were measured by analyzing the photomicrographs obtained using an image analysis system (Axiovert 200M, Carl Zeiss, Germany). The shape of *A. andersonii* was assumed to be an oval. The cell volume of the preserved *A. andersonii* was calculated according to the following equation: volume = $4/3\ \pi\ [(\text{cell length} + \text{cell width})/4]^3$.

4.3.6. Swimming speed

The swimming speed of *A. andersonii* cells growing autotrophically in f/2-Si medium, and of cells growing mixotrophically by feeding on *Pyramimonas* sp., were measured.

A dense culture (ca. 3000 cells ml^{-1}) of *A. andersonii* growing autotrophically in f/2-Si medium for 3 months under a 14:10 h light/dark cycle of 20 μE m^{-2} s^{-1}, was transferred to a 1000 ml PC bottle. An aliquot from the bottle was added to a 50 ml cell culture flask (BD Biosciences, MA, USA) and allowed to acclimate for 15 min. The video camera focused on one field (seen as one circle in a cell culture flask) under a dissecting microscope (SZX10, Olympus, Japan) at 20 ℃, and the swimming of *A. andersonii* cells was then recorded at a magnification of 32× using a video analysis system (Samsung Techwin, SRD-1673DN, Korea). Still images were taken using a CCD camera (Sony, DXC-C33, Japan). The mean and maximum swimming velocities were analyzed for all swimming cells moving

randomly, seen after the first 10 min. The average swimming speed was calculated based on the linear displacement of cells in 1 sec. during single-frame playback. The swimming speeds of 30 cells were measured.

A dense culture (ca. 4000 cells ml^{-1}) of *A. andersonii* growing mixotrophically on *Pyramimonas* sp. in f/2-Si medium under a 14:10 h light/dark cycle of 20 μE $m^{-2}s^{-1}$. Then, cells were starved for 2 weeks before transfer into 1000 ml PC bottles, after which swimming speeds of the algae were measured in the same manner described above.

A dense culture (ca. 2000 cells ml^{-1}) of *A. fraterculus* growing autotrophically in L1-Si medium under a 14:10 h light/dark cycle of 20 $m^{-2}s^{-1}$ were transferred into a 1000 ml PC bottle, after which swimming speeds were measured in the same manner described above.

The swimming speed of *A. affine* was obtained from Fraga et al. (1989).

4.3.7. Presence of saxitoxin (sxtA1, sxtA4) gene

To investigate whether the target species (*A. andersonii, A. affine*, and *A. fraterculus*) have putative saxitoxin genes or not, the presence of both *sxtA1* and *sxtA4* genes was tested by performing PCRs with extracted genomic DNA. To test the validity of this method, the presence of both *sxtA1* and *sxtA4* in *A. minutum* CCMP113 and CCMP1888 (which are known to have these two genes), was confirmed (Stüken et al., 2011; Murray et al., 2015).

Cells of *A. andersonii, A. affine, A. fraterculus*, and *A. minutum*

were concentrated by centrifuge, and their genomic DNA was extracted using an extraction kit (Bioneer, Korea). The PCR reactions were performed with a reaction mixture containing the same primer pairs (sxt001/sxt002 and sxt007/sxt008) and the same cycling conditions described in the previous studies (Stüken et al., 2011; Murray et al., 2015): (1) 94 ℃ for 3 min, 31× (94 ℃ for 30 s, 60 ℃ for 30 s, 68 ℃ for 1 min), 68 ℃ for 3 min for *sxtA1*; (2) 94 ℃ for 3 min, 31× (94 ℃ for 30 s, 57 ℃ for 30 s, 68 ℃ for 1 min), 68 ℃ for 3 min for *sxtA4*. DNA amplification was confirmed using HiQ^{TM} goRed (Hipurebio, Korea) with 1% agarose gel.

4.4. Results

4.4.1. Mixotrophic ability and feeding occurrences

Among the 20 algal prey species and micro-beads provided in this study, *A. andersonii* ingested *Teleaulax* sp. (Cryptophyte), *Pyramimonas* sp. (Prasinophyte), and *Heterocapsa rotundata* (Dinoflagellate), while *A. affine* and *A. fraterculus* did not ingest any prey items (Table 4.2, 4.3; Fig. 4.1, 4.2). However, *A. andersonii* did not ingest the other potential prey species (the haptophyte *Isochrysis galbana*, the diatom *Skeletonema* sp., the other cryptophytes *Storeatula major* and *Rhodomonas salina*, the raphidophytes *Heterosigma akashiwo* and *Chattonella ovata*, the mixotrophic dinoflagellates *Amphidinium carterae*, *Prorocentrum minimum*, *Prorocentrum donghaiense*, *Prorocentrum micans*, *Heterocapsa triquetra, Scrippsiella trochoidea, Cochlodinium polykrikoides, Akashiwo sanguinea,* and *Lingulodinium polyedrum*; and the

mixotrophic naked ciliate *Mesodinium rubrum*) even though it immobilized these potential prey (Table 4.2, 4.3, 4.4).

One *Teleaulax* cell, several ingested *Pyramimonas* cells, and one *H. rotundata* cell were found inside the protoplasm of *A. andersonii* cells (Fig. 4.1E, F, H, I, K, L). In addition, TEM micrographs confirmed that *A. andersonii* had food vacuoles containing ingested *Pyramimonas* and *Teleaulax* cells (Fig 4.2C, D, F, G). The chloroplasts of ingested *Pyramimonas* and *Teleaulax* cells inside the food vacuoles were similar to those of intact *Pyramimonas* and *Teleaulax* cells, but considerably different from the predator chloroplasts (Fig. 4.2A, G).

4.4.2. Feeding mechanism and time to ingest

Cells of *A. andersonii* immobilized several *H. rotundata* cells simultaneously and then engulfed an immobilized cell (Fig. 4.3). The time (mean $\pm$ standard error) for a captured *H. rotundata* cell to be engulfed by an *A. andersonii* cell was 17 $\pm$ 1 sec (n=3).

4.4.3. Immobilization and lysis of prey cells

After 48 h incubation with *A. andersonii* (concentrations = 2000–5000 cells ml^{-1}), most algal prey species were immobilized and further *Teleaulax* sp. and *Mesodinium rubrum* were lysed (Fig. 4.4A–D, Table 4.4). However, after 48 h incubation with *A. affine* (concentrations = 2000–3000 cells ml^{-1}), only *Pyramimonas* sp., *Teleaulax* sp., *Storeatula major*, *Rhodomonas salina*, *A. sanguinea*, and *M. rubrum* were immobilized and then lysed (Fig. 4.4E–G, Table

4.4). Moreover, after 48 h incubation with *A. fraterculus* (concentrations = 2000–3000 cells ml^{-1}), only *Teleaulax* sp., *S. major*, *R. salina*, *A. sanguinea*, and *M. rubrum* were immobilized and then lysed (Table 4.4).

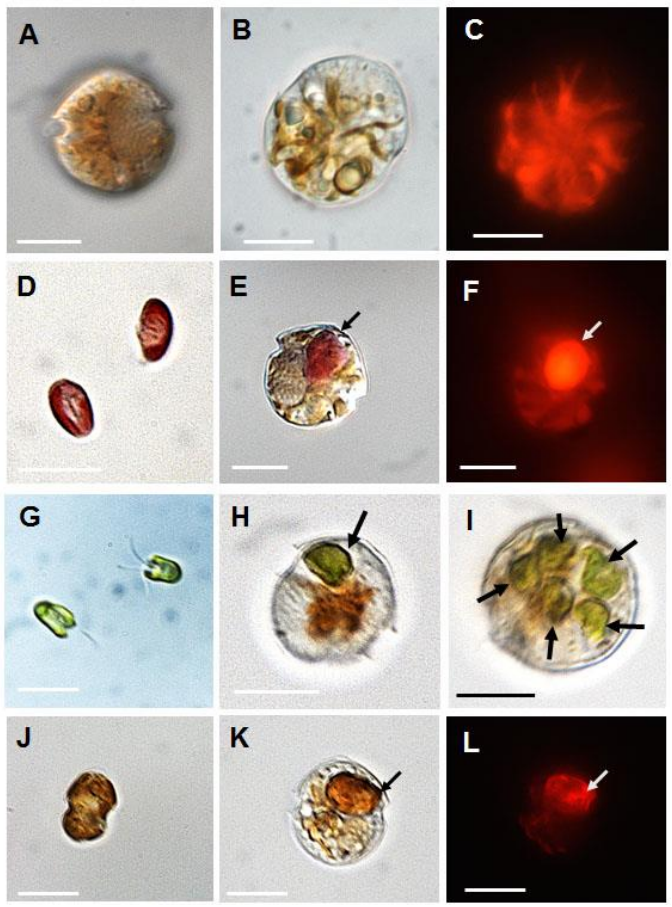

Fig. 4.1. *Alexandrium andersonii* and the algal prey species that were fed by *A. andersonii*. (A–C), *A. andersonii* cells growing autotrophically. (D), Intact *Teleaulax* sp. cells. (E–F), *A. andersonii* cell with an ingested *Teleaulax* sp. cell (arrow). (G), Intact *Pyramimonas* sp. cells. (H–I), *A. andersonii* cell with one or five ingested *Pyramimonas* sp. cells (arrows). (J), Intact *Heterocapsa rotundata*. (K–L), *A. andersonii* with an ingested *H. rotundata* cell (arrow). Scale bar = 10 μm.

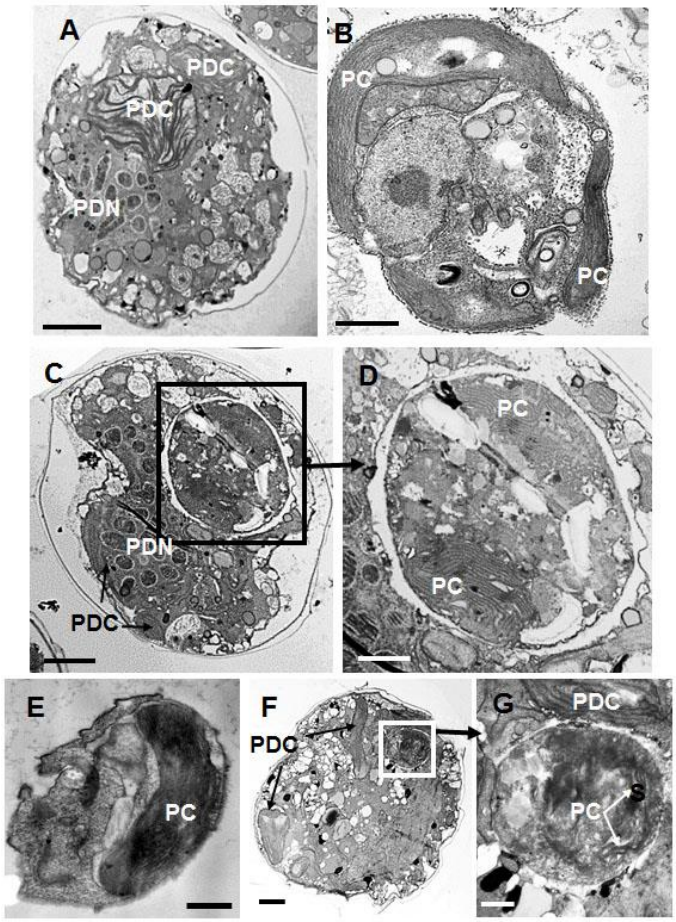

Fig. 4.2. Transmission electron micrographs (TEM) of *Alexandrium andersonii* and the algal prey species that were fed on by *A. andersonii*. (A), Unfed *A. andersonii* cell growing autotrophically. (B), A *Pyramimonas* sp. cell not ingested. (C), An *A. andersonii* cell with a food vacuole (box) containing an ingested *Pyramimonas* sp. cell. (D) Enlarged from (C). (E), A *Teleaulax* sp. cell not ingested. (F), An *A. andersonii* cell with a food vacuole (box) containing an ingested *Teleaulax* sp. cell. PDC: Predator's chloroplasts. PC: Prey's chloroplasts. Scale bar = 2 μm for (A), (C), and (F); 0.5 μm for (E) and (G); and 1 μm for (B) and (D).

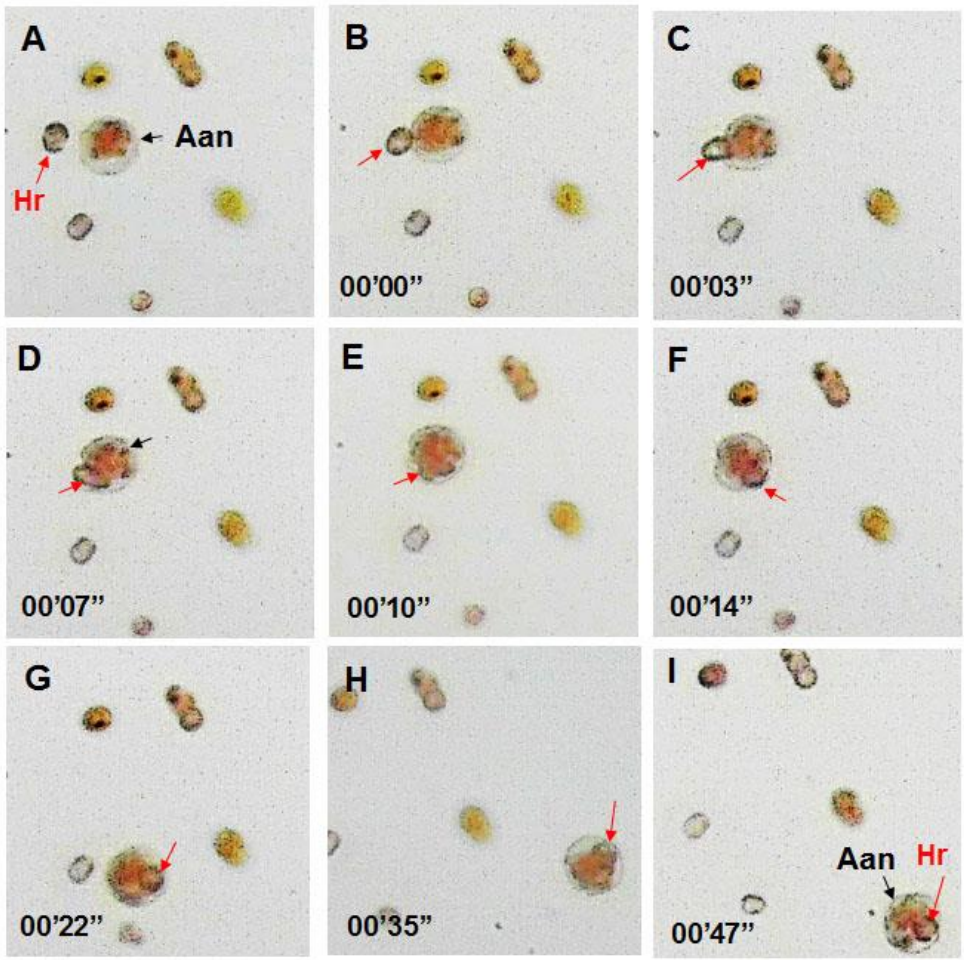

Fig. 4.3. Feeding process of *Alexandrium andersonii* (Aan, black arrow) feeding on *Heterocapsa rotundata* (Hr, red arrow). (A), An Aan cell approached a Hr cell. (B) and (C), the Aan cell captured and started to engulf the Hr cell. (D), the Aan cell engulfed half the prey cell body. (E–F), the Aan cell completely engulfed the prey cell. (G–I) leaving Aan cell. All predator and prey cells are the same cells. The numbers are min′ sec″.

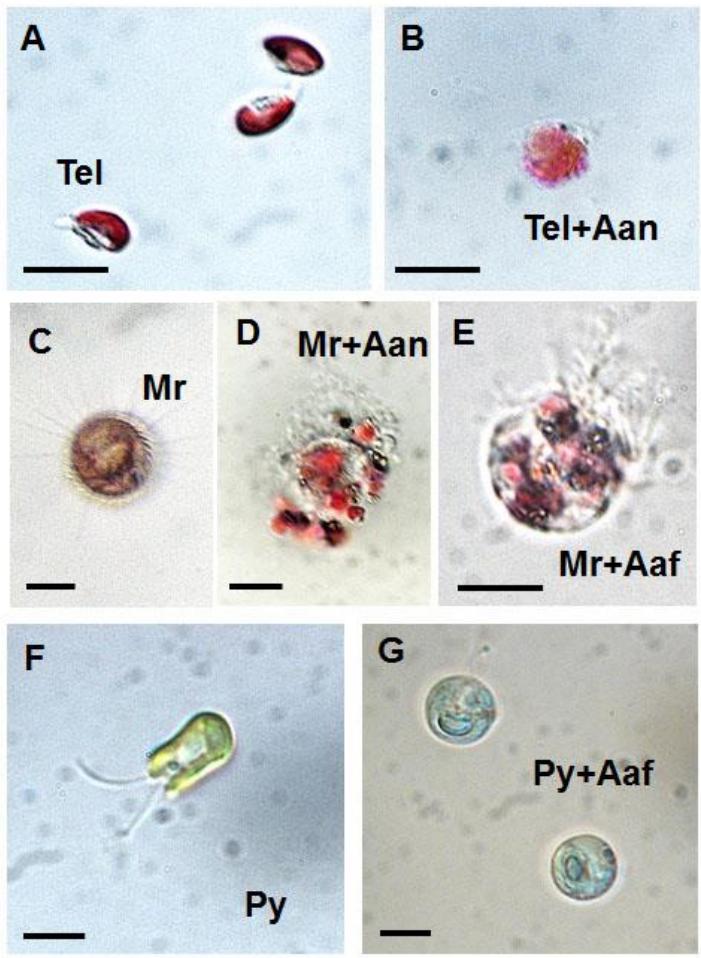

Fig. 4.4. Algal and ciliate cells lysed or deformed when incubated with *Alexandrium andersonii* (Aan) or *A. affine* cells (Aaf). (A), intact *Teleaulax* sp. cells (Tel). (B) A Tel cell lysed after being incubated with Aan for 1 h. (C), an intact *Mesodinium rubrum* (Mr) cell. (D), a Mr cell lysed after being incubated with Aan for 1 h. (E), a Mr cell lysed after being incubated with Aaf for 1 h. (F), an intact *Pyramimonas* sp. (Py) cell. (G) A Py cell lysed after being incubated with Aaf for 1 h. Scale bar = 10 μm for (A–E) and 5 μm for (F–G).

Table 4.3. Comparison of the prey species that the mixotrophic *Alexandrium* species were able to feed on. ESD, equivalent spherical diameter (μm) of: Aand, *A. andersonii*; Aaff, *A. affine*; Afra, *A. fraterculus*; Apsu, *A. pseudogonyaulax*; Atam, *A. tamarense*; Acat, *A. catenella*; Amin, *A. minutum*; Aphg, *A. pohangense*; Aost, *A. ostenfeldii*. T, thecate; AT, athecate (does not have thickened cellulose plates); B, body scales over the cell surface; Y, Feeding on the prey species; N, not able to feed on the species.

Potential prey species	ESD	Aand	Aaff	Afra	Apsu	Atam	Acat	Amin	Aphg	Aost
Cyanobacteria										
Synechococcus	1.0	N	N	N		Y	Y	Y		
Diatom										
Skeletonema spp.	5.9	N	N	N		Y	Y		N	
Prymnesiophyceae										
Isochrysis galbana	4.8	N	N	N		Y			N	
Prasinophytes										
Pyramimonas sp. (B)	5.6	Y	N	N						
Cryptophytes										
Teleaulax sp.	5.6	Y	N	N		Y			N	
Storeatula major	6.0	N	N	N					N	
Teleaulax acuta	7.1*				Y		N	N		
Rhodomonas salina	8.8	N	N	N		Y			N	
Raphidophytes										
Heterosigma akashiwo	11.5	N	N	N		Y			N	
Chatonella ovata	40.0	N	N	N						

Potential prey species	ESD	Aand	Aaff	Afra	Apsu	Atam	Acat	Amin	Aphg	Aost
Mixotrophic dionflagellates										
Heterocapsa rotundata (T, B)	9.5	Y	N	N	Y		N	N	N	
Amphidinium carterae (AT)	9.7	N	N	N		Y			N	
Prorocentrum minimum (T)	12.1	N	N	N		Y			N	
Prorocentrum donghaiense (T)	13.3	N	N	N		N				
Heterocapsa triquetra (T, B)	15.0	N	N	N	Y	N			N	
Gymnodinium aureolum (AT)	19.5								N	
Scrippsiella trochoidea (T)	22.8	N	N	N	N	N			N	
Cochlodinium polykrikoides (AT)	25.9	N	N	N		N			Y	
Prorocentrum micans (T)	26.6	N	N	N		N			N	
Akashiwo sanguinea (AT)	30.8	N	N	N		N			N	
Alexandrium tamarense (T)	32.6	N			N					
Gymnodinium catenatum (AT)	33.9					N			N	
Lingulodinium polyedrum (T)	38.2	N				N				
Dinophysis sp. (T)										Y
Naked ciliate										
Mesodinium rubrum	22.0	N	N	N	Y				N	
Unidentified ciliate										Y
Microbead										
Bacterium sized microbead A	1.9	N	N	N						
Microbead B	5.3	N	N	N						

number of eatable prey	3	0	0	4	8	2	1	1	2
number of tested prey	22	20	20	6	16	4	3	17	
Chain forming	N	Y	Y	N	Y	Y	Y	N	N
Reference		(1)		(2,3)	(4,5,6)	(2,5,6)	(2,6,7)	(8)	(9,10)

(1) This study, (2) Blossom et al. (2012), (3) Honsell et al. (1992), (4) Jeong et al. (2005b) (5) Yoo et al. (2009), (6) Jeong et al. (2005c) (7) Figueroa et al. (2007), (8) Lim et al. (2015), (9) Jacobson and Anderson (1996), (10) John et al. (2003); *, ESD data from Sommer et al. (2005).

Table 4.4. Comparison of the prey species that the mixotrophic *Alexandrium* species were able to immobilize (I) and/or lyse (L). ESD, equivalent spherical diameter (μm): Aand, *A. andersonii*; Aaff, *A. affine*; Afra, *A. fraterculus*; Apsu, *A. pseudogonyaulax*; Atam, *A. tamarense*; Acat, *A. catenella*; Amin, *A. minutum*; Aphg, *A. pohangense*; Aost, *A. ostenfeldii*. T, thecate; AT, athecate (does not have thickened cellulose plates); B, body scales over the cell surface.

Potential prey species	ESD	Aand	Aaff	Afra	Apsu	Atam	Acat	Amin	Aphg	Aost
Cyanobacteria										
Synechococcus sp.	1.0	–	–	–				–		
Diatom										
Skeletonema spp.	5.9	–	–	–		–	–		–	–
Prymnesiophyceae										
Isochrysis galbana	4.8	I	–	–		–			I	–
Prasinophytes										
Pyramimonas sp. (B)	5.6	I	I, L	–						
Cryptophytes										
Teleaulax sp.	5.6	I, L	I, L	I, L		–			L	–
Storeatula major	6.0	I	I, L	I, L					L	
Teleaulax acuta	7.1				I, L	L	L	–		
Rhodomonas salina	8.8	I	I, L	I, L		L	L	L	L	L
Raphidophytes										
Heterosigma akashiwo	11.5	I	–	–		–			I	–
Chatonella ovata	40.0	I	–	–						

Potential prey species	ESD	Aand	Aaff	Afra	Apsu	Atam	Acat	Amin	Aphg	Aost
Mixotrophic dionflagellates										
Heterocapsa rotundata (T, B)	9.5	I	–	–	I		I, L	–	I	
Amphidinium carterae (AT)	9.7	I	–	–		–			I	–
Prorocentrum minimum (T)	12.1	I	–	–		–			I	–
Prorocentrum donghaiense (T)	13.3	I	–	–		–				–
Heterocapsa triquetra (T, B)	15.0	I	–	–	I	–			I	–
Gymnodinium aureolum (AT)	19.5								I	
Scrippsiella trochoidea (T)	22.8	I	–	–	I	–			I	–
Cochlodinium polykrikoides (AT)	25.9	I	–	–		–			I	–
Prorocentrum micans (T)	26.6		–	–		–			I	–
Akashiwo sanguinea (AT)	30.8	I	I, L	I, L		–			I	–
Alexandrium tamarense (T)	32.6	I			I					
Gymnodinium catenatum (AT)	33.9					–			I	–
Lingulodinium polyedrum (T)	38.2	I				–				–
Dinophysis sp. (T)										
Naked ciliate										
Mesodinium rubrum	22.0	I, L	I, L	I, L	I, L				L	
Reference			(1)		(2)	(2, 3, 4)	(2, 3)	(3)	(4)	(3)

(1) This study, (2) Blossom et al. (2012), (3) Tillmann et al. (2008), (4) Tillmann et al. (2009), (5) Lim et al. (2015).

4.4.4. Growth and ingestion rates of *A. andersonii*

The specific growth rate of *A. andersonii* feeding on *Pyramimons* sp. was significantly affected by the mean prey concentration ($p<0.01$, ANOVA test) (Fig. 4.5). However, the specific growth rate of *A. andersonii* on *Pyramimons* sp. at mean prey concentrations < 649 ng C ml^{-1} (ca. 16,236 cells ml^{-1}) were not significantly different from that of *A. andersonii* without added prey ($p>0.1$, t−test). In contrast, the specific growth rates of *A. andersonii* on *Pyramimons* sp. at the higher mean prey concentrations were significantly greater than that of *A. andersonii* without added prey ($p<0.05$, t−test). When the data were fitted to Eq. (2), the maximum mixotrophic growth rate of *A. andersonii* on *Pyramimons* sp. under a 14:10 h light/dark cycle of 20 μE $m^{-2}s^{-1}$ was 0.432 d^{-1}, while the autotrophic growth rate was 0.243 d^{-1}.

With increasing mean prey concentration, the ingestion rate of *A. andersonii* increased rapidly at prey concentrations < 650 ng C ml^{-1}. (ca. 16,240 cells ml^{-1}), but became saturated at higher prey concentrations (Fig. 4.6). The maximum ingestion rate of *A. andersonii* on *Pyramimons* sp. was 1.03 ng C $predator^{-1}d^{-1}$ (25.6 cells $predator^{-1}d^{-1}$).

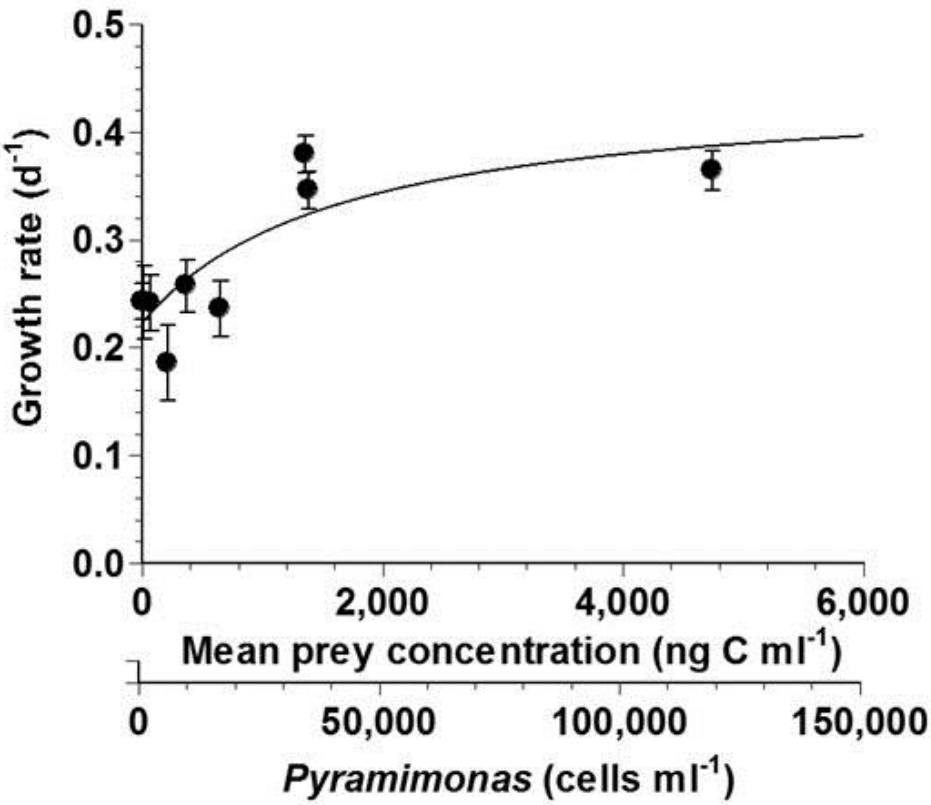

Fig. 4.5. Specific growth rates of *Alexandrium andersonii* eating *Pyramimonas* sp. as a function of mean prey concentration (x, ng C ml^{-1}). Symbols represent treatment means ± 1 SE. The curve is fitted by a Michaelis–Menten equation [Eq. (2)] using all treatments in the experiment. Growth rate (GR, d^{-1}) = 0.432 [(x + 751) / (714 + (x + 751))], r^2 = 0.527.

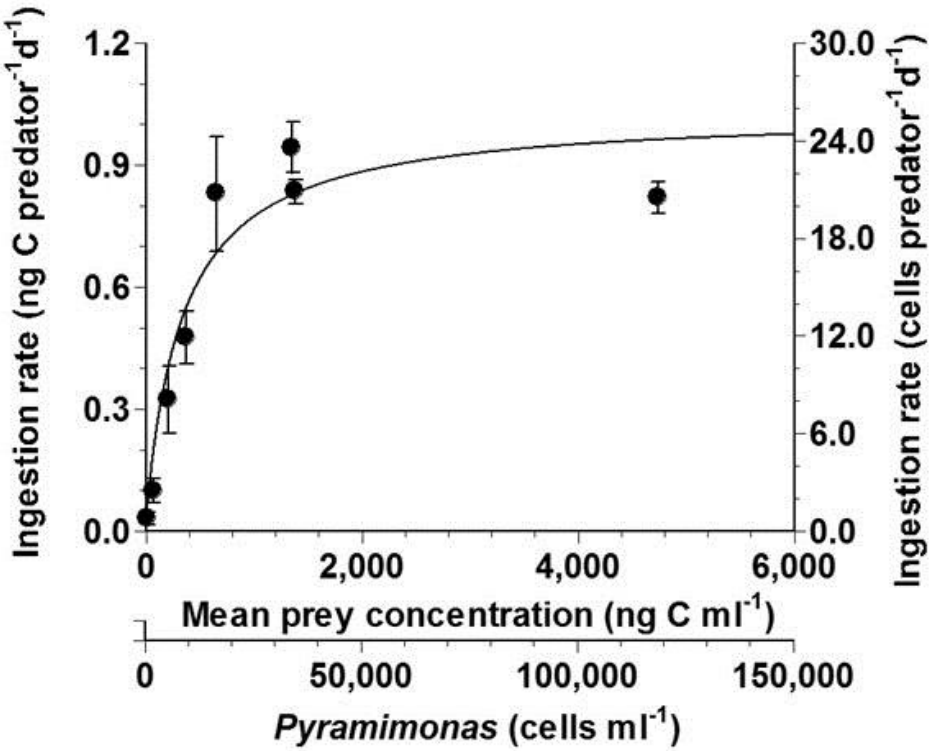

Fig. 4.6. Ingestion rates by *Alexandrium andersonii* of *Pyramimonas* sp. as a function of mean prey concentration (x, ng C ml^{-1}). Symbols represent treatment means ± 1 SE. The curve is fitted by a Michaelis–Menten equation [Eq. (3)] using all treatments in the experiment. Ingestion rate (IR, d^{-1}) = 1.03 [(x) / (335 + x))], r^2 = 0.854.

4.4.5. Cell volume

After a 4-d incubation, the mean cell volume of *A. andersonii* feeding on *Pyramimonas* sp. at the mean prey concentration of 1380 ng C ml^{-1} (3100 μm^3) was significantly greater than that when they were starved (2450 μm^3) ($p<0.05$, t-test), but that of *A. andersonii* feeding on *Pyramimonas* sp. at the other mean prey concentration was not significantly different from that when they were starved ($p>0.1$, t-test) (Fig. 4.7). The carbon contents of *A. andersonii* estimated from these cell volumes were 0.49-0.69 ng C per cell.

4.4.6. Swimming speed

The maximum swimming speed of *A. andersonii* growing mixotrophically on *Pyramimonas* sp. (n = 30) was 220 $\mu m\ s^{-1}$, while that of *A. andersonii* growing autotrophically (n = 30) was 150 $\mu m\ s^{-1}$ (Table 4.5). The average (± standard error) swimming speed of *A. andersonii* growing mixotrophically on *Pyramimonas* sp. [136 ± 44 $\mu m\ s^{-1}$] was significantly greater than that of *A. andersonii* growing autotrophically [59 ± 42 $\mu m\ s^{-1}$] ($p<0.001$, t-test).

The maximum and average (± standard error) swimming speed of non-chain forming *A. fraterculus* growing autotrophically was 680 $\mu m\ s^{-1}$ and 328 ± 123 $\mu m\ s^{-1}$ (n = 30), respectively (Table 4.5).

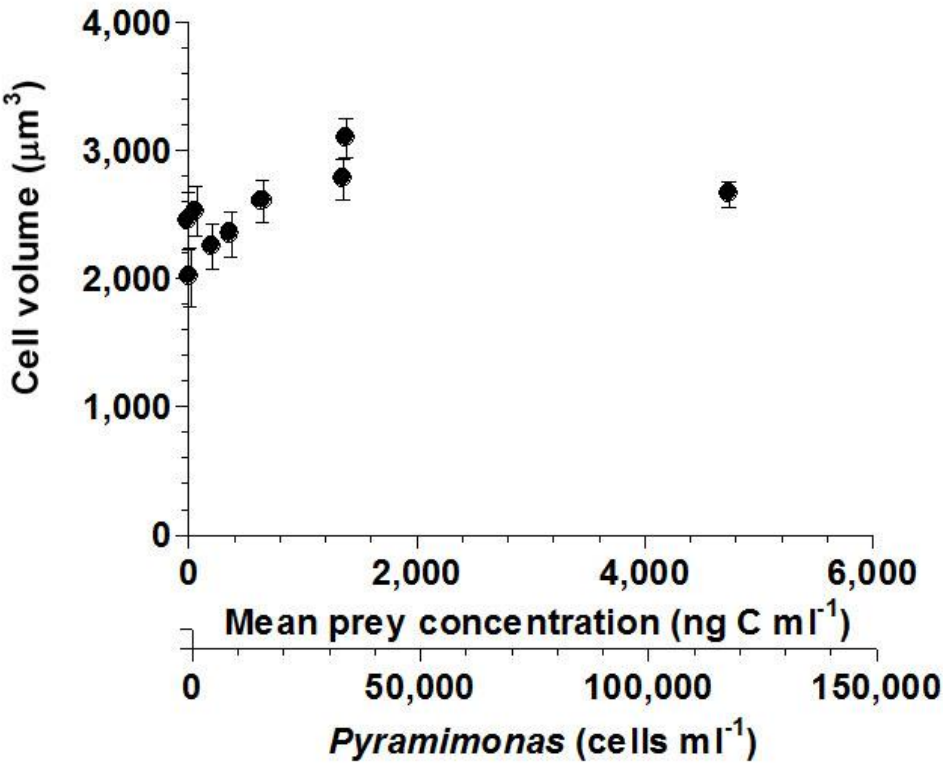

Fig. 4.7. Cell volume of *Alexandrium andersonii* eating *Pyramimonas* sp. after 4−day incubation as a function of mean prey concentration. Symbols represent treatment means ± 1 SE.

Table 4.5. Comparison of the maximum swimming speeds (μm s^{-1}) of (A) *Alexandrium* species whose mixotrophy have been revealed, and of the three *Alexandrium* species tested in this study and (B) the edible prey species of *A. andersonii* under the autotrophic (MSSA) and mixotrophic (MSSM) conditions. Temperatures (T, ℃). ESD is equivalent spherical diameter (μm).

A. *Alexandrium* spp.

Species	ESD*	T	MSSA (MSSM)	Ref
Alexandrium andersonii	14.9	20	150 (220)	This study
Alexandrium minutum	21.9	20	321	Lewis et al. (2006)
Alexandrium tamarense	24.3	20	249	Lewis et al. (2006)
Alexandrium catenella (single cell)	25.6	20	175	Karp-Boss et al. (2000)
Alexandrium affine	31.4	23	410	Fraga et al. (1989)
Alexandrium pohangense	32.0	20	340	Lim et al. (2015)
Alexandrium fraterculus (single cell)	32.3	20	680	This study
Alexandrium ostenfeldii	35.0	20	160	Lewis et al. (2006)

*, ESD of cells growing autotrophically.

B. Edible prey species of *Alexandrium andersonii*

Species	Taxa	MSSA	Reference
Teleaulax sp.	Cryptophyceae	143	Meunier et al. (2013)
Pyramimonas spp.	Prasinophyceae	558	Sym and Pienaar (1993)
Heterocapsa rotundata	Dinophyceae	564	Jakobsen et al. (2006)

4.4.7. Presence of SxtA genes

The Korean strains of *Alexandrium andersonii, A. affine*, and *A. fraterculus* used in this study had neither *sxtA1* nor *sxtA4* genes, while both genes were detected in the *A. minutum* strains (CCMP113 and CCMP1888).

4.5. Discussion

4.5.1. Mixotrophic ability of three *Alexandrium* species and kind of prey

This study clearly revealed that *A. andersonii* is a mixotrophic dinoflagellate, while *A. affine* and *A. fraterculus* lack mixotrophic ability. Therefore, *A. andersonii* is the 7th *Alexandrium* species whose mixotrophic ability has been discovered (Table 4.3). The size of *A. andersonii* is much smaller than *A. affine* and *A. fraterculus* (Table 4.5). In addition, the swimming speed of *A. andersonii* is much slower than that of *A. affine* and *A. fraterculus* (Table 4.5). In dinoflagellate feeding, larger predators have more of an advantage when feeding on large prey than do smaller predators (Jeong et al., 2010b). Thus, difference in size and slow swimming speed is likely not to be mainly responsible for this difference in the mixotrophic ability in these 3 *Alexandrium* species. Furthermore, *A. andersonii* is a non-chain forming species, while *A. affine* and *A. fraterculus* are chain forming species (Table 4.3). The mixotrophic species *A. pohangense*, *A. pseudogonyaulax*, and *A. ostenfeldii* are non-chain forming species (Honsell et al., 1992; John et al., 2003; Lim et al.,

2015), whereas the other mixotrophic species *A. tamarense*, *A. minutum*, and *A. catenella* are chain-forming species (Jeong et al., 2005b, 2005c; Yoo et al., 2009). Therefore, whether an *Alexandrium* species forms chains or not may not be responsible for possession of mixotrophic ability. Instead, *A. andersonii* may have genes related to phagotrophy, while *A. affine* and *A. fraterculus* may not have. It is worthwhile to investigate related genes by comparing transcriptome or proteome of *A. andersonii* with those of *A. affine* or *A. fraterculus*.

Cells of *A. andersonii* are able to feed on *Teleaulax* sp., *Pyramimonas* sp., and *Heterocapsa rotundata*, for which the ESDs are less than 10 μm. However, *A. andersonii* does not feed on *Isochrysis galbana*, *Skeletonema* sp., *Storeatula major*, *Rhodomonas salina*, and *Amphidinium carterae*, of which the sizes are similar to *Teleaulax* sp., *Pyramimonas* sp., and *H. rotundata*. Therefore, prey size may not be a critical factor affecting the feeding occurrence of *A. andersonii*. Even though *Teleaulax* sp., *S. major*, and *R. salina* are all cryptophytes, *A. andersonii* only ingested *Teleaulax* sp. In the phylogenetic trees based on rDNA, the clade containing *Teleaulax* is clearly divergent from the clade containing both *S. major* and *R. salina* (Marin et al., 1998; Hoef-Emden et al., 2002). Therefore, as prey for *A. andersonii,* there may be a big difference in genetics (and thus in biochemicals) at the genus level of the cryptophytes. This differential feeding of *A. andersonii* on these three cryptophyte genera may cause selection of dominant cryptophyte genera at sea. Furthermore, *Teleaulax* sp., *Pyramimonas* sp., and *H. rotundata* are cryptophyte, prasinophyte, and dinoflagellate, respectively. Furthermore, *Teleaulax* sp. do not have theca, *Pyramimonas* sp. have body scales, but *H. rotundata* has both theca and body scales.

Therefore, factors other than high level of taxa or the possession of body scale or theca are likely to affect the kind of prey selected by *A. andersonii*.

The predator *A. andersonii* has a greater number of prey items than *A. pohangense*, but less than *A. pseudogonyaulax* or *A. tamarense* (Table 4.3); *A. pohangense* is able to feed on only *Cochlodinium polykrikoides*, but *A. pseudogonyaulax* feeds on *Teleaulax acuta*, *Heterocapsa rotundata*, *Heterocapsa triquetra*, and *Mesodinium rubrum* (Blossom et al., 2012; Lim et al., 2015). Therefore, *A. andersonii* and *A. pseudogonyaulax* may compete for *Teleaulax* and *H. rotundata* prey.

Cells of *A. andersonii* engulf prey cells after immobilizing them. Similar feeding behaviors have been reported in *A. pohangense* and *A. pseudogonyaulax* (Blossom et al. 2012; Lim et al., 2015). However, *A. andersonii* does not form a mucus trap as *A. pseudogonyaulax* does. *A. affine* and *A. fraterculus* also immobilized *Teleaulax* sp. and/or *Pyramimonas* sp.; however, they did not feed on the potential prey. The maximum swimming speeds of the edible prey *Pyramimonas* and *Heterocapsa rotundata* are ca. 560 μm s^{-1}, which is greater than that of *A. andersonii* (ca. 150 μm s^{-1}; one of the slowest *Alexandrium* species), but comparable to that of *A. affine* and *A. fraterculus* (410–680 μm; Table 4.5). Therefore, immobilization of these prey species gives *A. andersonii* a big advantage for capturing tem. The time for a *H. rotundata* cell to be engulfed by *A. andersonii* (i.e., 15 sec) is similar to that by *A. pseudogonyaulax*, but much shorter than the time needed by the mixotrophic dinoflagellates *Gonyaulax polygramma* and *Lingulodinium polyedrum* to engulf prey cells similar in size to *H. rotundata*. This is true even though *G. polygramma* and *L. polyedrum*

are much larger than *A. andersonii*, but are comparable in size to *A. pseudogonyaulax* (Table 4.6). Therefore, immobilization of moving cells may enable *A. andersonii* to easily handle and engulf prey cells.

Chemicals produced by *A. andersonii*, *A. affine*, *A. fraterculus, A. pohangense, A. pseudogonyaulax*, *A. catenella*, and *A. tamarense* are known to lyse the bodies of diverse phytoplankton and heterotrophic protists after immobilization (Tillmann and John, 2002; Tillmann et al., 2008, 2009; Blossom et al., 2012; Kim et al., 2016). These predators may lose a chance to feed on prey cells if prey cells are completely lysed. However, lysing bodies of co-occurring phytoplankton and heterotrophic protists may allow *Alexandrium* spp. to eliminate these potential competitors or predators. The strains of *A. andersonii*, *A. affine*, and *A. fraterculus* used in this study were revealed by DNA analyses not to have saxitoxin genes. Thus, the chemicals for immobilization and/or lysis of potential prey cells appear not to be associated with saxitoxin. Tillmann and John (2002) and Kim et al. (2016) also suggested that chemicals related to immobilization and/or lysis of other protist cells caused by some *Alexandrium* species were not related to PSP toxins, but were caused by some unknown compounds. Therefore, it is worthwhile to identify the nature of the biochemicals used by *Alexandrium* for immobilization and/or lysis of prey cells.

Table 4.6. Comparison of time (FT, s^{-1}) for a prey cell to be engulfed by mixotrophic dinoflagellate predators that can immobilize prey cells, or not, when the prey sizes were similar. ESD, equivalent spherical diameter (μm); IM: Immobilization.

Species	ESD*	Prey	ESD	IM	FT	Ref.
Alexandrium andersonii	14.9	*Heterocapsa rotundata*	9.5	Y	17	(1)
Gonyaulax polygramma	32.5	*Amphidinium carterate*	9.7	N	291−346	(2)
Alexandrium pseudogonyaulax	35.4	*Heterocapsa rotundata*	9.5	Y	≤15	(3)
Lingulodinium polyedrum	38.2	*Heterosigma akashiwo*	11.5	N	180	(4)

*, ESD of cells growing autotrophically.

(1) This study, (2) Jeong et al. (2005a), (3) Blossom et al. (2012), (4) Jeong et al. (2005b)

4.5.2. Growth and ingestion rates

The autotrophic growth rates of the diverse strains of *Alexandrium andersonii* (0.05–0.32 d^{-1}, Frangópulos et al., 2004; Sampedro et al., 2013) are comparable to that of *A. pohangense, A. pseudogonyaulax, A. ostenfeldii*, or *A. minutum,* but lower than that of *A. catenella, A. affine, A. tamarense*, or *A. fundyense* (Table 4.7). The results of this study show that consumption of the optimal prey, *Pyramimonas* sp., elevates the growth rate of *A. andersonii* by 78% under the given conditions. Thus, in terms of growth rates, using a mixotrophic strategy, *A. andersonii* is able to compete with co-occurring *Alexandrium* species that have autotrophic growth rates higher than *A. andersonii*. In population dynamics models, the mixotrophic growth rate of *A. andersonii* should be used for k (growth rate) instead of the autotrophic growth rate when *A. andersonii* coexists with *Pyramimonas* species. The degree of elevation of the growth rate of *A. andersonii* through mixotrophy is greater than that of *A. pseudogonyaulax* (45%), but less than that of *A. pohangense* (390%). Interestingly, the degree of elevation through mixotrophy of each of these three *Alexandrium* species is the reverse of the number of prey species that each *Alexandrium* species is able to feed on. Thus, the degree of elevation through mixotrophy may trade off with diversity of prey items.

The maximum ingestion rate of *A. andersonii* on the optimal prey, *Pyramimonas* sp. is much lower than that of *A. pohangense* on the only prey, *Cochlodinium polykrikoides* (Table 4.7). The feeding behaviors of *A. andersonii* and *A. pohangense* are similar; they engulf

prey cells after immobilizing them (Lim et al., 2015). In general, maximum ingestion rates of mixotrophic or heterotrophic dinoflagellates increase with increasing body size (ESD) (Jeong et al., 2010b). The cells of *A. andersonii* are considerably smaller than those of *A. pohangense*. Therefore, compared to *A. pohangense*, the smaller size of *A. andersonii* may be partially responsible for the lower maximum ingestion rate, because the prey cells of both these *Alexandrium* predators are motionless when feeding is occurring.

The maximum mixotrophic growth rate of *Alexandrium andersonii* feeding on *Pyramimonas* sp. (0.432 d^{-1}) is similar to that of the dinoflagellate *Karlodinium armiger* feeding on *Pyramimonas orientalis* (0.45 d^{-1}), but much lower than that by the mixotrophic dinoflagellate *Ansanella granifera* on the same prey (1.426 d^{-1}) (Table 4.8). However, the maximum ingestion rate by *A. andersonii* of *Pyramimonas* sp. (1.03 ng C predator$^{-1}d^{-1}$) is much greater than that by *K. armiger* of *P. orientalis* (0.02 ng C predator$^{-1}d^{-1}$), but similar to that of *A. granifera* on the same prey (0.97 ng C predator$^{-1}d^{-1}$) (Berge et al., 2008; Lee et al., 2014c). Therefore, the growth efficiency of *A. andersonii* feeding on *Pyramimonas* sp. is much lower than that of *K. armiger* on *P. orientalis*. *A. andersonii* is an engulfment feeder, while *K. armiger* is a peduncle feeder. Thus, sucking partial prey materials through a peduncle may give greater growth efficiency than engulfing the entire body of prey. The larger size of *A. andersonii* (ESD = 14.9 μm) may be partially responsible for the lower growth rate than smaller *A. granifera* (ESD = 10.5 μm) because the maximum ingestion rates of these two predators are similar. When *Pyramimonas* spp. are abundant, the abundance of *A.*

andersonii and *K. armiger* are expected to be lower than that of *A. granifera* in natural environments.

Now, seven *Alexandrium* species have been revealed to be mixotrophic, but two *Alexandrium* species are revealed to lack mixotrophic ability when based on the prey organisms tested in this study. However, there are still several *Alexandrium* species for which mixotrophic ability has not yet been tested. To better understand the bloom dynamics of an *Alexandrium* species, interactions between *Alexandrium* species and co-occurring species, and potential horizontal gene transfer from prey to the *Alexandrium* species, first the mixotrophic ability of the *Alexandrium* species should be explored.

Table 4.7. Comparison of autotrophic growth rate (AG, d^{-1}), maximum mixotrophic growth rate (MMG, d^{-1}), elevated growth rate due to phagotrophy [EG = (MMG−AG)/AG ×100 (%)], and maximum ingestion rates (MIR, ng C $predator^{-1}$ d^{-1}) of *Alexandrium* species for which mixotrophy had been previously revealed, and of the three *Alexandrium* species tested in this study. NA indicates not available.

Species	ESD	Mixotr−ophy	Optimal prey	AG	MMG	EG	MIR	Ref
Alexandrium andersonii	14.9	O	*Pyramimonas* sp.	0.24	0.43	78	1.03	(1)
				0.31	NA		NA	(2)
Alexandrium minutum	21.9	O		0.30	NA		NA	(3)
Alexandrium tamarense	24.3	O		0.54	NA		NA	(4)
Alexandrium catenella	25.6	O		0.43	NA		NA	(5)
Alexandrium affine	31.4	X	None	0.49	NA		NA	(1,6)
Alexandrium pohangense	32.0	O	*Cochlodinium polykrikoides*	0.09	0.49	435	4.99	(7)
Alexandrium fraterculus	32.3	X	None	NA	NA		NA	(1)
Alexandrium ostenfeldii	35.0	O		0.22	NA		NA	(8)
Alexandrium pseudogonyaulax	35.4	O	*Heterocapsa rotundata*	0.22	0.32	45	NA	(9)

(1) This study, (2) Sampedro et al. (2013), (3) Frangópulos et al. (2004), (4) Yamamoto and Tarutani (1999), (5) Li et al. (2011), (6) Nguyen−Ngoc (2004), (7) Lim et al. (2015), (8) Jensen and Moestrup (1997), (9) Blossom et al. (2012).

Table 4.8. Comparison of the known mixotrophic dinoflagellate predators (MTD) of *Pyramimonas* as prey species. ESD is equivalent spherical diameter, MMG is maximum mixotrophic growth rate, and IR is maximum ingestion rates (MIR, ng C predator^{-1}d^{-1}).

MTD	ESD	Prey	Strain no.	ESD	MMG	MIR	Ref.
Ansanella granifera	10.5	*Pyramimonas* sp.	PSSH1204	5.6	1.43	0.97	(1)
Alexandrium andersonii	14.9	*Pyramimonas* sp.	PSSH1204	5.6	0.43	0.24	(1)
Karlodinium armiger	16.7	*Pyramimonas orientalis*	K-0003	5.6	0.45	0.02	(1)

(1) Lee et al. (2014c), (2) This study, (3) Berge et al. (2008)

Chapter 5.

Predation by common heterotrophic protists on the mixotrophic red-tide causative ciliate, *Mesodinium rubrum*

5.1. Abstract

Mesodinium rubrum is a cosmopolitan ciliate that often causes red tides. Predation by heterotrophic protists is a critical factor that affects the population dynamics of red tide species. However, there have been few studies on predators feeding on *M. rubrum.* To investigate heterotrophic protists grazing on *M. rubrum,* I tested whether the heterotrophic dinoflagellates *Gyrodiniellum shiwhaense*, *Gyrodinium dominans*, *Gyrodinium spirale*, *Luciella masanensis*, *Oblea rotunda*, *Oxyrrhis marina*, *Pfiesteria piscicida*, *Polykrikos kofoidii*, *Protoperidinium bipes*, and *Stoeckeria algicida*, and the ciliate *Strombidium* sp. preyed on *M. rubrum*. *G. dominans*, *L. masanensis*, *O. rotunda*, *P. kofoidii*, and *Strombidium* sp. preyed on *M. rubrum*. However, only *G. dominans* had a positive growth feeding on *M. rubrum*. The growth and ingestion rates of *G. dominans* on *M. rubrum* increased rapidly with increasing mean prey concentration < 321 ng C mL^{-1}, but became saturated or slowly at higher concentrations. The

maximum growth rate of *G. dominans* on *M. rubrum* was 0.48 d^{-1}, while the maximum ingestion rate was 0.55 ng C $predator^{-1}$ d^{-1}. The grazing coefficients by *G. dominans* on populations of *M. rubrum* were up to 0.236 h^{-1}. Thus, *G. dominans* may sometimes have a considerable grazing impact on populations of *M. rubrum*.

5.2. Introduction

Mesodinium rubrum is a globally distributed ciliate (Lindholm 1985, Crawford 1989, Williams 1996, Gibson et al. 1997) that sometimes causes red tides in coastal waters (Johnson et al. 2004, Yih et al. 2004, Hansen and Fenchel 2006, Hansen et al. 2013, Johnson et al. 2013, Kang et al. 2013). *M. rubrum* is capable of both photosynthesis and prey ingestion (Gustafson et al. 2000, Yih et al. 2004, 2013). In addition, this species is an important prey for some dinoflagellate predators (i.e., *Amylax triacantha, Alexandrium psedogonyaulax, Dinophysis* spp., *Neoceratium furca*, *Oxyphysis oxytoxoides*) and an effective grazer of cryptophytes (Yih et al. 2004, Park et al. 2006, 2011, 2013, Blossom et al. 2012, Hansen et al. 2013, Johnson et al. 2013).

The predation of *M. rubrum* by heterotrophic protists is one of the critical factors that affect the population dynamics of red tide species. Heterotrophic protists play an important role in marine food webs, as they connect phototrophic plankton to higher trophic levels (Stoecker and Capuzzo 1990, Sherr and Sherr 2002, Myung et al.

2011, Garzio and Steinberg 2013). However, there have been few studies on the feeding patterns of common heterotrophic protists that frequently co-occur with *M. rubrum*. *O. oxytoxioides* is the only heterotrophic dinoflagellate that is known to feed on *M. rubrum* (Park et al. 2011). However, the growth and ingestion rates and/or the impact of heterotrophic protist grazing on *M. rubrum* have not been reported.

Gyrodiniellum shiwhaense, Gyrodinium dominans, *Gyrodinium spirale*, *Luciella masanensis*, *Oblea rotunda*, *Oxyrrhis marina*, *Pfiesteria piscicida*, *Polykrikos kofoidii*, *Protoperidinium bipes*, and *Stoeckeria algicida*, and naked ciliates having sizes of 30-50 μm have been reported to be present in many waters (Strom and Buskey 1993, Kim and Jeong 2004, Jeong et al. 2004, 2005, 2006, 2007, 2011a, 2011b, Yoo et al. 2010, 2013a, Seuthe et al. 2011, Kang et al. 2013). Furthermore, they often co-occur with *M. rubrum* (Hansen et al. 1995, Bouley and Kimmerer 2006, Kang et al. 2013). Thus it is worthwhile to explore interactions between *M. rubrum* and these heterotrophic protists.

The results of the present study would provide a basis for understanding the interactions between *M. rubrum* and heterotrophic protists.

5.3. Materials and Methods

5.3.1. Preparation of experimental organisms

M. rubrum (MR-MAL01) was isolated from water samples collected from Gomso Bay, Korea (35° 40′ N, 126° 40′ E) in May 2001 at a water temperature and salinity of 18 °C and 31.5, respectively. A clonal culture of *M. rubrum* was established as in Yih et al. (2004). The culture was maintained with *Teleaulax* sp. (previously described as a cryptophyte) in 500-mL bottles on a shelf at 20 °C under an illumination of 20 μE m^{-2} s^{-1} of cool white fluorescent light on a 14 h:10 h light-dark cycle (Yih et al. 2004).

For the isolation and culture of the heterotrophic dinoflagellates *G. shiwhaense, G. dominans*, *G. spirale*, *L. masanensis*, *O. rotunda*, *O. marina*, *P. piscicida*, *P. kofoidii*, *P. bipes*, *S. algicida*, and the naked ciliate *Strombidium* sp. plankton samples were collected from the waters of coastal area in Korea in 2001-2013, and a clonal culture of each species was established by two serial single-cell isolations (Table 5.1).

The carbon contents for *M. rubrum* (0.43 ng C $cell^{-1}$, n=40), the heterotrophic dinoflagellates, and the ciliates were estimated from cell volume according to Menden-Deuer and Lessard (2000). The cell volume of the preserved predators after each feeding experiment was conducted was estimated using the methods of Kim and Jeong (2004) for *G. dominans* and *G. spirale*, the protocol of Jeong et al. (2008) for *O. marina*, and the methods of Jeong et al. (2001) for *P. kofoidii*. The

cell volume of *O. rotunda* was calculated with an assumption that its geometry is an ellipsoid

5.3.2. Feeding occurrence

Experiment 1 was designed to test whether *G. shiwhaense, G. dominans*, *G. spirale*, *L. masanensis*, *O. rotunda*, *O. marina*, *P. piscicida*, *P. kofoidii*, *P. bipes*, and *S. algicida*, and the naked ciliate *Strombidium* sp. were able to feed on *M. rubrum* in living status (Table 5.1).

Approximately 10,000 *M. rubrum* cells were added to each of the two 42-mL polycarbonate (PC) bottles containing each of the heterotrophic dinoflagellates (2,000-10,000 cells) and the ciliates (10-80 cells) (final *M. rubrum* prey concentration = ca. 1,000 - 5,000 cells mL^{-1}). One control bottle (without prey) was set up for each experiment. The bottles were placed on a plankton wheel rotating at 0.9 rpm and incubated at 20 °C under an illumination of 20 μE m^{-2} s^{-1} on a 14 h: 10h light-dark cycle.

Five milliliter aliquots were removed from each bottle after 1, 2, 6, and 24 h incubation and then transferred into 6-well plate. Approximately 200 cells in the plate chamber were observed under a dissecting microscope at a magnification of 10-63x (SZX10, Olympus, Japan) to determine whether the predators were able to feed on *M. rubrum*. Predator cells containing prey cells were transferred onto glass slides and then their photographs were taken at a magnification of 400-1000x with a camera mounted on an inverted microscope (Zeiss-Axiovert 200M, Carl Zeiss Ltd.,

Göttingen, Germany).

5.3.3. Prey concentration effects on growth and ingestion rates

Experiment 2 was designed to measure the growth and ingestion rates of *G. dominans* as a function of *M. rubrum* concentration.

Dense cultures of *G. dominans* growing on the algal prey listed in Table 5.1 were transferred to 500-mL PC bottles containing filtered seawater. The bottles were filled to capacity with freshly filtered seawater, capped, and placed on plankton wheels rotating at 0.9 rpm and incubated at 20° C under an illumination of 20 μE m^{-2} s^{-1} on a 14 h:10 h light-dark cycle. To monitor the conditions and interaction between the predator and prey species, the cultures were periodically removed from the rotating wheels, examined through the surface of the capped bottles using a dissecting microscope, and then returned to the rotating wheels. At timepoints at which prey cells were no longer present in ambient water, they were still observed inside the protoplasm of the predators. I therefore decided to starve the predators for 1 day in order to minimize possible residual growth resulting from the ingestion of prey during batch culture. After this incubation period, cell concentrations of *G. dominans* were determined in three 1-mL aliquots from each bottle using a light microscope, and the cultures were then used to conduct experiments.

For each experiment, the initial concentrations of *G. dominans* and *M. rubrum* were established using an autopipette to deliver predetermined volumes of known cell concentrations to the bottles.

Triplicate 42-mL PC experiment bottles (mixtures of predator and prey) and triplicate control bottles (prey only) were set up at each predator-prey combination. Triplicate control bottles containing only *G. dominans* were also established at one predator concentration. To obtain similar water conditions, the water of predator cultures was filtered through a 0.7-μm GF/F filter and then added to the prey control bottles in the same amount as the predator culture for each predator-prey combination. All bottles were then filled to capacity with freshly filtered seawater and capped. To determine the actual predator and prey densities at the beginning of the experiment, a 5-mL aliquot was removed from each bottle, fixed with 5% Lugol's solution, and examined using a light microscope to enumerate the cells in three 1-mL Sedgwick-Rafter chambers (SRCs). The bottles were refilled to capacity with freshly filtered seawater, capped, and placed on rotating wheels under the conditions described above. Dilution of the cultures associated with refilling the bottles was considered when calculating growth and ingestion rates. A 10-mL aliquot was taken from each bottle after 48-h incubation and fixed with 5% Lugol's solution, and the abundance of *G. dominans* and prey were determined by counting all or >300 cells in three 1-mL SRCs. Before taking the subsamples, the conditions of *G. dominans* and their prey were assessed using a dissecting microscope as described above.

The specific growth rate of *G. dominans*, μ (d^{-1}), was calculated as:

$$\mu = \frac{\mathrm{Ln}\,(P_t / P_0)}{t} \qquad (1)$$

where P_0 and P_t = the concentration of *G. dominans* at 0 d and 2 d, respectively.

Data for *G. dominans* growth rates were fitted to a Michaelis–Menten equation:

$$\mu = \frac{\mu_{max}\ (x - x')}{K_{GR} + (x - x')} \qquad (2)$$

where μ_{max} = the maximum growth rate (d^{-1}); x = prey concentration (cells mL^{-1} or ng C mL^{-1}), x' = threshold prey concentration (the prey concentration where $\mu = 0$), K_{GR} = the prey concentration sustaining ½ μ_{max}. Data were iteratively fitted to the model using DeltaGraph® (Delta Point).

Ingestion and clearance rates were calculated using the equations of Frost (1972) and Heinbokel (1978). The incubation time for calculating ingestion and clearance rates was the same as that for estimating the growth rate. Ingestion rate data for *G. dominans* were also fitted to a Michaelis–Menten equation:

$$IR = \frac{I_{max}\,(x)}{K_{IR} + (x)} \qquad (3)$$

where I_{max} = the maximum ingestion rate (cells $predator^{-1}\,d^{-1}$ or ng C $predator^{-1}\,d^{-1}$); x = prey concentration (cells mL^{-1} or ng $C^{-1}\,mL^{-1}$), and K_{IR} = the prey concentration sustaining ½ I_{max}.

Additionally, the growth and ingestion rates of *L. masanensis, O. rotunda,* and *Strombidium* sp. on *M. rubrum* prey at a single prey concentration at which both growth and ingestion rates of *G. dominans* on *M. rubrum* were saturated were measured as described above.

5.3.4. Cell volume of *Gyrodinium dominans*

After the 2-day incubation, the cell length and maximum width of *G. dominans* preserved in 5% acid Lugol's solution (n=20-30 for each prey concentration) were measured using an image analysis system on images collected with an inverted microscope (AxioVision 4.5, Carl Zeiss Ltd., Göttingen, Germany). The shape of *G. dominans* was estimated to 2 cones joined at the cell equator (= maximum width of the cell). The carbon content was estimated from cell volume according to Menden-Deuer and Lessard (2000).

5.3.5. Grazing impact.

I estimated grazing coefficients attributable to small heterotrophic *Gyrodinium* spp. (20 - 30 μm in cell length) on *Mesodinium* by combining field data on abundances of small *Gyrodinium* spp. and prey with ingestion rates of the predators on the prey obtained in the present study. I assumed that the ingestion rates of the other small heterotrophic *Gyrodinium* spp. on *M. rubrum* are the same as that of *G. dominans* (*G. spirale* is larger). The data on

the abundances of *M. rubrum* and co-occurring small heterotrophic *Gyrodinium* spp. used in this estimation were obtained from water samples collected in 2004-2005 from Masan Bay and in 2008-2009 from Shiwha Bay.

The grazing coefficients (g, h^{-1}) were calculated as:

$$g = CR \times GC \quad (4)$$

where CR is the clearance rate (mL $predator^{-1}h^{-1}$) of a predator on *M. rubrum* at a given prey concentration and GC is the predator concentration (cells mL^{-1}). CR' s were calculated as:

$$CR = IR(h)/X \quad (5)$$

where IR(h) is the ingestion rate (cells eaten $predator^{-1}\,h^{-1}$) of the predator on the prey and X is the prey concentration (cells mL^{-1}). CR' s were corrected using Q_{10} = 2.8 (Hansen et al. 1997) because in situ water temperatures and the temperature used in the laboratory for this experiment (20 °C) were sometimes different.

5.4. Results

5.4.1. Feeding occurrence

Among the predators tested in the present study, *G. dominans*, *L. masanensis*, *Oblea rotunda*, *P. kofoidii*, and *Strombidium* sp. preyed on *M. rubrum* (Fig. 5.1, Table 5.1). However, *G. shiwhaense*, *G. spirale*, *O. marina*, *P. piscicida*, *P. bipes*, and *S. algicida* did not attempt to attack, even when it encountered *M. rubrum*.

5.4.2. Growth and ingestion rates

The specific growth rates of *G. dominans* on *M. rubrum* increased rapidly with increasing mean prey concentration up to ca. 321 ng C mL^{-1} (746 cells mL^{-1}), but slowly at higher concentrations (Fig. 5.2). When the data were fitted to Eq. (2), the maximum specific growth rate (μ_{max}) of *G. dominans* on *M. rubrum* was 0.48 d^{-1}. The feeding threshold prey concentration for the growth of *G. dominans* (i.e. no growth) was 23.3 ng C mL^{-1} (54 cells mL^{-1}).

The ingestion rates of *G. dominans* on *M. rubrum* increased rapidly with increasing mean prey concentration up to ca. 321 ng C mL^{-1} (746 cells mL^{-1}), but became saturated at higher concentrations (Fig. 5.3). When the data were fitted to Eq. (3), the maximum ingestion rate (I_{max}) of *G. dominans* on *M. rubrum* was 0.55 ng C $predator^{-1}$ d^{-1} (1.3 cells $predator^{-1}$ d^{-1}). The maximum clearance

rate of *G. dominans* on *M. rubrum* was 0.14 μL predator^{-1} h^{-1}.

The growth rates of *L. masanensis, O. rotunda,* and *Strombidium* sp. on *M. rubrum* prey at single prey concentrations (995−1,130 ng C mL^{-1}) at which both growth and ingestion rates of *G. dominans* on *M. rubrum* were saturated were negative.

5.4.3. Grazing impact.

When the abundances of *M. rubrum* and small heterotrophic *Gyrodinium* spp. (20−30 μm in cell length) in Masan Bay in 2004−2005 and Shiwha Bay in 2008−2009 (n=121) were 1−1,014 cells mL^{-1} and 1−1,356 cells mL^{-1}, respectively, grazing coefficients attributable to small heterotrophic *Gyrodinium* spp. on co−occurring *M. rubrum* were up to 0.236 h^{-1} (Fig. 5.4).

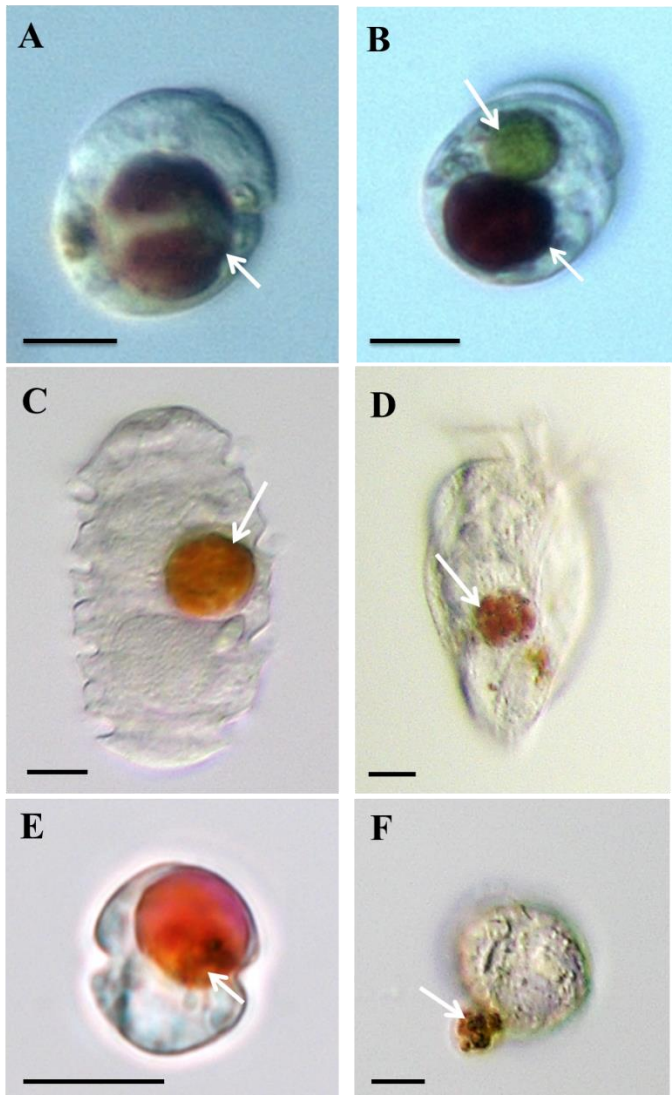

Fig. 5.1. Feeding by heterotrophic dinoflagellates on *Mesodinium rubrum*. (A–B) *Gyrodinium dominans* having 1–2 ingested *M. rubrum* cells. (C) *Polykrikos kofoidii*. (D) *Strombidium* sp., (E) *Luciella masanensis*, (F) *Oblea rotunda*. White arrows indicate prey (*M. rubrum*) materials. Scale bars = 10 μm.

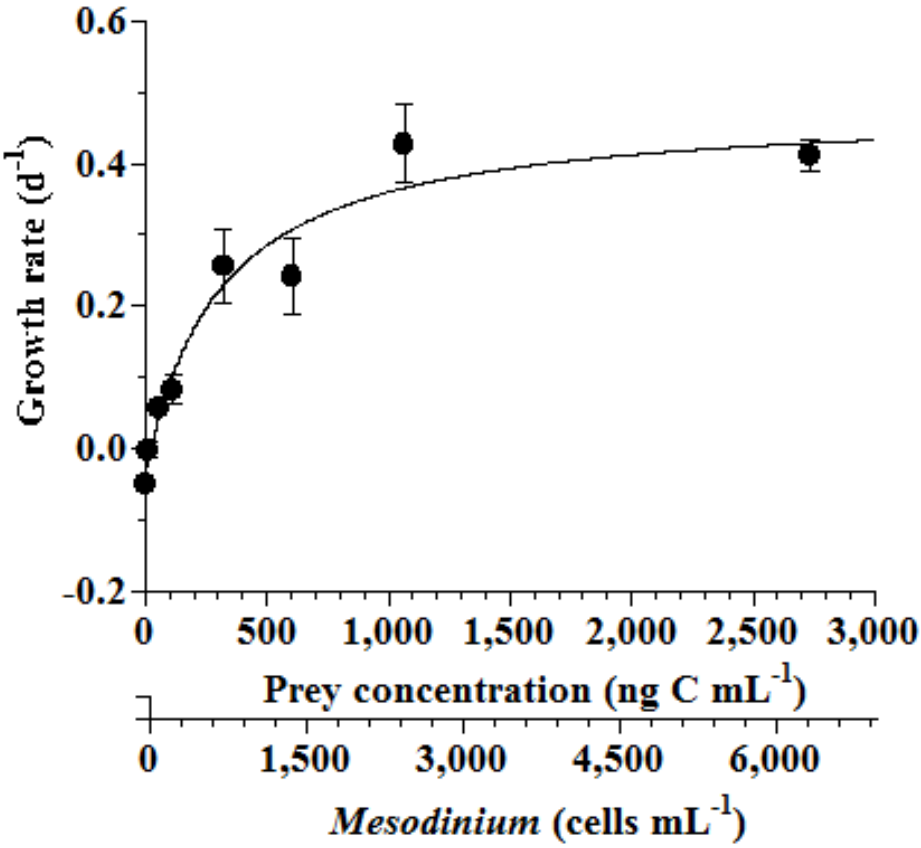

Fig. 5.2. Specific growth rate of the heterotrophic dinoflagellate *Gyrodinium dominans* on *Mesodinium rubrum* as a function of mean prey concentration (x). Symbols represent treatment means $\pm$ 1 SE. The curves are fitted by the Michaelis–Menten equation [Eq. (2)] using all treatments in the experiment. Growth rate (GR, d^{-1}) = 0.48 [(x − 23.3)/(325.7 + (x − 23.3))], r^2=0.881.

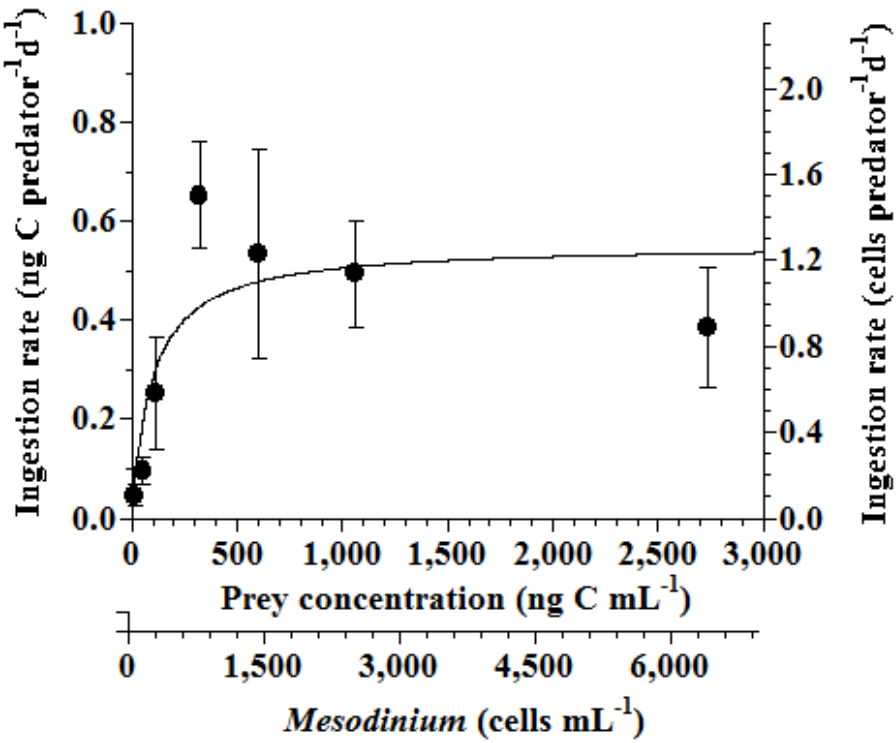

Fig. 5.3. Specific ingestion rates of the heterotrophic dinoflagellate *Gyrodinium dominans* on *Mesodinium rubrum* as a function of mean prey concentration (x). Symbols represent treatment means $\pm$ 1 SE. The curves are fitted by the Michaelis–Menten equation [Eq. (3)] using all treatments in the experiment. Ingestion rate (IR, ng C predator^{-1} d^{-1} = 0.55 [x/(94.6+ x)], r^2=0.453.

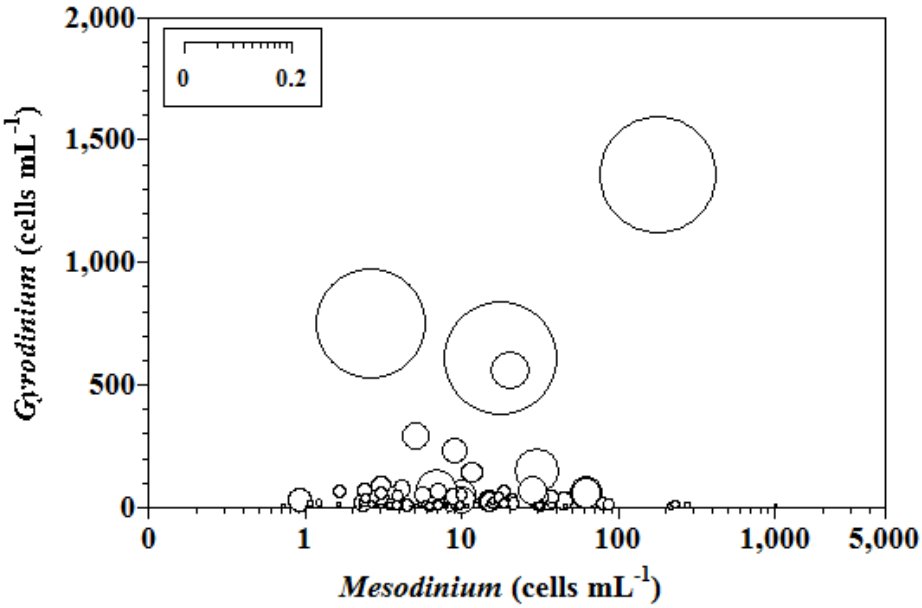

Fig. 5.4. Calculated grazing coefficients of small heterotrophic *Gyrodinium* spp. (A, n=121) in relation to the concentration of co-occurring *Mesodinium rubrum* (see text for calculation). Clearance rates, measured under the conditions provided in the present study, were corrected using Q_{10} = 2.8 (Hansen et al. 1997) because in situ water temperatures and the temperature used in the laboratory for this experiment (20 °C) were sometimes different. The scales of the circles in the inset boxes are g (d^{-1}).

Table 5.1. Conditions for the isolation and maintenance of the experimental organisms, and feeding occurrence (F) by diverse heterotrophic protistan predators.

	Type	FM	Strain isolation information				Prey species for maintenance	F
			Location	Time	T	S		
Predator								
Gyrodiniellum shiwhaense	HTD	PD	Shiwha	May. 2010	19.0	27.7	*Amphidnium carterae*	N
Gyrodinium dominans	HTD	EG	Masan	Nov. 2011	19.7	31.0	*Amphidnium carterae*	**Y**
Gyrodinium spirale	HTD	EG	Masan	May. 2009	19.7	31.0	*Prorocentrum minimum*	N
Luciella masanensis	HTD	PD	Shiwha	Apr. 2012	14.8	29.2	*Teleaulax* sp.	**Y**
Oblea rotunda	HTD	PA	Shiwha	Aug. 2010	26.8	23.7	*Prorocentrum minimum*	**Y**
Oxyrrhis marina	HTD	EG	Kunsan	May. 2001	16.0	27.7	*Amphidnium carterae*	N
Pfiesteria piscicida	HTD	PD	Jinhae	Feb. 2010	6.3	30.6	*Amphidnium carterae*	N
Polykrikos kofoidii	HTD	EG	Shiwha	Mar. 2010	9.3	23.4	*Lingulodinium polyedrum*	**Y**
Protoperidinium bipes	HTD	PA	Shiwha	Mar. 2012	6.4	27.8	*Skeletonema costatum*	N
Stoeckeria algicida	HTD	PD	Masan	Aug. 2007	24.5	29.7	*Heterosigma*	N

Strombidium sp.	NC	FF	Pohang	Jan. 2013	5.0	13.0	*akashiwo Heterocapsa rotundata*	Y
Prey								
Mesodinium rubrum	NC	EG	Gomso Bay	May. 2001	18	31.5	*Teleaulax* sp.	

HTD, Heterotrophic dinoflagellate; NC, Naked ciliate; FM, Feeding mechanism; PD, Peduncle feeder; EG, Engulfment feeder; PA, Pallium feeder; FF, filter feeder. T, Temperature (°C). S, Salinity. Y, Predator observed to feed on a living *M. rubrum* cell. N, Predator observed not to feed on a living *M. rubrum* cell.

5.5. Discussion

5.5.1. Predators

Among the heterotrophic dinoflagellates and a ciliate investigated in this study, *G. dominans*, *L. masanensis*, *O. rotunda*, *P. kofoidii*, and *Strombidium* sp. prey on *M. rubrum*. With respect to feeding mechanisms, *G. dominans*, *P. kofoidii*, and *Strombidium* sp. feed on prey by direct engulfment, but *L. masanensis*, and by a peduncle, and *O. rotunda* and by a pallium (Strom and Buskey 1993, Kim and Jeong 2004, Jeong et al. 2007, Yoo et al. 2010). Since organisms with different feeding modalities were able to graze on *M. rubrum*, I conclude that feeding mechanisms do not generally determine the ability of heterotrophic protists to feed on *M. rubrum*. In addition, the size range of the predators that can feed on *M. rubrum* is also wide, and thus this factor is also not a critical determinant of protist feeding on *M. rubrum*. *G. shiwhaense*, *G. spirale*, *O. marina*, *P. piscicida*, *P. bipes*, and *S. algicida* did not even attack *M. rubrum* when they encountered the ciliate. Thus, *G. dominans*, *L. masanensis*, *O. rotunda*, *P. kofoidii*, and *Strombidium* sp. may have an ability to detect *M. rubrum* cells by physical and/or chemical cues, while the other organisms may lack this feature.

M. rubrum usually stay motionless for a second, but swim or jump quickly. When it jumps, the maximum swimming speeds of *M. rubrum* are 2,217–12,000 μm s^{-1}, which are comparable to or greater than that of *G. dominans*, *O. rotunda*, *P. kofoidii*, and

Strombidium sp. (2,533, 420, 1,182, and 4,000 μm s^{-1}, respectively) (Barber and Smith Jr. 1981 cited by Smayda 2002, Crawford 1992, Buskey et al. 1993, Crawford and Lindholm 1997, Kim and Jeong 2004, Fenchel and Hansen 2006, Lee unpublished data). Therefore, *G. dominans*, *O. rotunda*, *P. kofoidii*, and *Strombidium* sp. are likely to capture *M. rubrum* when they are motionless and/or when *M. rubrum* bumps into them and then stuns them.

5.5.2. Growth and ingestion rates

G. dominans was the only predator whose growth actually increased when grazing on *M. rubrum* in this study, even though *L. masanensis*, *O. rotunda*, *P. kofoidii*, and *Strombidium* sp. also fed on *M. rubrum*. In addition, the mixotrophic dinoflagellates *Amylax triacantha* and *Dinophysis acuminata* are known to grow on *M. rubrum* (Park et al. 2006, 2013, Kim et al. 2008). Therefore, during red tides dominated by *M. rubrum*, *G. dominans*, *A. triacantha,* and *D. acuminata* are expected to be present. In contrast, *L. masanensis*, *O. rotunda*, *P. kofoidii*, and *Strombidium* sp. may be absent due to a lack of co-occurring alternative optimal prey species. The maximum growth rate of *G. dominans* on *M. rubrum* (0.48 d^{-1}) is lower than the mixotrophic growth rates of *A. triacantha* and *D. acuminata* on the same prey (0.68 d^{-1} and 0.91 d^{-1}, respectively) (Table 5.2). A lower ingestion rate of *G. dominans* on *M. rubrum* (0.55 ng C $predator^{-1}$ d^{-1}) when compared with *A. triacantha* (2.54 ng C $predator^{-1}$ d^{-1}) and *D. acuminata* (1.30 ng C $predator^{-1}$ d^{-1}) may be partially responsible

for this lower growth rate. During *M. rubrum* red tides, *G. dominans* may be less abundant than *A. triacantha* and *D. acuminata*. However, *G. dominans* can grow on diverse algal prey species, while *A. triacantha* and *D. acuminata* can only grow on *M. rubrum* (Nakamura et al. 1992, 1995, Kim and Jeong 2004, Park et al. 2006, 2013, Kim et al. 2008, Jeong et al. 2011a, 2014, Yoo et al. 2010, 2013b). Thus, the abundance of *G. dominans* in the period of red tides that are not associated with *M. rubrum* may be greater than those of *A. triacantha* and *D. acuminata*. I suggest that future studies should compare the relative abundances of these three predators, and their grazing impact on prey populations, during *M. rubrum*–associated red tides.

The maximum growth rate (μ_{max}) of *G. dominans* on *M. rubrum* (0.48 d^{-1}) is comparable to that on the mixotrophic dinoflagellates *Heterocapsa triquetra* and *Karenia mikimotoi*, and the raphidophyte *Chattonella antique*, but higher than that on the mixotrophic dinoflagellate *Biecheleria cincta*, the cryptophyte *Rhodomonas salina*, and the chlorophyte *Dunaliella teriolecta* (Table 5.3). However, the μ_{max} of *G. dominans* on *M. rubrum* is lower than that observed with the mixotrophic dinoflagellates *Gymnodinium aureolum, Prorocentrum minimum,* and *Symbiodinium voratum*, the euglenophyte *Eutrepsiella gymnastica*, and the diatom *Thalassiosira* sp. (Table 5.3). *M. rubrum*, these mixotrophic dinoflagellates, and the raphidophyte cause red tides in the waters of many countries (Crawford 1989, Heil et al. 20005, Jeong et al. 2011a, 2013, Park et al. 2013, Yih et al. 2013). *G. dominans* is likely to be more abundant during *M. rubrum* red tides than during *B. cincta*, *R. salina*, or *D.*

teriolecta red tides, but less abundant during *E. gymnastica, G. aureolum,* or *P. minimum* red tides.

The maximum rate at which *G. dominans* can ingest *M. rubrum* is one of the lowest among the algal prey species, with the exception of *B. cincta* and comparable to that on *R. salina* (Table 5.3). Interestingly, *M. rubrum* and *Rhodomonas* spp. exhibit jumping behaviors (Fenchel and Hansen 2006, Berge et al. 2008). These jumping behaviors of *M. rubrum* may act as an anti-predation behavior. However, the ratio of the maximum growth rate relative to the maximum ingestion rate (RMGI) of *G. dominans* on *M. rubrum* is greater than that on any other algal prey, with the exception of *P. minimum*. Therefore, *M. rubrum* is likely to be the most nutritious algal prey for *G. dominans*, *P. minimum* notwithstanding.

In the numerical response of *G. dominans* to four algal prey species, the feeding threshold prey concentration for growth of *G. dominans* on *M. rubrum* is lower than that of *E. gymnastica* or *G. aureolum,* but higher than that of *S. voratum* (Fig. 5.5A, Table 5.3). Therefore, *G. dominans* may preferentially grow on *M. rubrum* rather than on *E. gymnastica* or *G. aureolum* at low prey concentrations. The K_{GR} (the prey concentration sustaining ½ μ_{max}) of *G. dominans* on *M. rubrum* is greater than that on *G. aureolum,* and *S. voratum,* but lower than that on *E. gymnastica.* Therefore, the growth of *G. dominans* on *M. rubrum* is more sensitive to a change in prey concentration than the same parameter in *E. gymnastica*, but less sensitive than *G. aureolum,* and *S. voratum*. The functional response of *G. dominans* feeding on diverse algal prey species follows a Holling type II pattern

(Holling 1959). With respect to the functional response of *G. dominans* to eight algal prey species, the K_{IR} (the prey concentration sustaining ½ I_{max}) when grown on *M. rubrum* is greater than that obtained with *R. salina*, *P. minimum*, *D. teriolecta,* and *H. triquetra,* but lower than that obtained with *E. gymnastica, G. aureolum,* and *S. voratum* (Fig. 5.5B). Therefore, the ingestion of *G. dominans* on *M. rubrum* is more sensitive to a change in prey concentration than *E. gymnastica, G. aureolum,* and *S. voratum*, but less sensitive than *R. salina*, *P. minimum*, *D. teriolecta,* and *H. triquetra*.

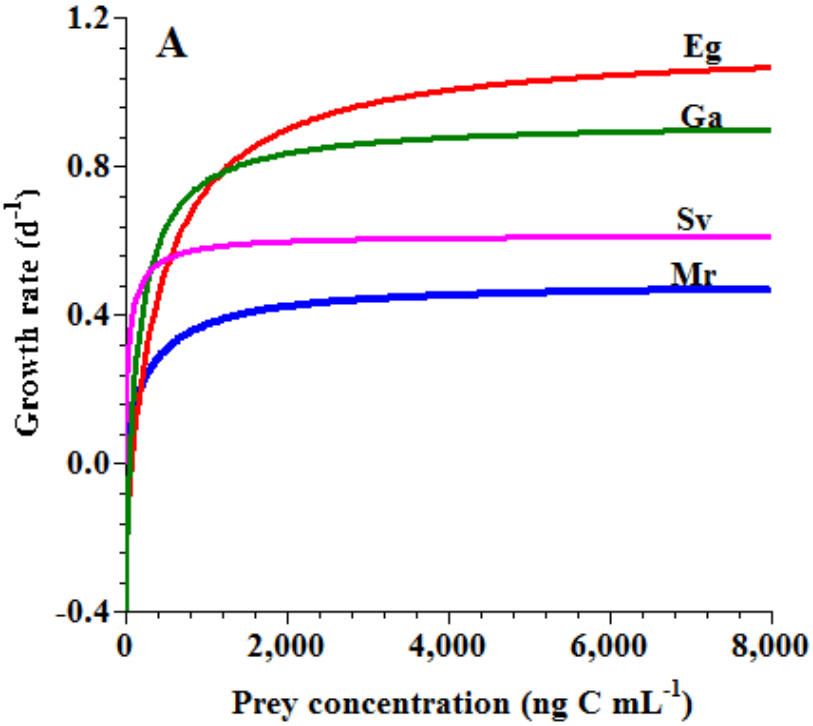

Fig. 5.5A. A comparison of the numerical responses of the heterotrophic dinoflagellate *Gyrodinium dominans* feeding on diverse prey related to prey concentration. Rates are corrected to 20 °C using Q_{10} = 2.8 (Hansen et al. 1997). *Eutreptiella gymnastica* (Eg, Euglenophyte), *Gymnodinium aureolum* (Ga, Mixotrophic dinoflagellate), *Mesodinium rubrum* (Mr, mixotrophic ciliate), *Symbiodinium voratum* (Sv, mixotrophic dinoflagellate), *Heterocapsa triquetra* (Ht, Mixotrophic dinoflagellate), *Dunaliella tertiolecta* (Dt, Chlorophyte), *Prorocentrum minimum* (Pm, mixotrophic dinoflagellate), *Rhodomonas salina* (Rs, cryptophyte). All responses in A were fitted to Eq. 2, whereas those in B were fitted to Eq. 3.

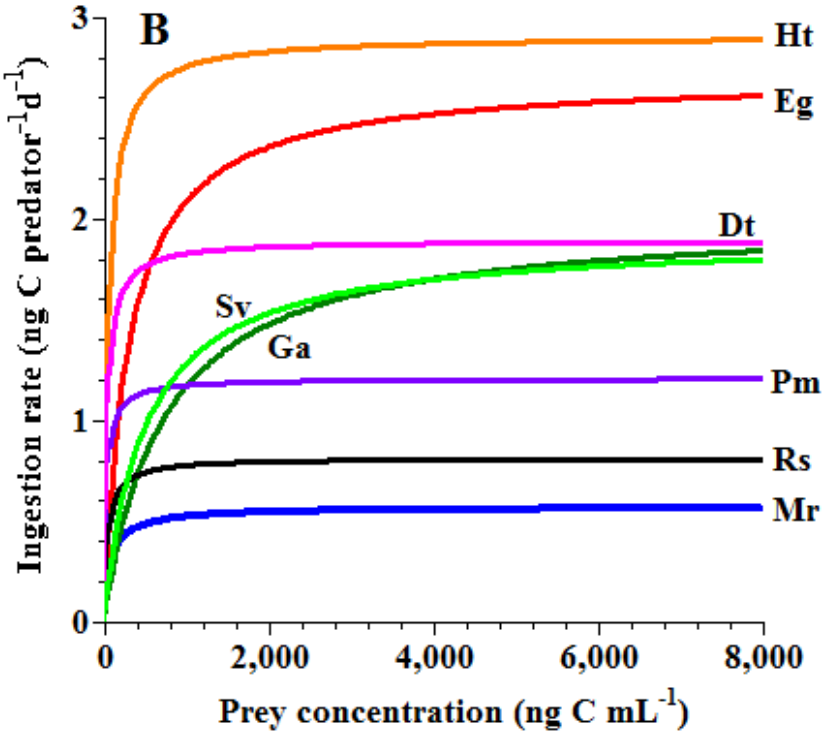

Fig. 5.5B. A comparison of the functional responses of the heterotrophic dinoflagellate *Gyrodinium dominans* feeding on diverse prey related to prey concentration. Rates are corrected to 20 °C using Q_{10} = 2.8 (Hansen et al. 1997). *Eutreptiella gymnastica* (Eg, Euglenophyte), *Gymnodinium aureolum* (Ga, Mixotrophic dinoflagellate), *Mesodinium rubrum* (Mr, mixotrophic ciliate), *Symbiodinium voratum* (Sv, mixotrophic dinoflagellate), *Heterocapsa triquetra* (Ht, Mixotrophic dinoflagellate), *Dunaliella tertiolecta* (Dt, Chlorophyte), *Prorocentrum minimum* (Pm, mixotrophic dinoflagellate), *Rhodomonas salina* (Rs, cryptophyte). All responses in A were fitted to Eq. 2, whereas those in B were fitted to Eq. 3.

Table 5.2. Growth and ingestion rates of dinoflagellate predators when feeding on *Mesodinium rubrum*.

Predators	ESD	Type	Feeding mechanism	GR	IR	Reference
Gyrodinium dominans	20.0	HTD	Engulfment	0.48	0.55	This study
Amylax triacantha	30.0	MTD	Engulfment	0.68	2.54	Park et al. (2013)
Dinophysis acuminata	35.0	MTD	Peduncle	0.91	1.30	Kim et al. (2008)

HTD, heterotrophic dinoflagellate; MTD, mixotrophic dinoflagellate; GR, growth rate (d^{-1}); IR, ingestion rate (ng C predator^{-1} d^{-1}).

Table 5.3. Comparison of growth and grazing data for *Gyrodinium dominans* on diverse prey species.

Prey species	Type	ESD	MGR	K_{GR}	x'	MIR	K_{IR}	RMGI	Reference
Thalassiosira sp.	DIA	5.4	0.73			–		–	Nakamura et al. (1995)
Rhodomonas salina	CR	6.5	0.21			0.8	49	0.21	Calbet et al. (2013)
Dunaliella teriolecta	CH	6.5	0.28			1.9	37	0.12	Calbet et al. (2013)
Symbiodinium voratum	MTD	11.1	0.61	65	0.4	1.9	493	0.32	Jeong et al. (2014)
Prorocentrum minimum	MTD	12.1	1.13			1.2	31	0.94	Kim and Jeong (2004)
Biecheleria cincta	MTD	12.2	0.07			0.1		0.54	Yoo et al. (2013b)
Eutreptiella gymnastica	EU	12.6	1.13	499	106	2.7	299	0.42	Jeong et al. (2011a)
Heterocapsa triquetra	MTD	15.3	0.54			2.9	56	0.23	Nakamura et al. (1995)
Karenia mikimotoi	MTD	16.8	0.48			–		–	Nakamura et al. (1995)
Gymnodinium aureolum	MTD	19.5	0.92	207	76	2.0	727	0.46	Jeong et al. (2010)
Mesodinium rubrum	MNC	22.0	0.48	326	23	0.6	95	0.87	This study
Chatonella antique	RA	35.3	0.50			2.3		0.22	Nakamura et al. (1992)

ESD, equivalent spherical diameter, μm; MGR, maximum growth rate, d^{-1}; K_{GR}, the prey concentration sustaining ½ μ_{max}, ng C mL^{-1}; x', threshold prey concentration, ng C mL^{-1}; MIR, maximum ingestion rate, ng C predator $^{-1}$ d^{-1}; K_{IR}, the prey concentration sustaining ½ I_{max}, ng C mL^{-1}; RMGI, ratio of MGR relative to MIR. Rates are corrected to 20 °C using Q_{10} = 2.8 (Hansen *et al.*, 1997). DIA, diatom; CR, cryptophyte; CH, chlorophyte; MTD, mixotrophic dinoflagellate; EU, euglenophyte; MNC, mixotrophic naked ciliate; RA, raphidophyte.

5.5.3. Grazing impact

To our knowledge, prior to this study, there had been no reports on the impact of protist grazing on algal populations. Grazing coefficients derived from studies in Masan Bay in 2004–2005 and Shiwha Bay in 2008–2009 show that up to 21% of *M. rubrum* populations can be removed by small *Gyrodinium* populations in approximately 1 d. Therefore, small heterotrophic *Gyrodinium* spp. can have a considerable grazing impact on populations of *M. rubrum* under suitable conditions. *G. dominans* is one of the few protistan grazers that are able to feed on *M. rubrum*, and is the only protistan grazer with a documented grazing impact on *M. rubrum* abundance. This finding should be taken into consideration when developing models to explain the red tide dynamics of *M. rubrum*.

Chapter 6.
Nutrient conditions altering effects of warming on phytoplankton production in coastal waters

6.1. Abstract

Phytoplankton production in coastal waters of temperate regions is a critical concern because it greatly affects seafood production, human health, and recreational activities. However, the effects of warming on phytoplankton production in these regions are not well understood. Nutrient concentrations in these waters have been increasing or decreasing depending on the policies of each country. Thus, the effects that nutrient concentration may have on the impact of future warming on phytoplankton production should be assessed. These effects were revealed to be critical when assessed by comparing phytoplankton biomasses between experiments under 64 different initial conditions formed by combining 4 different water temperatures (i.e., ambient, +2, +4, and +6 °C) and 2 different nutrient conditions (i.e., non-enriched and enriched) using natural water sampled 8 times at intervals of 1-2 months. Under non-enriched conditions, the effects of temperature elevation on phytoplankton production were inconsistent (i.e., positive, negative, or negligible) irrespective of temperature elevation, whereas under enriched conditions, the effects were all positive. The ratio of initial nitrate concentration to Chl-a concentration [NCCA, μM (μg L^{-1})$^{-1}$]

mainly determined the directionality of the temperature effect. With a few exceptions, when the NCCA value in the ambient or nutrient-enriched waters was > 1.5, temperature elevation increased phytoplankton production. The exceptions were caused by grazing impact by protistan grazers. If grazing impact by protistan grazers was high (0.6-5.0 d^{-1}), impact of warming on phytoplankton production was bumped. This study suggests that the NCCA value is the critical factor affecting coastal phytoplankton production in periods of global warming.

6.2. Introduction

Global warming increases seawater temperature, and many models have predicted ca. 2-6 °C increases of global temperature in the next 100 years (Belkin, 2009; Gaedke et al., 2010; Sommer and Lengfelnner, 2008; IPCC, 2013). Thus, seawater temperature will increase in the future, which may affect the production of marine organisms and eventually the structure and functions of marine ecosystems (Isla et al., 2008; Boyce et al., 2010; Defriez et al., 2016). Phytoplankton is an essential component of marine ecosystems (Jeong et al., 2012; Barton et al., 2016) and important prey for diverse commercially important marine animals (Brown et al., 2010; Woodworth-Jefcoats et al., 2013), but phytoplankton sometimes causes harmful algal blooms and resultant great losses in the aquaculture and tourism industries (Anderson, 1995; Glibert et al., 2014). Thus, its production is a critical factor affecting seafood production, human health, and the economy. Coastal waters are

important to humans because most seafood harvesting, aquaculture, water supply activities, and human recreation occur in these waters (Canuel et al., 2012; Bianchi et al., 2013). However, these coastal waters are likely to be affected more easily by global warming and eutrophication (Canuel et al., 2012; Hewitt et al., 2016) due to their relatively small size, restricted circulation, and freshwater inputs than oceanic waters (Lee, 2012). Thus, in general, the effects of water temperature elevation and nutrient concentration change on the eco-physiology of marine phytoplankton and in turn its production may be greater in coastal waters than in oceanic waters, so the combined effects and interaction between these two critical factors should be investigated.

Nutrient concentrations, one of the major factors affecting phytoplankton production, drastically change in coastal waters due to freshwater input carrying high nutrients, change in populations in coastal cities, use of fertilizations, and artificial constructions etc. (Humborg et al., 1997; Turner et al., 2003; Zhou et al., 2008; Kim et al., 2011; Glibert et al., 2014). However, effects of nutrient changes on impact by warming on phytoplankton production have not been well understood yet. The results of exploring these effects may give a clue in controlling water treatment systems of each country to maintain optimal harvest of healthy sea foods and clean water bodies in global warming period in the future.

Although many models for predicting effects of global warming or nutrient enrichments on phytoplankton production have been established, real values of critical parameters for the models are lacking because there have been only a few enclosure studies on

acquiring values of the parameters and also trends in the parameters (Sommer & Lengfellner, 2008; Lassen et al., 2010; Calbet et al., 2014; Lewandowska et al., 2014).

Therefore, to investigate effects of nutrient conditions on impact by warming on phytoplankton production in coastal waters, I collected water samples from a shallow semi-closed bay, Shiwha Bay in Korea 8 times at 1-2 month intervals from March 2011 to January 2012 and then incubated under 8 different initial conditions by combining 4 different water temperature (i.e., ambient water temperature, +2, +4, and +6 ℃) and 2 different nutrient conditions (i.e., non-enriched and enriched). The results of this study from provide a basis on understanding nutrient conditions altering effects of warming on phytoplankton production in coastal waters and a guideline for each country's policy on managing nutrient concentrations in its coastal waters.

6.3. Material and methods

6.3.1. Sampling and establishing experimental and control incubation bottles

Seawater samples of 400 L were collected from the surface at a station in Shiwha Bay, Korea, in March, April, May, July, August, October, and December 2011 and January 2012. The collected seawater was immediately moved to the laboratory, and zooplankton was screened out with a 200-μm mesh. The concentrations of nitrite plus nitrate (described as nitrate in this paper), phosphate, and silicate of the seawater were measured using a 2-channel nutrient auto-analyzer (QuAAtro, Germany). Then, the seawater samples were gently mixed and evenly distributed into 24 10-L transparent polycarbonate (PC) bottles and maintained for ca. 12 h at ambient temperature inside two different temperature-controlled chambers. Predetermined amounts of nitrate (NO_3), phosphate (PO_4), and silicate (SiO_2) were added (nutrient enriched, ER) to 12 10-L PC bottles to make the target final concentrations of ~200 μM for NO_3, ~12 μM for PO_4 (N:P = 16:1), and ~100 μM for SiO_2, respectively, which include almost the maximum nitrate concentrations observed in the major rivers of the world (Turner et al., 2003). Trace metals and vitamins were also added based on the f/2 medium (Guillard and Ryther, 1962). The waters in the other 12 10-L PC bottles were not enriched (NE) (i.e., the nutrient concentrations were the same as those of the ambient waters). Triplicate ER bottles and triplicate NE bottles were placed inside one of the four different temperature-

controlled chambers for the ambient water temperature (T) experiment. In the same manner, triplicate ER and triplicate NE bottles were set up for each of the elevation by 2 ℃ (T+2 ℃), 4 ℃ (T+4 ℃), and 6 ℃ (T+6 ℃) experiments. All bottles were capped loosely and incubated at the target temperature under an illumination of 50 μE m^{-2} s^{-1} of cool-white fluorescent light in a 14:10 h light-dark cycle.

6.3.2. Subsampling and analyses of components

Each experiment lasted for 14 days and subsamples were taken every day. The first incubation period, from Day 0 to Day 7, was considered to be a temperature acclimation period; thus, after the 6^{th} day sub-sampling, the concentrations of the nutrients were measured and additional nutrients were added after 7^{th} day subsampling to the ER and NE bottles to make the target concentrations of NO_3, PO_4, and SiO_2. These second-treatment bottles were incubated again as described above. Thus, the second incubation period from Day 7.5 (Day 8 for April 2011 without the additional 7.5 d nutrients added due to scarcely consumed nutrients during days 0-7) to Day 14 were considered as the actual experimental period.

I subsampled 500-mL aliquots from each of the 24 bottles each day. For the chlorophyll-a (Chl-a) analysis, a 100-mL aliquot (50-mL aliquot when a bloom occurred) from each bottle was gently filtered through a GF/F filter and the filter paper was placed in a 15-mL falcon tube. A 10-mL volume of acetone was added to the tube

and then the tube was sonicated for 10 min and placed in dark chamber at 4 °C for one night. The supernatant after centrifugation was carefully taken and then the Chl-a concentration was measured using a 10-AU Turner fluorometer (Turner Designs, Sunnyvale, CA, USA). For nutrient analysis, duplicate 20-mL aliquot was taken from each bottle and placed in a HDPE bottle after filtering through GF/F. The concentrations of NO_3, PO_4, and SiO_2 were analyzed every day using a 2-channel nutrient auto-analyzer (QuAAtro, Germany).

For the determination of plankton abundances, a 20-mL aliquot was taken from each bottle and fixed with Lugol's acid solution. Phytoplankton, heterotrophic dinoflagellates, and ciliates were enumerated in a Sedgwick-Rafter chamber by counting >200 cells or all for each species in x50-200 using light microscopy (BX51, Olympus, Japan).

6.3.3. Data analyses

The ratio of the concentration of NO_3 relative to that of Chl-a (hereafter NCCA) was calculated by dividing the initial concentration NO_3 by the initial concentration of Chl-a (see Fig. 6.2).

The Chl-a concentration in each bottle was measured on a daily basis and an accumulated Chl-a concentration [$Chl_{acc(t=0-14d)}$] was calculated as follows:

$$Chl_{acc(t=0-14d)} = [Chl_{acc(t=0d)} + Chl_{acc(t=1d)} + \cdots + Chl_{acc(t=14d)}] \quad \text{(eq. 1)}$$

As described above, I considered the first 7 days (Day 0 to Day

7) to be a biological acclimation period for each target temperature and the latter 7 days (Day 7.5 to 14) to be the actual response period. Thus, to compare the accumulated Chl-a among all the treatments, the Chl-a concentration accumulated from Day 7.5 to Day 14 in each treatment [hereafter $Chl_{acc(t=7.5-14d)}$] was calculated as follows:

$$Chl_{acc(t=7.5-14d)} = Chl_{acc(t=14d)} - Chl_{acc(t=7.5d)} \quad \text{(eq. 2)}$$

where t = elapsed days.

The t-test was used to test whether the $Chl_{acc(t=0-14d)}$ or $Chl_{acc(t=7.5-14d)}$ of one treatment was greater or smaller than that of the control in each month (Zar, 1999).

To test whether our results could be used in marine environments of other countries, I reanalyzed the results from mesocosm experiments conducted in coastal waters off of Norway (Lassen et al., 2010 and Calbet et al., 2014). Using the Chl-a data obtained in those studies, values of $Chl_{acc(t=7-14d)}$ were calculated in the same manner used in this study. However, a statistical analysis of the differences between control and treatment was not performed because the actual value of each datum was not provided in these studies.

6.3.4. Grazing impact by heterotrophic protistan grazers

Grazing coefficients (impact) of protistan (unicellular) grazers on populations of phytoplankton were calculated by combining field

data on abundances of the predator and the prey with ingestion rates of the predator on the prey as in our previous study (Jeong et al., 2004, 2006). The carbon of phytoplankton (i.e., prey) was calculated by converting chlorophyll-a concentration to carbon content using the general ratio of carbon to chlorophyll-a of ~40 mgC $mgChl^{-1}$ (Westberry et al., 2016). The abundances of the protistan grazers were determined by enumerating cells on 1-mL Sedgwick-Rafter chambers under light microscopy (detailed list described in Table 6.2). In this calculation, I assumed that all *Pfiesteria*-like dinoflagellates were *Pfiesteria piscicida*, that all *Gyrodinium* spp. whose size was less than 50 μm were *Gyrodinium dominans*, and that all 20-50 μm sized naked ciliates were *Strobilidium* sp. because these are abundant in this study area (e.g.Kang *et al.*, 2013) and because their ingestion rates on phytoplankton are available (Jeong et al. 2004, 2006, 2011; Yih et al. 2004).

All data were fitted using DeltaGraph 4.0 (Red Rock Software, USA).

6.4. Results

6.4.1. Physical, chemical, and biological properties of the ambient and experimental waters

I collected water samples from a shallow bay of Korea 8 times from March 2011 to January 2012 (Table 6.1 and Fig. 6.1) and then incubated under 8 different conditions by combining 4 different water

temperature (i.e., ambient temperature, +2, +4, and +6 °C) and 2 nutrient conditions (i.e., non-enriched and enriched). The ambient water temperature (AWT) increased from 4 °C in March 2011 to 27 °C in August 2011, then decreased to 0.2 °C in January 2012 (Table 6.1 and Fig. 6.1). The salinities in July and August 2011 were 6.5 and 15.0, respectively, but they were within 24.2–31.1 in the other months (Table 6.1 and Fig. 6.1). The ranges of the nutrient concentrations of the sampled waters were 0.04–106.7 μM for nitrate plus nitrite (NO_3), 0.7–38.4 μM for ammonium (NH_4), 0–0.5 μM for phosphate (PO_4), and 0.02–76.5 μM for silicate concentrations (SiO_2) (Table 6.1 and Fig. 6.1). The chlorophyll-a concentrations ranged from 3.5–5.7 μg l^{-1} in April 2011 to 96.8–103.3 μg l^{-1} in January 2012 (Table 6.1 and Fig. 6.1). The average ratio of the concentration of NO_3 to chlorophyll-a [hereafter NCCA, μM (μg l^{-1})$^{-1}$] in the water samples was 3.3–4.0 in March, April, and August 2011, 1.2–1.7 in May, July, and October 2011, but only 0.0–0.5 in December 2011 to January 2012 (Fig. 6.2A). Under the nutrient-enriched (ER) conditions, the initial average NCCA became $\geq$15 in March–August 2011, 7.7–9.2 in October to December 2011, but 1.8–3.1 in July 2011 and January 2012 (Fig. 6.2B). The three most dominant phytoplankton groups at the beginning of the experiments were diatoms, phototrophic dinoflagellates, and cryptophytes (Fig. 6.3).

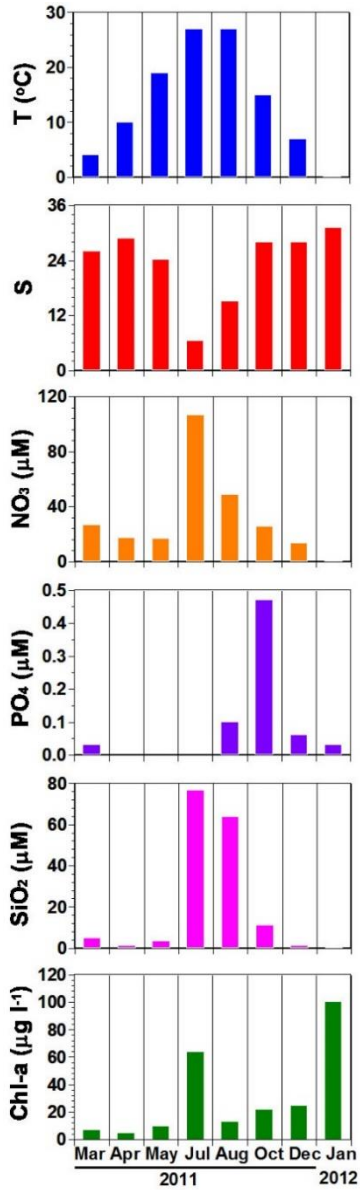

Fig. 6.1. Temporal variations in temperature (T), salinity (S), nitrate (NO_3), phosphate (PO_4), silicate (SiO_2), and chlorophyll-a (Chl-a) in the surface waters collected from Shiwha Bay, Korea, from March 2011 to January 2012.

Table 6.1. Sampling and initial conditions.

A. Non-enriched conditions

Y/M	T	S	Initial concentrations of nutrients and chl-a under the ambient condition (±SE)				
			NO3	HN4	PO4	SiO2	Chl a
2011 03	4.3	26.1	26.7 (0.9)	24.3 (0.3)	0.03 (0.01)	4.7 (0.1)	6.9 (0.3)
2011 04	10.5	28.8	16.8 (0.2)	7.1 (0.3)	0.01 (0.01)	1.1 (0.2)	5.7 (0.5)
2011 05	19.0	24.2	16.6 (0.1)	6.6 (0.2)	0.00 (0.00)	3.3 (0.1)	10.3 (0.6)
2011 07	26.8	6.5	106.7 (0.4)	11.5 (0.7)	0.00 (0.00)	76.5 (0.6)	61.8 (1.4)
2011 08	27.0	15.0	48.7 (0.8)	11.9 (0.3)	0.10 (0.02)	63.7 (0.1)	12.9 (0.5)
2011 10	15.3	28.0	25.4 (0.2)	38.4 (0.6)	0.47 (0.02)	11.1 (0.1)	21.5 (0.5)
2011 12	7.0	28.0	13.1 (0.1)	0.6 (0.0)	0.06 (0.01)	1.1 (0.0)	25.4 (0.2)
2012 01	0.2	31.1	0.04 (0.04)	0.7 (0.0)	0.03 (0.01)	0.02(0.01)	103.3(0.5)

B. Enriched conditions

Y/M	T	S	Initial concentrations of nutrients and chl−a under the enriched condition (±SE)				
			NO3	HN4	PO4	SiO2	Chl a
2011 03	4.3	26.1	235.9 (10.2)	14.4 (1.2)	15.7 (0.5)	84.4 (4.2)	7.4 (0.3)
2011 04	10.5	28.8	193.7 (0.3)	5.9 (0.1)	12.3 (0.0)	86.8 (0.7)	3.5 (0.3)
2011 05	19.0	24.2	175.0 (0.9)	7.1 (0.4)	10.8 (0.1)	109.9 (0.1)	9.3 (0.6)
2011 07	26.8	6.5	202.8 (0.4)	7.6 (0.3)	8.1 (0.22)	99.7 (0.5)	65.7 (0.8)
2011 08	27.0	15.0	197.5 (4.3)	11.1 (0.7)	14.5 (0.1)	97.7 (0.7)	13.5 (0.4)
2011 10	15.3	28.0	173.7 (3.4)	38.3 (1.3)	12.6 (0.1)	91.1 (0.7)	22.5 (0.4)
2011 12	7.0	28.0	211.6 (0.7)	0.6 (0.0)	12.9 (0.8)	95.3 (0.8)	23.3 (0.5)
2012 01	0.2	31.1	168.0 (2.2)	0.7 (0.0)	12.6 (0.2)	103.4 (1.1)	96.8 (1.7)

Sampling month and initial water temperature (°C), salinity, initial nutrients (μM and initial Chlorophyll−a ($\mu g\ l^{-1}$).

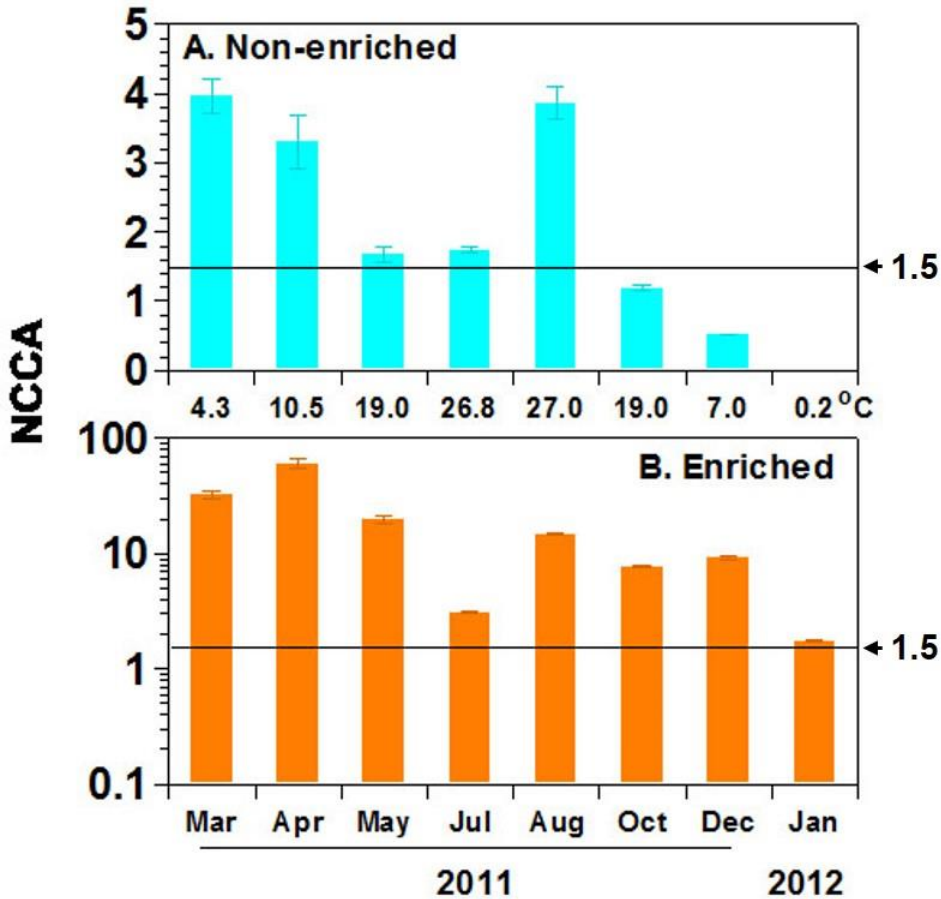

Fig. 6.2 The ratio of nitrate plus nitrite (NO_3) concentration to chlorophyll-a concentration [NCCA, μM (μg L^{-1})$^{-1}$] at the beginning of the experiments from March 2011 to January 2012 under the non-enriched (A) and enriched (B) conditions.

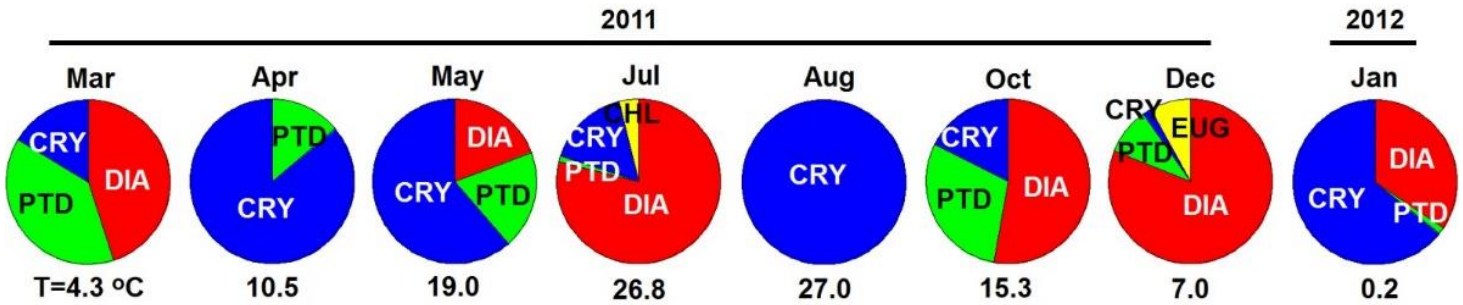

Fig. 6.3 The ratio (%) of the abundances of the 5 most dominant phytoplankton groups in the water samples collected from Shiwha Bay from March 2011 to January 2012. T, initial water temperature (°C); PTD, phototrophic dinoflagellates; DIA, diatoms; CRY, cryptophytes; CHL, chlorophytes; EUG, euglenophytes.

6.4.2. Combined effect of elevated temperature and nutrient enrichment on the accumulated chlorophyll-a concentration

The Chl-a concentrations accumulated from Day 0 to Day 14 [hereafter $chl_{acc(t=0-14d)}$] under the 8 different month conditions showed clear patterns (Fig. 6.4).

Under the non-enriched (NE) condition, the $chl_{acc(t=0-14d)}$ values at +2 °C were significantly higher than those at the ambient water temperatures (AWT) in 2 months, lower in 1 month, but showed no difference in 5 months (Fig 6.4A; $p < 0.05$ or $p > 0.05$, t-test). The $chl_{acc(t=0-14d)}$ at +4 °C were significantly higher than those at the AWT in 5 months, lower in 2 months, but showed no difference in 1 month (Fig 6.4A; $p < 0.05$ or $p > 0.05$). Moreover, the $chl_{acc(t=0-14d)}$ at +6 °C were significantly higher than those at the AWT in 4 months, lower in 3 months, but showed no difference in 1 month (Fig 6.4A; $p < 0.05$ or $p > 0.05$). Thus, under the NE conditions, the effects of warming on $chl_{acc(t=0-14d)}$ were either positive, negative, or negligible irrespective of the temperature elevation of the coastal waters. However, if the effects were either positive or negative, the +4 and +6 °C conditions resulted in warming effects on $chl_{acc(t=0-14d)}$ that were larger than those caused by the +2 °C condition. Under the ER conditions, the $chl_{acc(t=0-14d)}$ were significantly higher than those at the AWT in all months regardless of temperature elevations (Fig. 6.4B; $p < 0.05$).

Using the same data shown in Fig. 6.4 but considering the first 7 days to be an acclimation period, the Chl-a concentrations

accumulated from Day 7.5 (i.e., just after addition of nutrients to make the concentrations as much as at Day 0; see details in Methods) to Day 14 [hereafter $chl_{acc(t=7.5-14d)}$] under the 64 different initial conditions were compared (Fig. 6.5). Under the NE conditions, the $chl_{acc(t=7-14d)}$ at elevated water temperature (EWT) were significantly higher than those at AWT in March, April, and July 2011, but lower from October 2011 to January 2012 (Fig. 6.5; $p < 0.05$, t-test). However, under ER conditions, the $chl_{acc(t=7.5-14d)}$ at EWT were significantly higher than those at AWT in all months (Fig 6.5; $p < 0.05$). Thus, nutrient enrichment is likely to enhance the effects of warming on $chl_{acc(t=7.5-14d)}$.

Next, the criterion for positive or negative effects is considered. Under NE, the average ratios of the concentration of NO_3 to that of chlorophyll-a (NCCA) from March to August 2011 were from 1.7-4.0, whereas those from October 2011 to January 2012 were from 0-1.2 (Fig. 6.2). Furthermore, under ER conditions, the NCCA in all months ranged from 1.8-60.3. Conclusively, with two exceptions in May and August 2011, when NCCA was $\geq$ 1.7, the $chl_{acc(t=7.5-14d)}$ at EWT was significantly higher than that at AWT, whereas when NCCA was $\leq$ 1.2, the $chl_{acc(t=7-14d)}$ at EWT was significantly lower than or not significantly different from that at AWT. In May and August 2011, when the two exceptions occurred, the calculated initial grazing impact by heterotrophic protistan grazers was high (Fig. 6.6).

The dominant heterotrophic protists at the beginning of the experiments were heterotrophic dinoflagellates and/or ciliates (detailed list in Table 6.2). The calculated grazing impact by

populations of these grazers was highest in August 2011 (5.0 d^{-1}, which is equivalent to 99% of the phytoplankton populations being removed by the grazer populations in 1 d) and second-highest in May 2011 (0.60 d^{-1}) (Table 6.2, Fig. 6.6). The grazing impact was 0.47 d^{-1} in April and October 2011, but was very low (<0.1 d^{-1}) in the other months (Table 6.2, Fig. 6.6).

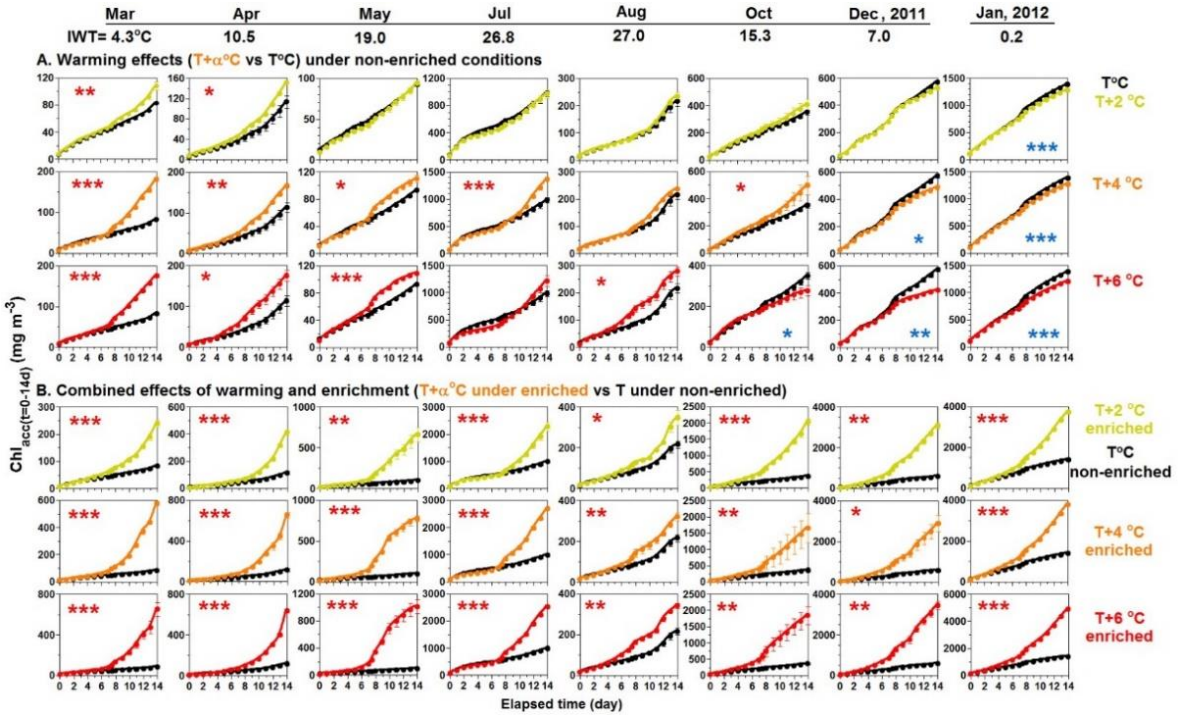

Fig. 6.4. Daily variations in accumulated chlorophyll-a concentrations under 8 different conditions. Red stars indicate an increase, and blue stars indicate a decrease.

*, $p < 0.05$; **, $p < 0.01$; ***, $p < 0.001$; t-test.

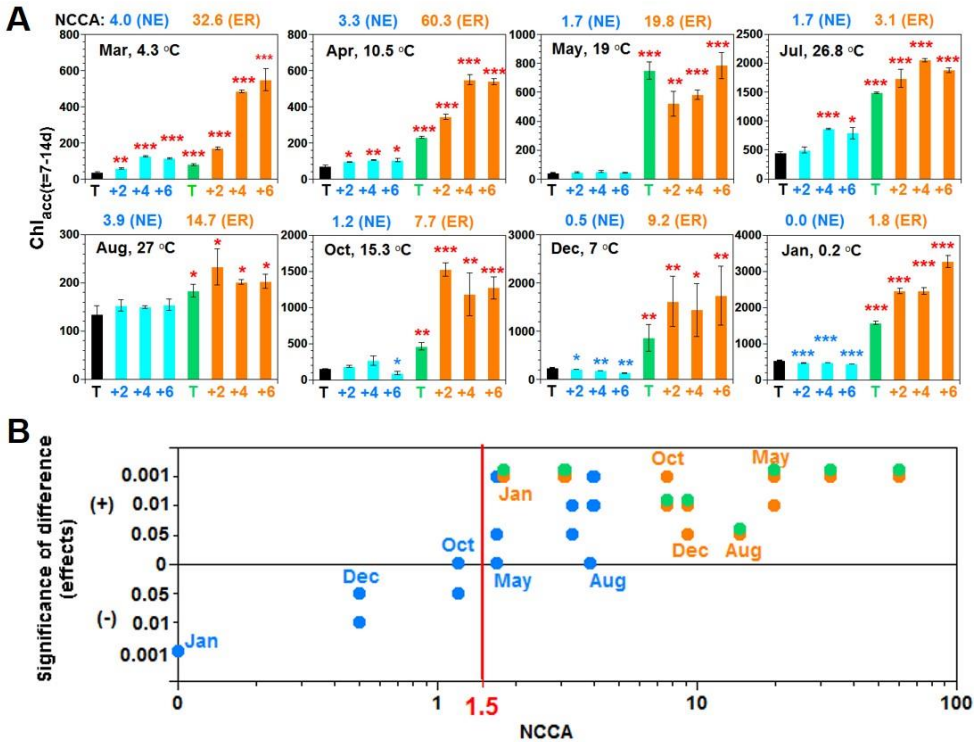

Fig. 6.5. Comparison of the accumulated chlorophyll-a concentrations under the control and experimental conditions (A), and significance of their differences (B). (A) Black bars: ambient water temperature (T) under the non-enriched conditions in each month. Blue bars: T+2, T+4, and T+6 °C under the non-

enriched conditions. Green bars: T under the enriched conditions. Orange bars: T+2, T+4, and T+6 ℃ under the enriched conditions. Red stars indicate an increase and blue stars indicate a decrease compared to the control conditions (t-test). *, $p < 0.05$; **, $p < 0.01$; ***, $p < 0.001$. (B) Blue circle: T+2, T+4, and T+6 ℃ under the non-enriched conditions. Green circle: T under the enriched conditions. Orange circle: T+2, T+4, and T+6 ℃ under the enriched conditions.

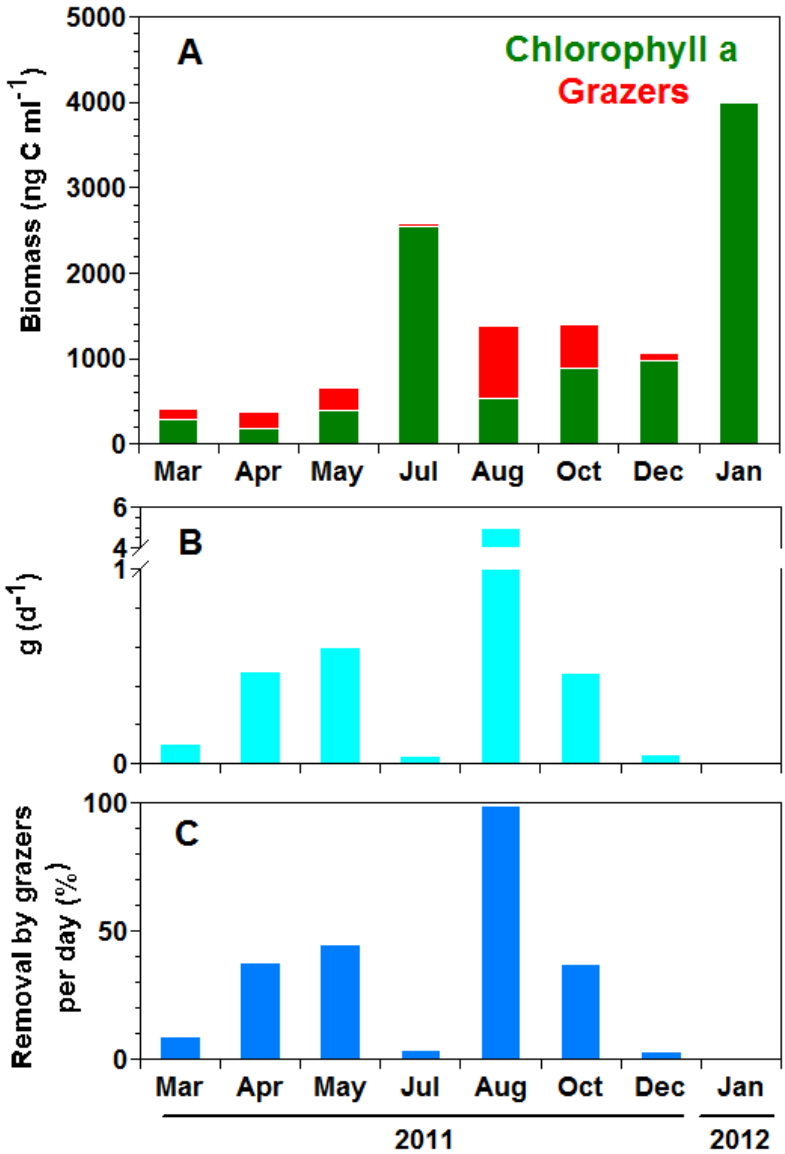

Fig. 6.6. Initial biomass of chlorophyll-a and protistan grazers (ng C mL^{-1}, A), calculated grazing impact by the grazers on phytoplankton (d^{-1}, B), and removal by grazers per day (%, C).

6.5. Discussion

The results of this study clearly show that the impact by elevated water temperature on phytoplankton production is affected significantly by nutrient conditions. Furthermore, the NCCA critically influences the effect of the nutrient conditions. Based on the results under the 64 different conditions in this study, the critical value of NCCA was determined to be ~1.5. Theoretically, the Redfield ratio of C:N is 106:16 (i.e., ca. 6.6) and C:Chl-a is ca. 40:1, thus N:Chl-a is ca. 6 (Redfield, 1958; Westberry et al., 2016). This value is much greater than the value of 1.5 (NCCA) obtained as the criterion for positive effect in this study. Thus, phytoplankton in coastal waters can grow under conditions in which NCCA is much lower than the N:Chl-a in phytoplankton cells. Otherwise, the dominant phytoplankton may have N:Chl-a lower than 6 or reserve nitrogen within their cells (Bode et al., 1997).

There are only two studies providing available data for exploring the effects of warming and/or nutrient enrichment on phytoplankton production in enclosures (Lassen et al., 2010; Calbet et al., 2014). Whether the critical value of 1.5 is applicable to other environments in various temperate regions can be tested by reanalyzing the available data produced by these two studies. In Lassen et al. (2010) that investigated the impact by warming (T+3 and T+6 °C) on phytoplankton production without enrichment in Norwegian waters in January and February 2003, when the NCCA ranged from 25-50, $chl_{acc(t=7-14d)}$ values in both the T+3 and T+6 °C

conditions were greater than those in AWT (Fig. 6.6A–B). In Calbet et al. (2014), which explored the effects of warming (T+3 °C) and nutrient enrichment on phytoplankton production in Norwegian waters in January 2011, the NCCA in the ambient water was 0.4, but that in the enriched waters became 5.4–5.9. At the initial water temperature of 12.3 °C, the $chl_{acc(t=7-14d)}$ in the enriched waters were greater than that in the non-enriched ambient water (Fig. 6.6C). The $chl_{acc(t=7-14d)}$ in the enriched waters at T °C was higher than that in the non-enriched ambient water at T °C, even though the $chl_{acc(t=7-14d)}$ at T+3 °C under the enriched conditions was lower than that at T °C, as shown in May 2011 in our study. In conclusion, in these two studies, when NCCA was $\geq$ 5.4, the impact by warming on phytoplankton production was positive. Thus, our critical value can be used in these waters.

In August 2011, the grazing impact by heterotrophic protistan grazers on phytoplankton was very high (mortality rate of phytoplankton = ~5 d^{-1}), which caused the effects of warming on phytoplankton growth to be negligible under the NE condition and relatively low under the ER condition. Grazing by predators is known to affect phytoplankton biomass at sea (Tillmann, 2004; Calbet, 2008; Marinov et al., 2013; Lee et al., 2014) and grazing or grazing pattern can be changed depending on ecosystem shift driven by warming (Defriez et al., 2016). Both heterotrophic protistan (i.e., heterotrophic dinoflagellates and ciliates) and metazoan (i.e., copepods, cladocerans, and larvae of benthos) grazers are able to feed on diverse phytoplankton species. However, the grazing impact

by heterotrophic protistan grazers on phytoplankton in coastal waters is usually much greater than that by metazoan grazers because the abundances of heterotrophic protists are ca. 100–10,000 times higher than those of metazoan grazers, even though the ingestion rates of heterotrophic protists are ca. 10–100 times lower than those of metazoan grazers (Kim et al., 2013; Yoo et al., 2013b). Therefore, this study indicates that high grazing impact by heterotrophic protistan grazers can sometimes mask the effects of warming on phytoplankton production.

Although many models have been used to predict the effects of global warming or nutrient enrichment on phytoplankton production (Bopp et al., 2001; Sarmiento et al., 2004; Gregg et al., 2005; Marinov et al., 2010; Steinacher et al., 2010), measured values of critical parameters for the models are lacking because there have been only a few enclosure studies on acquiring values of the parameters and also trends of the parameters (Sommer and Lengfellner, 2008; Lassen et al., 2010; Sommer and Lewandowska, 2011; Calbet et al., 2014; Lewandowska et al., 2014). Furthermore, only two studies have examined the combined effects of global warming and nutrient enrichment on phytoplankton production using enclosures (Calbet et al., 2014; Lewandowska et al., 2014). However, these studies explored the combined effects under a single initial temperatures; the initial and changed temperatures were 11 °C and −3 and +3 °C or 12.3 °C and +3 °C, respectively. Furthermore, the nitrate (NO_3) concentrations of the ambient waters under NE and ER conditions were 0.11 and 0.12–0.14 μM, and ~0.9 and ~11–14 μM, respectively.

However, the range of water temperatures in global coastal waters is −8 to 35 ℃ (Alaska and Pacific coastal), and that of NO_3 is 0–200 μM (NOAA; Colern, 2001; Zhou et al., 2008; Hayn et al., 2014). In this study, the initial temperatures and NO_3 concentrations in the ambient seawaters were 0.2−27 ℃ and 0−107 μM−NO_3, respectively and thus elevated water temperature and enriched NO_3 concentrations tested were 2.2−33 ℃ and 168−236 μM−NO_3, respectively. Thus, the ranges of 0.2−33 ℃ and 0−236 μM−NO_3 in this study may cover those in most of coastal environments at present and in the future. Therefore, to understand the combined effects of global warming and eutrophication on phytoplankton production better, experiments using phytoplankton populations collected from natural environments in wider ranges of water temperature and nutrient concentrations should be explored.

Many studies have predicted that global warming will lower phytoplankton biomass in the future because stronger thermoclines would limit mixing between oligotrophic surface waters and eutrophic deep waters and consequently lower the flux of nutrients into surface waters (Behrenfeld et al., 2006, 2015; Doney, 2006; Boyce et al., 2010; Lewandowska et al., 2014). However, this prediction does not consider changes in nutrient concentrations in coastal environments and according to the result of recent study analyzed 50 years data suggested increased phytoplankton production by global warming in North Atlantic subpolar region due to increased nutrient concentrations from deepened thermocline depth (Martinez et al., 2016). The results of this study show that nutrient conditions, NCCA

rather than absolute concentration, influence the effects of warming on phytoplankton. Therefore, I suggest that the effects of NCCA should be considered when running prediction models of phytoplankton dynamics in the warm and/or eutrophic world of the future. To increase the phytoplankton biomass available for larvae of commercially important fish and benthos in coastal waters, NCCA should be elevated by controlling the nutrient load in freshwater input. To the contrary, to reduce harmful algal blooms, NCCA should be reduced. Thus, the results of exploring these effects may provide a basis for understanding how nutrient conditions may alter the effects of warming on phytoplankton production in coastal waters and also provide some information useful for controlling the water treatment systems of each country to maintain an optimal harvest of healthy sea foods and also clean bodies of water in the global warming period of the future.

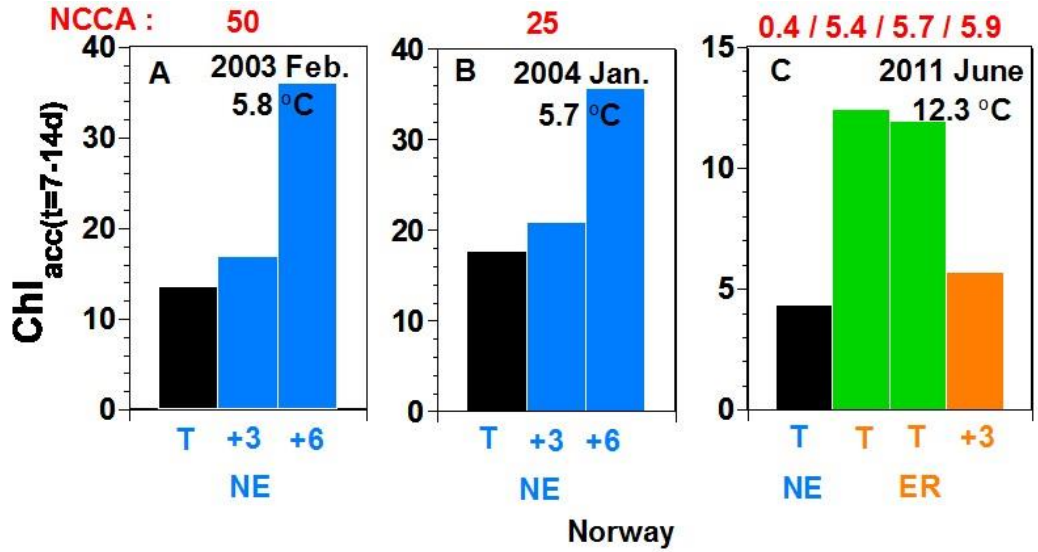

Fig. 6.7. The calculated chlorophyll-a concentration accumulated from Day 7 to Day 14 [$Chl_{acc(t=7-14d)}$] under control and experimental conditions in coastal waters off Norway. The original data in (A, B) were obtained from Lassen et al. (2010) and those in (C) were from Calbet et al. (2014). black bars indicate T, blue bars indicate T+3 or T+6 °C elevated water temperature, green bars indicate enriched, and orange bars indicate both elevated water temperature and NO_3 conditions (T+3 °C).

Table 6.2. Dominant potential protistan grazers and their grazing impacts on phytoplankton.

Y/M	T	S	Dominant potential protistan grazers	g(d^{-1})
2011 03	4.3	26.1	*Pfiesteria piscicida* and *Strobilidium* sp.	0.10
2011 04	10.5	28.8	*P. piscicida, Gyrodinium* sp., and *Protoperidinium bipes*	0.47
2011 05	19.0	24.2	*P. piscicida, Strobilidium* sp., and *P. bipes*	0.60
2011 07	26.8	6.5	*Strobilidium* sp. and *Gyrodinium dominans*	0.04
2011 08	27.0	15.0	*P. piscicida, Strobilidium* sp., *P. bipes, G. dominans*, and *Mesodinium rubrum*	5.00
2011 10	15.3	28.0	*P. piscicida* and *P. bipes*	0.47
2011 12	7.0	28.0	*P. piscicida, Strobilidium* sp., *M. rubrum,* and *P. bipes*	0.05
2012 01	0.2	31.1	*Strobilidium* sp.	0.00

Grazing impacts (g) were calculated using data on the initial abundances of potential heterotrophic protistan grazers and phytoplankton prey (expressed as chlorophyll-a concentration) and the ingestion rates of the predators on prey. See the references listed in the Methods section for the calculation.

Chapter 7.
Overall discussion

The ultimate goals of this thesis study is to comprehensive understandings of response by structures and functions of marine ecosystems to environmental changes such as global warming and eutrophication and response by phytoplankton food webs which is carrying out biogeochemical cycle. Thus, understanding current status of structures and functions of marine ecosystems is important to predict future variable effects on marine environments because global warming and eutrophication are accelerating and serious environmental concerns (Nixon, 1995; Barnett et al., 2005; IPCC, 2013; Codhe et al., 2015). In addition, the eco-physiological research about 4,000 phytoplankton plus unidentified species is the most essential factor to better understand biogeochemical cycles in marine food webs. For these reasons, I started firstly with environmental field study and investigated physical, chemical, and biological characteristics of Korean coastal waters (Chapter 2). And then to better understand protistan dynamics in food webs, I investigated the strategy of survival, growth, and competition of the newly described mixotrophic dinoflagellate, *Gymnodinium smaydae* by acquiring nutrients from ingesting other protistan species (Chapter 3). In addition, the strategy of toxic mixotrophic dinoflagellates, *Alexandrium andersonii, A. affine*, and *A. fraterculus* to survive by using allelopathic effects and feeding other protists was also investigated (Chapter 4). Moreover, to better understand red-tide dynamics, I investigated predation by common heterotrophic

protists on the mixotrophic red-tide ciliate, *Mesodinium rubrum* (Chapter 5). Finally, I planned the study that combined global warming and eutrophication effects on phytoplankton dynamics to predict next 100 years by conducting bottle incubations with environmental samples for 8 months. Experiments under 64 different initial conditions formed by combining 4 different water temperatures (i.e., ambient, +2, +4, and +6 °C) and 2 different nutrient conditions (i.e., non-enriched and enriched) using natural water sampled 8 times at intervals of 1-2 months (Chapter 6).

Mixotrophy in protistan species. Diatoms are generally known as dominant species in coastal waters near river flows because they may less sensitive to salinity and require lower nutrient concentrations to response (i.e., half saturation value), and relative rapid growth rates than other groups (Margalef, 1978; Odebrecht et al., 2014). However, dinoflagellates have complicated characteristics because they have narrow survival salinity range than diatoms, relative higher nutrient requirements, different feeding mechanisms, prey preference, and/or migration ability (Smayda and Reynolds, 2003; Godhe et al., 2015; Jeong et al., 2010b, 2015). In this thesis, I revealed that new food web pathway of *G. smaydae*. Mixotrophy is another strategy of acquiring nutrients by ingesting prey species to elevate growth rates. Prey species can be bacteria, small flagellates, phylogenetically close species, bigger flagellates, and/or their predators. Dinoflagellates is believed to evolve in diverse way by feeding on preys in easy way. *G. smaydae* has revealed as the most fast mixotrophically growing dinoflagellates in the world. 3-4 divisions per day (i.e., the maximum specific growth rate = 2.23 d^{-1}) of *G. smaydae* is comparable to those of diatoms. Also, I revealed

that *Alexandrium andersonii* which was isolated Jinhae Bay have ability to conduct both phototrophy and mixotrophy. The harmful effects and mixotrophic ability of *Alexandrium andersonii* was not reported in previous studies even though *Alexanderium* species belong to harmful group and give great concerns for the people who work in aquaculture industry and related officials. In this study, I firtst reported that *A. andersonii* kill other protistan species by immobilizing and lysing regardless of feeding. In addition, *A. andersonii* elevetated growth rates almost twice after feeding *Pyramimonas* sp.. Moreover, *A. affine and A. fraterculus* have immobilization or lytic effects on other protists. These allelopathic mechanism is also outcompeting strategy to survive and uptake nutrients by removing potential competitors. Therefore, these mixotrophic or harmful dinoflagellates may have potential to occur red tides if NCCA properly decrease in Korean coastal waters.

Red tide control by heterotrophic protists. *Mesodinium rubrum* is cosmopolitan red tide species and obligate mixotrophic species by feeding only *Teleaulax* species. *Mesodinium* frequently occur red tides in Korean coastal waters during last three decades and provided potentially harmful to aquaculture industries and coastal benthic ecosystems (Yih et al., 2013). *M. rubrum* is also a good prey for *Dinophysis* species, thus first successful *Dinophysis* spp. culture was established using *M. rubrum*. Moreover, both *M. rubrum* and *Dinophysis* spp. are known as kleptoplastidic (i.e., retention of plastids obtained from ingested algal prey) species using chloroplasts acquired from cryptophytes. However, *Dinophysis* is harmful and responsible for DSP (Diarrhetic Shellfish Poison) production. Thus, investigations of heterotrophic protistan species feeding *on M.*

rubrum and finding *Gyrodinium dominans* as an optimal predator in this study provide important informations to better understand evolutionary directionality and red-tide mitigation using biological methods.

Global warming and eutrophication. In both coastal waters, Gwangyang Bay and Shiwha Bay in Korea, serial correlations among sum of precipitation over ten days, salinity, and nitrate concentrations were decided whether dominant phytoplankton is diatom, dinoflagellate, and /or small flagellates. Diatom and dinoflagllates are two of the major dominant phytoplankton groups and they contribute ~80% of total phytoplankton (Sournia et al., 1991). Diatoms are known as good prey for aquatic animals, while dinoflagellates are sometimes harmful for them (Cloern et al., 1983). In addition, if the ratio of initial nitrate concentration to Chl-a concentration [NCCA, μM (μg L^{-1})$^{-1}$] value is > 1.5, temperature elevation increased phytoplankton production. Thus, I additionally investigated feed-back analysis by applying the theory from chapter 6 to chapter 2 field data. Calculated NCCA value was high during the study periods, even though the trend decreased from 5.8-20.3 in 2011 and 0.5-15.6 in 2012 to 1.1-3.1 in 2013 in Gwangyang Bay (Fig. 7.1; Table 7.1). In addition, water temperature also increased by ~1 ℃ from 14.7-15.7 ℃ in 2011 to 15.8-16.5 ℃ in 2012 and 2013 (Table 7.1) Thus, the response by Chlorophyll-a was increased from 0.9-1.2 in 2011 to 3.0-6.4 in 2012 and 2013 (Fig. 7.1; Table 7.1). Therefore, water temperature is expected to elevate continuously due to global warning in Gwangyang Bay and the major factor of nitrate flowing into the Gwangyang Bay is precipitation. If frequency of precipitation increase, NCCA value will increase and

phytoplankton production dominated by diatom is expected to increase. Otherwise, frequency of precipitation decrease, NCCA value will lower and harmful algal blooms dominated by dinoflagellates is expected to increase in Gwangyang Bay (Fig. 7.2).

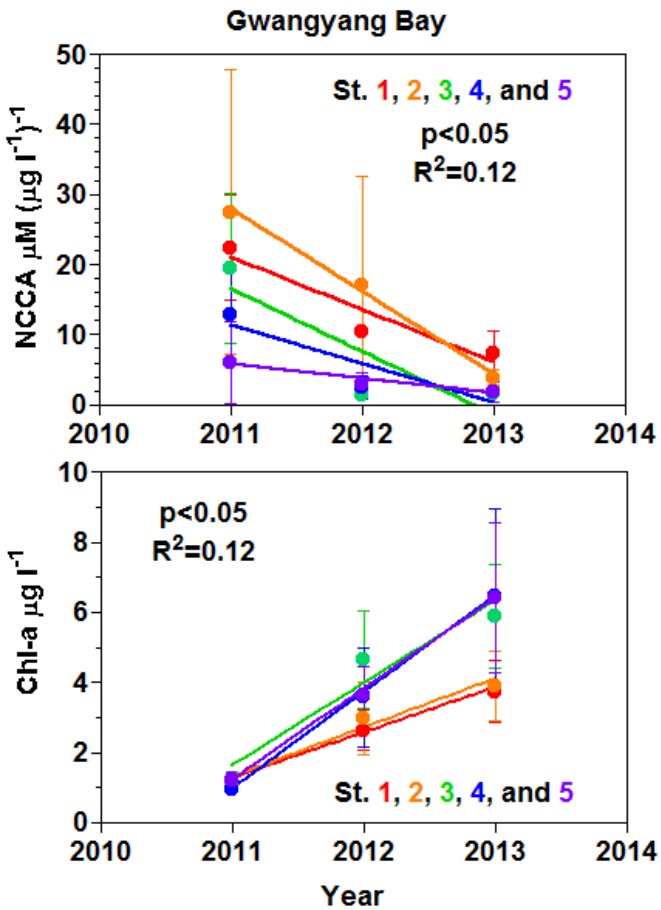

Fig. 7.1. The ratio of initial nitrate concentration to Chlorophyll-a concentration [NCCA, μM ($\mu g\ L^{-1}$)$^{-1}$] and Chlorophyll-a ($\mu g\ L^{-1}$) concentrations in Gwangyang Bay from 2011 to 2013.

Table 7.1. Field stations (see chapter 2), year, water temperature (℃), salinity, ratio of initial nitrate concentration to Chlorophyll−a concentration [NCCA, μM (μg L^{-1})$^{-1}$] and Chlorophyll−a concentration (μg L^{-1}) in Gwangyang Bay from 2011 to 2013.

station	year	Temperature		Salinity		NCCA		Chlorophyll −a	
		Average	SE	Average	SE	Average	SE	Average	SE
St. 1	2011	15.7	4.6	21.7	5.5	22.4	7.5	1.2	0.2
St. 1	2012	16.1	4.2	27.4	4.5	10.4	7.2	2.6	0.6
St. 1	2013	15.8	3.8	24.9	2.3	7.4	3.1	3.7	0.9
St. 2	2011	15.4	4.5	24.2	6.2	27.5	20.3	1.1	0.2
St. 2	2012	16.5	4.3	27.9	4.7	17.0	15.6	3.0	1.0
St. 2	2013	16.2	3.6	28.2	1.5	3.9	1.2	3.9	1.0
St. 3	2011	14.9	4.2	28.9	4.3	19.5	10.7	1.2	0.3
St. 3	2012	16.3	4.3	31.8	1.6	1.3	0.5	4.7	1.4
St. 3	2013	16.4	3.4	31.0	0.8	1.6	1.1	5.9	1.5
St. 4	2011	15.2	4.1	29.4	3.6	12.8	6.5	0.9	0.0
St. 4	2012	16.4	4.4	31.7	1.7	2.5	1.6	3.6	1.4
St. 4	2013	16.4	3.4	31.2	0.8	1.8	1.5	6.4	2.5
St. 5	2011	14.7	3.0	30.4	2.9	5.9	5.8	1.2	0.1
St. 5	2012	15.8	4.0	31.1	2.2	2.8	1.8	3.6	0.9
St. 5	2013	15.9	3.5	31.5	0.7	1.8	1.5	6.4	2.1

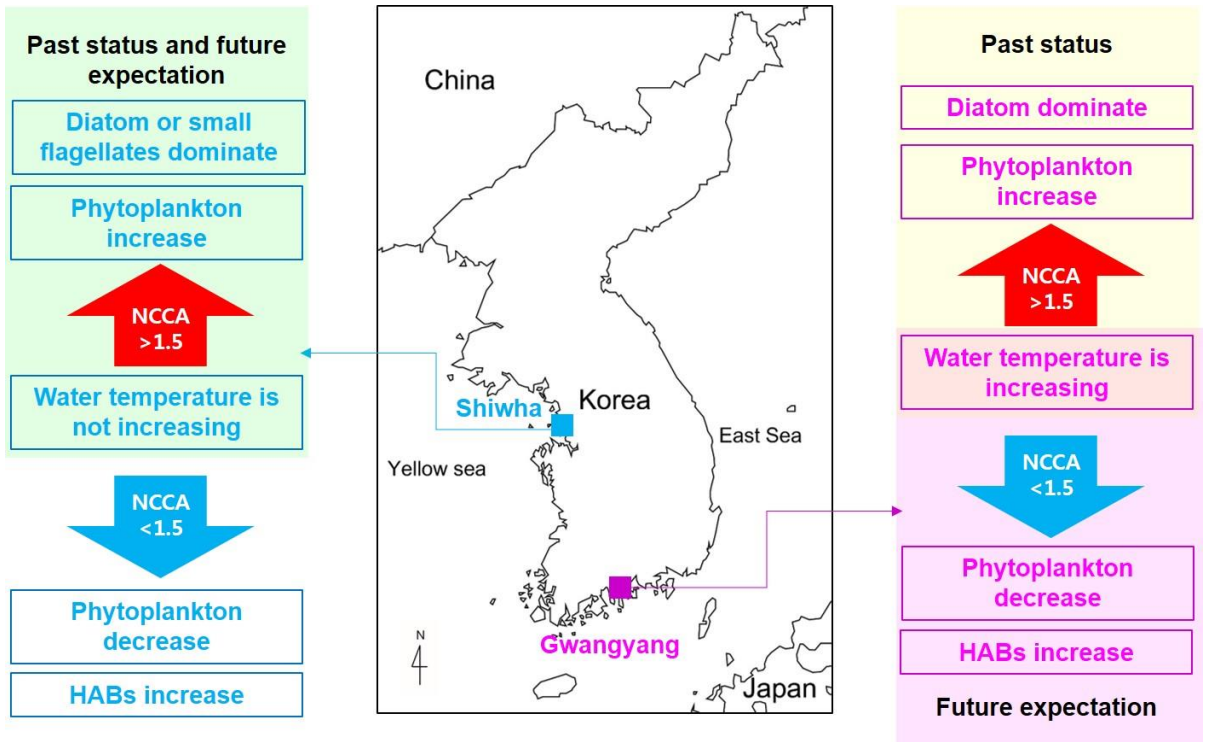

Fig. 7.2. Two major field study area, Gwangyang Bay located in Southern Korea and Shiwha Bay located in western Korea, in this thesis. Indicated conceptual past status and future expectation model in two regions.

Similarly, data based on every March to December from 2010 to 2013 in Shiwha Bay was analyzed (Lee et al., unpublished data). Distinct water temperature increase was not observed in Shiwha Bay unlike in Gwangyang Bay (Table 7.2). In addition, NCCA and Chlorophyll-a concentration clearly showed increasing even though statistically not correlated (Fig. 7.3; Table 7.2). Shiwha Bay is semi-enclosed bay and there have been reported frequent red tides and high biomass compared to other Korean coastal waters (Kang et al., 2013) since dike has established. In addition, diverse artificial construction has been occurred for long time there such as establishing dike, opening water gates to improve water quality, and establishing and operating tidal power plants (Kang et al., 2013). Thus, the enclosed Shiwha bay may be affected not only meteorological effects but other artificial interactions. Moreover, dinoflagellates and small flaglellates are known to grow well and occur blooms in stagnant waters, stagnant semi-enclosed bay seem to provide outgrowing benefits to small flagellates and dinoflagellates than diatoms even though high nitrogen loads of fresh waters originated from three big near cities. Therefore, water temperature is expected not to seriously elevate by global warming in Shiwha Bay and more investigations should be explored to predict phytoplankton production by future climate changes in Shiwha Bay.

Therefore, people who works related fishery must consider which dominant phytoplankton groups and specific species give positive or negative effects on their specific fishery cultivations. And then feedback to the people who manage sewage treatment plant and coastal environmental manager to control the effective nutrient levels to minimize economic losses.

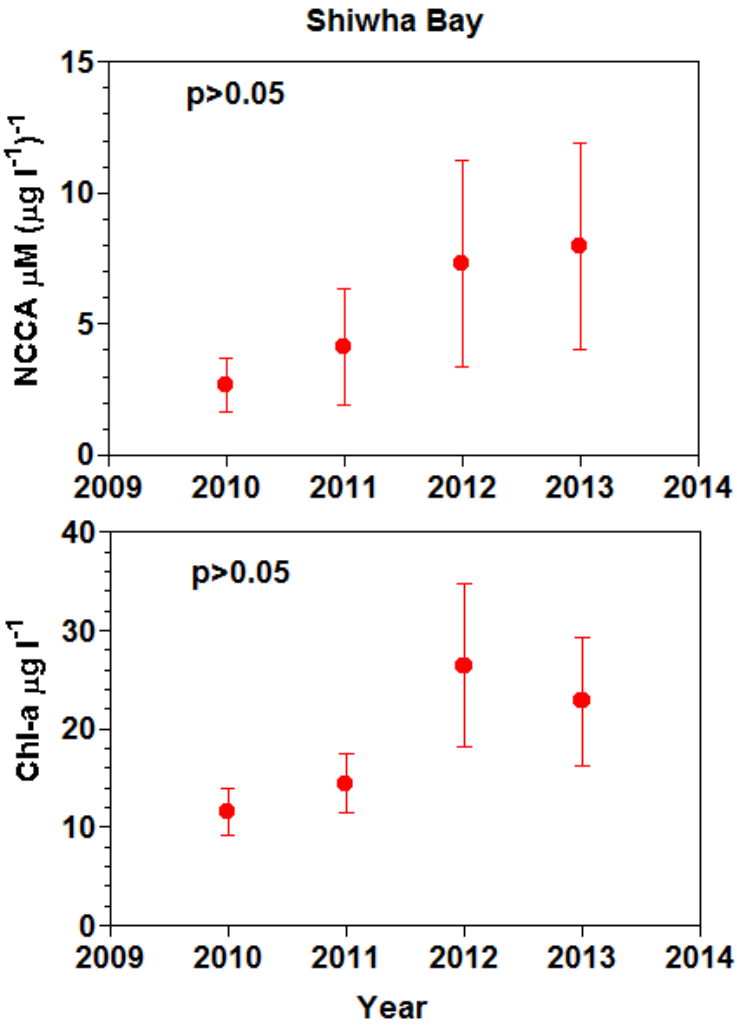

Fig. 7.3. The ratio of initial nitrate concentration to Chlorophyll-a concentration [NCCA, μM $(\mu g\ L^{-1})^{-1}$] and Chlorophyll-a ($\mu g\ L^{-1}$) concentrations in Shiwha Bay from 2010 to 2013.

Table 7.2. Year, water temperature (°C), salinity, ratio of initial nitrate concentration to Chlorophyll−a concentration [NCCA, μM (μg L^{-1})$^{-1}$] and Chlorophyll−a concentration (μg L^{-1}) Shiwha Bay from March to December in every year during 2010 to 2013.

Month, Year	Temperature		Salinity		NCCA		Chlorophyll −a		n
	Average	SE	Average	SE	Average	SE	Average	SE	
Mar to Dec, 2010	17.4	2.5	22.0	1.4	2.7	1.0	11.6	2.4	11
Mar to Dec, 2011	16.8	2.5	21.1	2.6	4.1	2.2	14.5	3.0	11
Mar to Dec, 2012	17.5	2.7	24.0	2.8	7.3	3.9	26.4	8.3	10
Mar to Dec, 2013	17.7	2.9	23.2	1.6	8.0	3.9	22.8	6.5	11

Bibliography

Adolf, J.E., Stoecker, D.K. & Harding L.W. (2006). The balance of autotrophy and heterotrophy during mixotrophic growth of *Karlodinium micrum* (Dinophyceae). *J. Plankton. Res.* **7**, 737-751

Anderson, D.M. (1995). Toxic red tides and harmful algal blooms: A practical challenge in coastal oceanography. *Rev. Geophys.* **33**, 1189-1200.

Anderson, D.M. (1995). The ecology and oceanography of harmful algal blooms—a national research agenda. Woods Hole Oceanographic Institution, 66 pp

Anderson, D.M., Alpermann, T.J., Cembella, A.D., Collos, Y., Masseret, E. & Montresor, M. (2012). The globally distributed genus *Alexandrium*: multifaceted roles in marine ecosystems and impacts on human health. *Harmful Algae* **14**, 10-35.

Balzano, L., Recht, B. & Nowak, R. (2010). High-dimensional matched subspace detection when data are missing. In 2010 IEEE International Symposium on Information Theory (pp. 1638-1642). IEEE.

Balech, E. (1990). Four new dinoflagellates. Helgoländer Meeresuntersuchungen, **44**(3-4), 387-396.

Band-Schmidt, C.J., Lilly, E.L. & Anderson, D.M. (2003). Identification of *Alexandrium affine* and *A. margalefii* (Dinophyceae) using DNA sequencing and LSU rDNA-based RFLP-PCR assays. *Phycologia* **42**(3), 261-268.

Barnett, T.P., Adam, J.C. & Lettenmaier, D.P. (2005). Potential impacts of a warming climate on water availability in snow-dominated regions. *Nature* **438**(7066), 303-309.

Barber, R.T. & Smith Jr., W.O. (1981). The role of circulation, sinking and vertical migration in physical sorting of phytoplankton in the upwelling center at 15° S. In: Richards, F.A. (Ed.), Coastal Upwelling. Coastal and Estuarine Sciences 1, American Geophysical Union, Washington, DC, pp. 366-371.

Barton, A.D., Irwin, A.J., Finkel, Z.V. & Stock, C.A. (2016). Anthropogenic climate change drives shift and shuffle in North Atlantic phytoplankton communities. *P. Natl. Acad. Sci. USA* **113**, 2964-2969.

Baek, S.H., Kim, D., Son, M., Yun, S.M. & Kim, Y.O. (2015). Seasonal distribution of phytoplankton assemblages and nutrient-enriched bioassays as indicators of nutrient limitation of phytoplankton growth in Gwangyang Bay, Korea. *Estuar. Coast. Shelf S.* **163**, 265-278.

Behrenfeld, M.J., O'Malley, R.T., Siegel, D.A., McClain, C.R., Sarmiento, J.L., Feldman, G.C., Milligan, A.J., Falkowski, P.G., Letelier, R.M. & Boss, E.S. (2006). Climate-driven trends in contemporary ocean productivity. *Nature*, **444**, 752-755.

Belkin, I.M. (2009). Rapid warming of large marine ecosystems. *Prog. Oceanogr.* 81, 207–213.

Berge, T., Hansen, P.J. & Moestrup, Ø. (2008). Prey size spectrum and bioenergetics of the mixotrophic dinoflagellate *Karlodinium armiger*. *Aquat. Microb. Ecol.* 50, 289–299.

Bianchi, T.S., Allison, M.A. & Cai, W.J. (2013). Biogeochemical Dynamics at Major River–Coastal Interfaces: Linkages with Global Change, pp. xiii.

Blossom, H.E., Daugbjerg, N. & Hansen, P.J. (2012). Toxic mucus traps: A novel mechanism that mediates prey uptake in the mixotrophic dinoflagellate *Alexandrium pseudogonyaulax*. *Harmful Algae* 17, 40–53.

Bockstahler, K.R. & Coats, D.W. (1993a). Grazing of the mixotrophic dinoflagellate *Gymnodinium sanguineum* on ciliate population of Chesapeake Bay. *Mar. Biol.* 116, 447–487.

Bockstahler, K.R. & Coats, D.W. (1993b). Spatial and temporal aspects of mixotrophy in Chesapeake Bay dinoflagellates. *J. Eukaryot. Microbiol.* 40, 49–60.

Bode, A., Botas, J.A. & Fernandez, E. (1997). Nitrate storage by phytoplankton in a coastal upwelling environment. *Mar. Biol.* 129, 399–406.

Bopp, L., Monfray, P., Aumont, O., Dufresne, J., Treut, H.L., Madec, G., Terray, L & Orr, J. (2001). Potential impact of climate change on marine export production. *Global Biogeochem. Cy.* 15, 81–99.

Bouley, P. & Kimmerer, W.J. (2006). Ecology of a highly abundant, introduced cyclopoid copepod in a temperate estuary. *Mar. Ecol. Prog. Ser.* **324**, 219-228.

Boyce, D.G., Lewis, M.R. & Worm, B. (2010). Global phytoplankton decline over the past century. *Nature* **466**, 591-596.

Brown, C.J., Fulton, E.A., Hobday, A.J., Matear, R.J., Possingham, H.P., Bulman, C., Christensen, V., Forrest, R.E., Gehrke, P.C., Gribble, N.A., Griffiths, S.P., Lozano-Montes, H., Martin, J.M., Metcalf, S., Okey, T.A., Watson, R. & Richardson, A.J. (2010). Effects of climate-driven primary production change on marine food webs: implications for fisheries and conservation. *Global Change Biol.* **16**, 1194-1212.

Burkholder, J.M., Noga, E.J., Hobbs, C.W., Glasgow, H.B.Jr. & Smith, S.A. (1992). New "phantom" dinoflagellate is the causative agent of major estuarine fish kills. *Nature* **358**, 407-410.

Burkholder, J.M., Glibert, P.M. & Skelton, H.M. (2008). Mixotrophy, a major mode of nutrition for harmful algal species in eutrophic waters. *Harmful Algae* **8**, 77-93.

Buskey, E.J. Coulter, C. & Strom, S. (1993). Locomotory patterns of microzooplankton: potential effects on food selectivity of larval fish. *Bull. Mar. Sci.* **53**, 29-43.

Calbet, A. (2008). The trophic roles of microzooplankton in marine systems. *ICES Journal of Marine Science: Journal du Conseil* **65**, 325-331.

Calbet, A., Isari, S., Martínez, R.A., Saiz, E., Garrido, S., Peters, J., Borrat, R.M. & Alcaraz, M. (2013). Adaptations to feast and famine in different strains of the marine heterotrophic dinoflagellates *Gyrodinium dominans* and *Oxyrrhis marina*. *Mar. Ecol. Prog. Ser.* **483**, 67-84.

Calbet, A., Sazhin, A.F., Nejstgaard, J.C., Berger, S.A., Tait, Z.S., Olmos, L., Sousoni, D., Isari, S., Martínez, R.A., Bouquet, J., Thompson, E.M., Båmstedt, U. & Jakobsen, H.H. (2014). Future Climate Scenarios for a Coastal Productive Planktonic Food Web Resulting in Microplankton Phenology Changes and Decreased Trophic Transfer Efficiency. *PloS one* **9**, e94388.

Canuel, E.A., Cammer, S.S., McIntosh, H.A. & Pondell, C.R. (2012). Climate change impacts on the organic carbon cycle at the land-ocean interface. *Annu. Rev. Earth Pl. Sc.* **40**, 685-711.

Caron, D.A. & Hutchins, D.A. (2013) The effects of changing climate on microzooplankton grazing and community structure: drivers, predictions and knowledge gaps. *J. Plankton Res.* **35**, 235-252.

Ciminiello, P., Fattorusso, E., Forino, M. & Montresor, M. (2000). Saxitoxin and neosaxitoxin as toxic principles of *Alexandrium andersoni* (Dinophyceae) from the Gulf of Naples, Italy. *Toxicon* **38**(12), 1871-1877.

Cloern, J.E., Alpine, A.E., Cole, B.E., Wong, R.L., Arthur, J.F. & Ball, M.D. (1983). River discharge controls phytoplankton dynamics in the northern San Francisco Bay estuary. *Estuar. Coast. Shelf S.* **16**(4), 415-429.

Cloern, J.E. (2001). Our evolving conceptual model of the coastal eutrophication problem. *Mar. Ecol. Prog. Ser.* **210**, 223-253.

Crawford, D. W. (1989). *Mesodinium rubrum*: The phytoplankter that wasn't. *Marine ecology progress series* Oldendorf **58**:161-174.

Crawford, D.W. (1992). Metabolic cost of motility in planktonic protists: theoretical considerations on size scaling and swimming speed. *Microb. Ecol.* **24**, 1-10.

Crawford, D.W. & Lindholm, T. (1997). Some observations on vertical distribution and migration of the phototrophic ciliate *Mesodinium rubrum* (*Myrionecta rubra*) in a stratified brackish inlet. Aquat. Microb. Ecol. **13**, 267-274.

Defriez, E.J., Sheppard, L.W., Reid, P.C. & Reuman, D.C. (2016). Climate change-related regime shifts have altered spatial synchrony of plankton dynamics in the North Sea. *Global Change Biol.* **22**, 2069-2080.

Doney, S.C. (2006). Oceanography: Plankton in a warmer world. *Nature* **444**, 695-696.

Falkowski, P.G., Katz, M.E., Knoll, A.H., Quigg, A., Raven, J.A., Schofield, O. & Taylor, F.J.R. (2004). The evolution of modern eukaryotic phytoplankton. *Science* **305**(5682), 354-360.

Falkowski, P.G. & Raven, J.A. (2013). Aquatic photosynthesis. Princeton University Press.

Fenchel, T. & Hansen, P.J. (2006). Motile behaviour of the bloom-forming ciliate *Mesodinium rubrum*. *Mar. Biol. Res.* **2**, 33-40.

Figueroa, R.I., Garces, E. & Bravo, I. (2007). Comparative study of the life cycles of *Alexandrium tamutum* and *Alexandrium minutum* (Gonyaulacales, Dinophyceae) in culture. *J. Phycol.* **43**(5), 1039-1053.

Fraga, S., Gallager, S.M. & Anderson, D.M. (1989). Chain-forming dinoflagellates: an adaptation to red tides. Red tides: biology, environmental science and toxicology. Elsevier, New York, 281-284.

Frangópulos, M., Guisande, C. & Maneiro, I. (2004). Toxin production and competitive abilities under phosphorus limitation of *Alexandrium* species. *Harmful Algae* **3**(2), 131-139.

Frost, B.W. (1972). Effects of size and concentration of food particles on the feeding behavior of the marine planktonic copepod *Calanus pacificus*. *Limnol. Oceanogr.* **17**, 805-815.

Gaedke, U., Ruhenstroth-Bauer, M., Wiegand, I., Tirok, K., Aberle, N., Breithaupt, P., Lengfellner, K., Wohlers, J. & Sommer, U. (2010). Biotic interactions may overrule direct climate effects on spring phytoplankton dynamics. *Global Change Biol.* **16**, 1122-1136.

Garzio, L.M. & Steinberg, D.K. (2013). Microzooplankton community composition along the Western Antarctic Peninsula. *Deep Sea Res. Pt I: Oceanographic Research Papers* **77**. 36-49.

Gibson, J.A., Swadling, K.M., Pitman, T.M. & Burton, H.R. (1997). Overwintering populations of *Mesodinium rubrum* (Ciliophora: Haptorida) in lakes of the Vestfold Hills, East Antarctica. *Polar Boil.* **17**:175-179.

Glibert, P.M., Burkholder, J.M., Kana, T.M., Alexander, J., Skelton, H. & Shilling, C. 2009. Grazing by *Karenia brevis* on *Synechococcus* enhances its growth rate and may help to sustain blooms. *Aquat. Microb. Ecol.* **55**, 17–30.

Glibert, P.M., Icarus Allen, J., Artioli, Y.J., Beusen, A., Bouwman, L., Harle, J. & Holmes, R. (2014). Vulnerability of coastal ecosystems to changes in harmful algal bloom distribution in response to climate change: projections based on model analysis. *Global Change Biol.* **20**, 3845–3858.

Godhe, A., Narayanaswamy, C., Klais, R., Moorthy, K.V., Ramesh, R., Rai, A. & Reddy, H.V. (2015). Long–term patterns of net phytoplankton and hydrography in coastal SE Arabian Sea: What can be inferred from genus level data? *Estuar. Coast. Shelf S.* **162**, 69–75.

Goldman, J.C., Dennett, M.R. & Gordin, H. (1989). Dynamics of herbivorous grazing by the heterotrophic dinoflagellate *Oxyrrhis marina*. *J. Plankton Res.* **11**, 391–407.

Gómez, F. (2012). A quantitative review of the lifestyle, habitat and trophic diversity of dinoflagellates (Dinoflagellata, Alveolata). *Syst. Biodivers.* **10**(3), 267–275.

Gregg, W.W., Casey, N.W. & McClain, C.R. (2005). Recent trends in global ocean chlorophyll. *Geophys. Res. Lett.* **32**, L03606.

Guillard, R.R.L. & Ryther, J.H. (1962). Studies of marine planktonic diatoms. I. *Cyclotella nana* Hustedt and *Detonula confervacea* (Cleve) Grun. Can. *J. Microbiol.* **8**, 229–239.

Gustafson, D.E., Stoecker, D.K., Johnson, M.D., Van Heukelem, W.F. & Sneider, K. (2000). Cryptophyte algae are robbed of their organelles by the marine ciliate *Mesodinium rubrum*. *Nature* **405**, 1049–1052.

Hansen, P.J. (1992). Prey size selection, feeding rates and growth dynamics of heterotrophic dinoflagellates with special emphasis on *Gyrodinium spirale*. *Mar. Biol.* **114**, 327–334.

Hansen, P.J., Nielsen, T.G. & Kaas, H. (1995). Distribution and growth of protists and mesozooplankton during a bloom of *Chrysochromulina* spp. (Prymnesiophyceae, Prymnesiales). *Phycologia* **34**, 409–416.

Hansen, P.J., Bjornsen, P.K. & Hansen, B.W. (1997). Zooplankton grazing and growth: scaling within the 2–2,000–μm body size range. *Limnol. Oceanogr.* **42**, 687–704.

Hansen, P.J. & Fenchel, T. (2006). The bloom–forming ciliate *Mesodinium rubrum* harbours a single permanent endosymbiont. *Mar. Biol. Res.* **2**, 169–177.

Hansen, P.J., Nielsen, L.T., Johnson, M., Berge, T. & Flynn, K.J. 2013. Acquired phototrophy in *Mesodinium* and *Dinophysis*–A review of cellular organization, prey selectivity, nutrient uptake and bioenergetics. *Harmful Algae* **28**, 126–139.

Harvey, E.L., Jeong, H.J. & Menden–Deuer, S. (2013). Avoidance and attraction: Chemical cues influence predator–prey interactions of planktonic protists. *Limnol. Oceanogr.* **58**(4), 1176–1184.

Hayn, M., Howarth, R., Marino, R., Ganju, N., Berg, P., Foreman, K.H., Giblin, A.E. & McGlathery, K. (2014). Exchange of nitrogen and phosphorus between a shallow lagoon and coastal waters. *Estuar. Coast.* **37**, 63-73.

Heil, C.A., Glibert, P.M. & Fan, C. (2005). *Prorocentrum minimum* (Pavillard) Schiller: A review of a harmful algal bloom species of growing worldwide importance. *Harmful Algae* **4**, 449-470.

Heinbokel, J.F. (1978). Studies on the functional role of tintinnids in the Southern California Bight. I. Grazing and growth rates in laboratory cultures. *Mar. Biol.* **47**, 177-189.

Herbeck, L.S., Unger, D., Krumme, U., Liu, S.M. & Jennerjahn, T.C. (2011). Typhoon-induced precipitation impact on nutrient and suspended matter dynamics of a tropical estuary affected by human activities in Hainan, China. *Estuar. Coast. Shelf S.* **93**(4), 375-388.

Hewitt, J.E., Ellis, J.I. & Thrush, S.F. (2016). Multiple stressors, nonlinear effects and the implications of climate change impacts on marine coastal ecosystems. *Global Change Biol.* **22**, 2665-2675.

Hoef-Emden, K., Martin, B. & Melkonian, M. (2002). Nuclear and nucleomorph SSU rDNA phylogeny in the cryptophyta and the evolution of cryptophyte Diversity. *J. Mol. Evol.* **55**, 161-179.

Holling, C.S. (1959). Some Characteristics of Simple Types of Predation and Parasitism. *Can. Entomol.* **91**, 385-398

Honsell, G., Boni, L., Cabrini, M. & Pompei, M. (1992). Toxic or potentially toxic dinoflagellates from the Northern Adriatic Sea. *Sci. Total Environ.* 107-113

Humborg, C., Ittekkot, V., Cociasu, A. & Bodungen, B. V. (1997). Effect of Danube River dam on Black Sea biogeochemistry and ecosystem structure. *Nature* **386**, 385-388.

IPCC (2013). Climate Change 2013: The Physical Science Basis. In: *Contribution of Working Group I to the Fifth Assessment Report of the Intergovernmental Panel on Climate Change* (eds Stocker TF, Qin D, Plattner G-K, Tignor M, Allen SK, Boschung J, Nauels A, Xia Y, Bex V, Midgley PM). Cambridge University Press, Cambridge, UK.

Isla, J.A., Lengfellner, K. & Sommer, U. (2008). Physiological response of the copepod Pseudocalanus sp. in the Baltic Sea at different thermal scenarios. *Global Change Biol.* **14**, 895-906.

Jacobson, D.M. & Anderson, D.M. (1986). Thecate heterotrophic dinoflagellates: Feeding behavior and mechanisms. *J. Phycol.* **22**, 249-258.

Jacobson, D.M. & Anderson, D.M. (1996). Widespread phagocytosis of ciliates and other protists by marine mixotrophic and heterotrophic thecate dinoflaegllates. *J. Phycol.* **32**(2), 279-285.

Jakobsen, H.H., Everett, L.M. & Strom, S.L. (2006). Hydromechanical signaling between the ciliate *Mesodinium pulex* and motile protist prey. *Aquat. Microb. Ecol.* **44**(2), 197–206.

Jensen, M.Ø. & Moestrup, Ø. (1997). Autecology of the toxic dinoflagellate *Alexandrium ostenfeldii*: life history and growth at different temperatures and salinities. *Eur. J. Phycol.* **32**(01), 9–18.

Jeong, H.J., Shim, J.H., Kim, J.S., Park, J.Y., Lee, C.W. & Lee, Y. (1999). The feeding by the thecate mixotrophic dinoflagellate *Fragilidium* cf. *mexicanum* on red tide and toxic dinoflagellate. *Mar. Ecol. Prog. Ser.* **176**, 263–277.

Jeong, H.J., Kim, S.K., Kim, J.S., Kim, S.T., Yoo, Y.D. & Yoon, J.Y. (2001). Growth and grazing rates of the heterotrophic dinoflagellate *Polykrikos kofoidii* on red-tide and toxic dinoflagellates. *J. Eukaryot. Microb.* **48**, 298–308.

Jeong, H.J., Kim, J.S., Yoo, Y.D., Kim, S.T., Kim, T.H., Park, M.G., Lee, C.H., Seong, K.A., Kang, N.S. & Shim, J.H. (2003). Feeding by the Heterotrophic Dinoflagellate *Oxyrrhis marina* on the Red-Tide Raphidophyte *Heterosigma akashiwo*: a Potential Biological Method to Control Red Tides Using Mass-Cultured Grazers. *J. Eukaryot. Microb.* **50**(4), 274–282.

Jeong, H.J., Yoo, Y.D., Kim, S.T. & Kang, N.S. (2004). Feeding by the heterotrophic dinoflagellate *Protoperidinium bipes* on the diatom *Skeletonema costatum*. *Aquat. Microb. Ecol.* **36**(2), 171–179.

Jeong, H.J., Yoo, Y.D., Seong, K.A., Kim, J.H., Park, J.Y., Kim, S.H., Lee, S.H., Ha, J.H. & Yih, W.H. (2005a). Feeding by the mixotrophic dinoflagellate *Gonyaulax polygramma*: mechanisms, prey species, the effects of prey concentration, and grazing impact. *Aquat. Microb. Ecol.* **38**, 249-257.

Jeong, H.J., Yoo, Y.D., Park, J.Y., Song, J.Y., Kim, S.T., Lee, S.H., Kim, K.Y. & Yih, W.H. (2005b). Feeding by the phototrophic red-tide dinoflagellates: five species newly revealed and six species previously known to be mixotrophic. *Aquat. Microb. Ecol.* **40**, 133-155.

Jeong, H.J., Park, J.Y., Nho, J.H., Park, M.O., Ha, J.H., Seong, K.A., Chang, J., Seong, C.N., Lee, K.Y. & Yih, W.H. (2005c). Feeding by the red-tide dinoflagellates on the cyanobacterium *Synechococcus*. *Aquat. Microb. Ecol.* **41**, 131-143.

Jeong, H.J., Kim, J.S., Kim, J.H., Kim, S.T., Seong, K.A., Kim, T.H., Song, J.Y. & Kim, S.K. (2005d). Feeding and grazing impact by the newly described heterotrophic dinoflagellate *Stoeckeria algicida* on the harmful alga *Heterosigma akashiwo*. *Mar. Ecol. Prog. Ser.* **295**, 69-78.

Jeong, H.J., Ha, J.H., Park, J.Y., Kim, J.H., Kang, N.S., Kim, S., Kim, J.S., Yoo, Y.D. & Yih, W.H. (2006). Distribution of the heterotrophic dinoflagellate *Pfieteria piscicida* in Korean waters and its consumption of mixotrophic dinoflagellates, raphidophytes, and fish blood cells. *Aquat. Microb. Ecol.* **44**, 263-278.

Jeong, H.J., Ha, J.H., Yoo, Y.D., Park, J.Y., Kim, J.H., Kang, N.S., Kim, T.H., Kim, H.S. & Yih, W.H. (2007). Feeding by the *Pfiesteria*-like heterotrophic dinoflagellate *Luciella masanensis*. *J. Eukaryot. Microbiol.* **54,** 231-241.

Jeong, H.J., Seong, K.A., Yoo, Y.D., Kim, T.H., Kang, N.S., Kim, S., Park, J.Y., Kim, J.S., Kim, G.H. & Song, J.Y. (2008). Feeding and grazing impact by small marine heterotrophic dinoflagellates on heterotrophic bacteria. *J. Eukaryot. Microbiol.* **55,**271-288.

Jeong, H.J., Yoo, Y.D., Kang, N.S., Rho, J.R., Seong, K.A., Park, J.W., Nam, G.S. & Yih, W.H. (2010a). Ecology of *Gymnodinium aureolum*. I. Feeding in western Korean waters. *Aquat. Microb. Ecol.* **59**, 239-255.

Jeong, H.J., Yoo, Y.D., Kim, J.S., Seong, K.A., Kang, N.S. & Kim, T.H. (2010b). Growth, feeding, and ecological roles of the mixotrophic and heterotrophic dinoflagellates in marine planktonic food webs. *Ocean Science Journal* **45**(2), 65-91

Jeong, H.J., Kim, T.H., Yoo, Y.D., Yoon, E.Y., Kim, J.S., Seong, K.A., Kim, K.Y., Park, J.Y. (2011a). Grazing impact of heterotrophic dinoflagellates and ciliates on common red-tide euglenophyte *Eutreptiella gymnastica* in Masan Bay, Korea. *Harmful Algae* **10**(6), 576-588.

Jeong, H.J., Lee, K.H., Yoo, Y.D., Kang, N.S. & Lee, K.T. (2011b). Feeding by the newly described, nematocyst-bearing heterotrophic dinoflagellate *Gyrodiniellum shiwhaense*. *J. Eukaryot. Microbiol.* **58**, 511-524.

Jeong, H.J., Yoo, Y.D., Kang, N.S., Lim, A.S., Seong, K.A., Lee, S.Y., Lee, M.J., Lee, K.H., Kim, H.S., Shin, W., Nam, S.W., Yih, W. & Lee, K. (2012). Heterotrophic feeding as a newly identified survival strategy of the dinoflagellate *Symbiodinium*. *Proc. Natl. Acad. Sci.* **109**, 12604-12609.

Jeong, H.J., Yoo, Y.D., Lim, A.S., Kim, T.W., Lee, K. & Kang, C.K. (2013a). Raphidophyte red tides in Korean waters. *Harmful Algae* **30**, S41-S52.

Jeong, H.J., Yoo, Y.D., Lee, K.H., Kim, T.H., Seong, K.A., Kang, N.S., Lee, S.Y., Kim, J.S., Kim, S. & Yih, W.H. (2013b). Red tides in Masan Bay, Korea in 2004-2005: I. Daily variations in the abundance of red-tide organisms and environmental factors. *Harmful Algae,* **30**, S75-S88.

Jeong, H.J., Lim, A.S., Yoo, Y.D., Lee, M.J., Lee, K.H., Jang, T.Y. & Lee, K. (2014). Feeding by Heterotrophic Dinoflagellates and Ciliates on the Free-living Dinoflagellate *Symbiodinium* sp.(Clade E). *J. Eukaryot. Microbiol.* **61**:27-41.

Jeong, H.J., Lim, A.S., Franks, P.J., Lee, K.H., Kim, J.H., Kang, N.S., Lee, M.J., Jang, S.H., Lee, S.Y., Yoon, E.Y., Park, J.Y., Yoo, Y.D., Seong, K.A., Kwon, J.E. & Jang, T.Y. (2015). A hierarchy of conceptual models of red-tide generation: Nutrition, behavior, and biological interactions. *Harmful Algae* **47**, 97-115.

John, U., Cembella, A., Hummert, C., Elbrächter, M., Groben, R. & Medlin, L. (2003). Discrimination of the toxigenic dinoflagellates *Alexandrium tamarense* and *A. ostenfeldii* in co-occurring natural populations from Scottish coastal waters. *Eur. J. Phycol.* **38**(1), 25-40.

Johnson, M.D., Tengs, T., Oldach, D.W., Delwiche, C.F. & Stoecker, D.K. (2004). Highly Divergent SSU rRNA Genes Found in the Marine Ciliates *Myrionecta rubra* and *Mesodinium pulex*. *Protist* **155**, 347-359.

Johnson, M.D. (2011). The acquisition of phototrophy: adaptive strategies of hosting endosymbionts and organelles. *Photosynthesis research*, **107**(1), 117-132.

Johnson, M.D., Stoecker, D.K. & Marshall, H.G. (2013). Seasonal dynamics of *Mesodinium rubrum* in Chesapeake Bay. *J. Plankton Res.* **35**:877-893.

Kang, N.S., Lee, K.H., Jeong, H.J., Yoo, Y.D., Seong, K.A., Potvin, É., Hwang, Y.J. & Yoon, E.Y. (2013). Red tides in Shiwha Bay, western Korea: a huge dike and tidal power plant established in a semi-enclosed embayment system. *Harmful Algae* **30**, S114-S130.

Kang, N.S., Jeong, H.J., Lee, S.Y., Lim, A.S., Lee, M.J., Kim, H.S. & Yih, W.H. (2013). Morphology and molecular characterization of the epiphytic benthic dinoflagellate *Ostreopsis* cf. *ovata* in the temperate waters off Jeju Island, Korea. *Harmful Algae* **27**, 98-112.

Kang, N.S., Jeong, H.J., Moestrup, Ø., Lee, S.Y., Lim, A.S., Jang, T.Y., Lee, K.H., Lee, M.J., Jang, S.H., Potvin, É., Lee, S.K. & Rho, J.H. (2014). *Gymnodinium smaydae* n. sp., a new planktonic phototrophic dinoflagellate from the coastal waters of western Korea: morphology and molecular characterization. *J. Eukaryotic Microbiol.* **61**(2), 182-203.

Kang, N.S., Jeong, H.J., Yoo, Y.D., Yoon, E.Y., Lee, K.H., Lee, K. & Kim, K.H. (2011). Mixotrophy in the newly described phototrophic dinoflagellate *Woloszynskia cincta* from western Korean waters: Feeding mechanism, prey species, and effect of prey concentration. *J. Eukaryotic Microbiol.* **58**(2), 152-170

Karp-Boss, L., Boss, E. & Jumars, P.A. (2000). Motion of dinoflagellates in a simple shear flow. *Limnol. Oceanogr.* **45**(7), 1594-1602.

Kemp, W.M., Smith, E.M., Marvin-DiPasquale, M. & Boynton, W.R. (1997). Organic carbon-balance and net ecosystem metabolism in Chesapeake Bay. Mar. Ecol. Prog. Ser. **150**, 229-248

Kim, J.S., Jeong, H.J., Yoo, Y.D., Kang, N.S., Kim, S.K., Song, J.Y., Lee, M.J., Kim, S.T., Kang, J,H., Seong, K.A. & Yih, W.H. (2013). Red tides in Masan Bay, Korea, in 2004-2005: III. Daily variations in the abundance of mesozooplankton and their grazing impacts on red-tide organisms. *Harmful algae* **30**, S102-S113.

Kim, K.T., Lee, S.H., Kim, E.S., Cho, S.R. & Park, C.K. (2002). Behavior of heavy metals in the surface waters of the Lake Shihwa and its tributaries. *Journal of the Korean Society for Marine Environment & Energy*, **5**(1), 51-67.

Kim, T.W., Lee, K., Najjar, R.G., Jeong, H.D. & Jeong, H.J. (2011). Increasing N abundance in the northwestern Pacific Ocean due to atmospheric nitrogen deposition. *Science* **334**, 505-509.

Kim, T.W., Najjar, R.G. & Lee, K. (2014). Influence of precipitation events on phytoplankton biomass in coastal waters of the eastern United States. *Global Biogeochem. Cy.* **28**(1), 1-13.

Kim, T.W., Kim, D., Baek, S.H. & Kim, Y.O. (2015). Human and riverine impacts on the dynamics of biogeochemical parameters in Kwangyang Bay, South Korea revealed by time-series data and multivariate statistics. *Mar. Pollut. Bull.* **90**(1), 304-311.

Kim, J.S. & Jeong, H.J. (2004). Feeding by the heterotrophic dinoflagellates *Gyrodinium dominans* and *Gyrodinium spirale* on the red-tide dinoflagellate *Prorocentrum minimum*. *Mar. Ecol. Prog. Ser.* **280**, 85-94.

Kim, J.H., Jeong, H.J., Lim, A.S., Rho, J.R. & Lee, S.B. (2016). Killing potential protist predators as a survival strategy of the newly described dinoflagellate *Alexandrium pohangense*. *Harmful Algae* **55**, 41-55.

Kim, S., Kang, Y.G., Kim, H.S., Yih, W., Coats, D.W. & Park, M.G. (2008). Growth and grazing responses of the mixotrophic dinoflagellate *Dinophysis acuminata* as functions of light intensity and prey concentration. *Aquat. Microb. Ecol.* **51**, 301-310.

Klais, R., Cloern, J.E. & Harrison, P.J. (2015). Resolving variability of phytoplankton species composition and blooms in coastal ecosystems. *Estuar. Coast. Shelf S.* **162**, 4-6.

Lagos, N. (2003). Paralytic shellfish poisoning phycotoxins: occurrence in South America. *Comments on Toxicology* **9**(2), 175-193.

Lassen, M.K., Nielsen, K.D., Richardson, K., Garde, K. & Schlüter, L. (2010). The effects of temperature increases on a temperate phytoplankton community—a mesocosm climate change scenario. *J. Exp. Mar. Biol. Ecol.* **383**, 79-88.

Lee, F.W.F., Morse, D. & Lo, S.C.L. (2009). Identification of two plastid proteins in the dinoflagellate *Alexandrium affi*ne that are substantially down-regulated by nitrogen-depletion. *J. Proteome Res.* **8**(11), 5080-5092.

Lee, K.H. (2012). Response by phytoplankton and heterotrophic protists collected from Shiwha Bay, Korea in cold seasons to water temperature increase. MS Thesis. Seoul National University, Korea.

Lee, K.H., Jeong, H.J., Park, K., Kang, N.S., Yoo, Y.D., Lee, M.J., Lee, J.W., Lee, S.J., Kim, T.K., Kim, H.S. & Noh, J.H. (2013). Morphology and molecular characterization of the epiphytic dinoflagellate *Amphidinium massartii*, isolated from the temperate waters off Jeju Island, Korea. *Algae* **28**(3), 213–231.

Lee, K.H., Jeong, H.J., Jang, T.Y., Lim, A.S., Kang, N.S., Kim, J.H., Kim, K.Y., Park, K.T. & Lee, K., 2014a. Feeding by the newly described mixotrophic dinoflagellate *Gymnodinium smaydae*: Feeding mechanism, prey species, and effect of prey concentration. *J. Exp. Mar. Biol. Ecol.* **459**, 114–125.

Lee, K.H., Jeong, H.J., Yoon, E.Y., Jang, S.H., Kim, H.S. & Yih, W. 2014b. Feeding by common heterotrophic dinoflagellates and a ciliate on the red-tide ciliate *Mesodinium rubrum*. *Algae* **29**(2), 153–163.

Lee, S.K., Jeong, H.J., Jang, S.H., Lee, K.H., Kang, N.S., Lee, M.J. & Potvin, E. (2014c). Mixotrophy in the newly described dinoflagellate *Ansanella granifera*: feeding mechanism, prey species, and effect of prey concentration. *Algae* **29**(2), 137–152.

Lee, M.J., Jeong, H.J., Lee, K.H., Jang, S.H., Kim, J.H. & Kim, K.Y. (2015). Mixotrophy in the nematocyst-taeniocyst complex-bearing phototrophic dinoflagellate *Polykrikos hartmannii*. *Harmful Algae* **49**, 124–134.

Lewandowska, A.M., Boyce, D.G., Hofmann, M., Matthiessen, B., Sommer, U. & Worm, B. (2014). Effects of sea surface warming on marine plankton. *Ecol. Let.* **17**, 614-623.

Lewis, N.I., Xu, W., Jericho, S.K., Kreuzer, H.J., Jericho, M.H. & Cembella, A.D. (2006). Swimming speed of three species of *Alexandrium* (Dinophyceae) as determined by digital in-line holography. *Phycologia* **45**(1), 61-70.

Li, A., Stoecker, D.K. & Coats, D. W. (2000). Mixotrophy in *Gyrodinium galatheanum* (dinophyceae): grazing responses to light intensity and inorganic nutrients. *J. Phycol.* **36**, 33-45.

Li, T.S., Yu, R.C. & Zhou, M.J. (2011). Short-term effects of different nitrogen substrates on growth and toxin production of dinoflagellate *Alexandrium catenella* Balech (strain ACDH). *Harmful algae* **12**, 46-54.

Lim, A.S., Jeong, H.J., Kim, J.H., Jang, S.H., Lee, M.J. & Lee, K. (2015). Mixotrophy in the newly described dinoflagellate *Alexandrium pohangense*: A specialist for feeding on the fast-swimming ichthyotoxic dinoflagellate *Cochlodinium polykrikoides*. *Harmful Algae* **49**, 10-18.

Lim, P.T. & Ogata, T. (2005). Salinity effect on growth and toxin production of four tropical Alexandrium species (Dinophyceae). *Toxicon* **45**(6), 699-710.

Lindholm, T. (1985). *Mesodinium rubrum*—a unique photosynthetic ciliate. *Adv. Aquat. Microbial.* **3**, 1-48.

MacKenzie, L., de Salas, M., Adamson, J. & Beuzenberg, V. (2004). The dinoflagellate genus *Alexandrium* (Halim) in New Zealand coastal waters: comparative morphology, toxicity and molecular genetics. *Harmful Algae* **3**(1), 71-92.

Mallin, M.A., Paerl, H.W., Rudek, J. & Bates, P.W. (1993). Regulation of estuarine primary production by watershed rainfall and river flow. *Mar. Ecol. Prog. Ser.* **93**, 199-199.

Margalef, R. (1978). Life-forms of phytoplankton as survival alternatives in an unstable environment. *Oceanol. Acta* **1**(4), 493-509.

Marin, B., Klingberg, M. & Melkonian, M. (1998). Phylogenetic relationships among the Cryptophyta: analyses of nuclear-encoded SSU rRNA sequences support the monophyly of extant plastid-containing lineages. *Protist* **149**(3), 265-276.

Marinov, I., Doney, S.C. & Lima, I.D. (2010). Response of ocean phytoplankton community structure to climate change over the 21st century: partitioning the effects of nutrients, temperature and light. *Biogeosciences*, **7**, 3941-3959.

Marinov, I., Doney, S.C., Lima, I.D., Lindsay, K., Moore, J.K. & Mahowald, N. (2013). North-South asymmetry in the modeled phytoplankton community response to climate change over the 21st century. *Global Biogeochem. Cy.* **27**, 1274-1290.

Martinez, E., Raitsos, D.E. & Antoine, D. (2016). Warmer, deeper, and greener mixed layers in the North Atlantic subpolar gyre over the last 50 years. *Global Change Biol.*, **22**, 604-612.

Mateo, P.P., Hemminga, M.A. & Peene, J. (2001). Measurement of seagrass production using the ^{13}C stable isotope compared with classical O_2 and ^{14}C methods. *Mar. Ecol. Prog. Ser.* **223**,157-165.

McClain, C.R. (2009). A decade of satellite ocean color observations. *Annu. Rev. Mar. Sci.* **1**, 19-42.

McQuatters-Gollop, A., Reid, P.C., Edwards, M., Burkill, P.H., Castellani, C., Batten, S., Gleskes, W., Beare, D., Bidigare, R.R., Head, E., Johnson, R., Kahru, M., Koslow, J.A. & Pena, A. (2011). Is there a decline in marine phytoplankton? *Nature* **472**(7342), E6-E7.

Menden-Deuer, S. & Lessard, E. (2000). Carbon to volume relationships for dinoflagellates, diatoms, and other protist plankton. *Limnol. Oceanogr.* **45**, 569-579.

Meunier, C.L., Schulz, K., Boersma, M. & Malzahn, A.M. (2013). Impact of swimming behaviour and nutrient limitation on predator-prey interactions in pelagic microbial food webs. *J. Exp. Mar. Biol. Ecol.* **446**, 29-35.

Mitra, A. & Flynn, K.J. (2010). Modelling mixotrophy in harmful algal blooms: More or less the sum of the parts? *J. Marine Syst.* **83**(3), 158-169.

Mitra, A., Flynn, K.J., Tillmann, U., Raven, J.A., Caron, D., Stoecker, D.K., Not, F., Hansen, P.J., Hallegraeff, G., Sanders, R., Wilken, S., McManus, G., Johnson, M., Pitta, P., Våge, S., Berge, T., Calbet, A., Thingstad, F., Jeong, H.J., Burkholder, J., Glibert, P.M., Granéli, E. & Lundgren, V. (2016). Defining planktonic protist functional groups on mechanisms for energy and nutrient acquisition: incorporation of diverse mixotrophic strategies. *Protist* **167**(2), 106-120.

Murray, S.A., Diwan, R., Orr, R.J., Kohli, G.S. & John, U. (2015). Gene duplication, loss and selection in the evolution of saxitoxin biosynthesis in alveolates. *Mol. Phylogen. Evol.* **92**, 165-180.

Myung, G., Kim, H.S., Park, J.S., Park, M.G. & Yih, W. (2011). Population growth and plastid type of *Myrionecta rubra* depend on the kinds of available cryptomonad prey. *Harmful Algae* **10**, 536-541.

Nagai, S., Nishitani, G., Takano, Y., Yoshida, M. & Takayama, H. (2009). Encystment and excystment under laboratory conditions of the nontoxic dinoflagellate *Alexandrium fraterculus* (Dinophyceae) isolated from the Seto Inland Sea, Japan. *Phycologia* **48**(3), 177-185.

Nakamura, Y., Suzuki, S.Y. & Hiromi, J. (1995). Growth and grazing of a naked heterotrophic dinoflagellate, *Gyrodinium dominans*. *Aquat. Microb. Ecol.* **9**, 157-164.

Nakamura, Y., Yamazaki, Y. & Hiromi, J. (1992). Growth and grazing of a heterotrophic dinoflagellate, *Gyrodinium dominans*, feeding on a red tide flagellate, *Chattonella antiqua*. *Mar. Ecol. Prog. Ser.* **82**, 275-279.

Nakanishi, K., Masao, A., Sako, Y., Ishida, Y., Muguruma, H. & Karube, I. (1996). Detection of the red tide-causing plankton *Alexandrium affine* by a piezoelectric immunosensor using a novel method of immobilizing antibodies. *Analytical letters* **29**(8), 1247-1258.

Naustvoll, L.J. (2000). Prey size spectra and food preferences in thecate heterotrophic dinoflagellates. *Phycologia* **39**(3), 187-198.

Nguyen-Ngoc, L. (2004). An autecological study of the potentially toxic dinoflagellate *Alexandrium affine* isolated from Vietnamese waters. *Harmful Algae* **3**(2), 117-129.

Nixon, S.W. (1995). Coastal marine eutrophication: a definition, social causes, and future concerns. *Ophelia* **41**(1), 199-219.

NOAA, www.nodc.noaa.gov-water temperature table of all coastal regions.

Nielsen, L.T. & Kiørboe, T. (2015). *The ISME journal* **9**(10), 2117-2127.

Omachi, C.Y., Tamanaha, M.D.S. & Proença, L.A.D.O. (2007). Bloom of *Alexandrium fraterculus* in coastal waters off Itajaí, SC, Southern Brazil. *Braz. J. Oceanogr.* **55**(1), 57-61.

Odebrecht, C., Du Preez, D.R., Abreu, P.C. & Campbell, E.E. (2014). Surf zone diatoms: a review of the drivers, patterns and role in sandy beaches food chains. *Estuarine, Estuar. Coast. Shelf S.* **150**, 24–35.

Odebrecht, C., Abreu, P.C. & Carstensen, J. (2015). Retention time generates short–term phytoplankton blooms in a shallow microtidal subtropical estuary. *Estuar. Coast. Shelf S.* **162**, 35–44.

Orr, R.J., Stüken, A., Rundberget, T., Eikrem, W. & Jakobsen, K.S. (2011). Improved phylogenetic resolution of toxic and non–toxic *Alexandrium* strains using a concatenated rDNA approach. *Harmful Algae* **10**(6), 676–688.

Park, J., Jeong, H.J., Yoo, Y.D. & Yoon, E.Y. (2013). Mixotrophic dinoflagellate red tides in Korean waters: distribution and ecophysiology. *Harmful Algae* **30**, S28–S40.

Park, M.G., Kim, S., Kim, H.S., Myung, G., Kang, Y.G. & Yih, W. (2006). First successful culture of the marine dinoflagellate *Dinophysis acuminata*. *Aquat. Microb. Ecol.* **45**, 101–106.

Park, M.G., Lee, H., Kim, K.Y. & Kim, S. (2011). Feeding behavior, spatial distribution and phylogenetic affinities of the heterotrophic dinoflagellate *Oxyphysis oxytoxoides*. *Aquat. Microb. Ecol.* **62**, 279–287.

Park, M.G., Kim, M. & Kang, M. (2013). A Dinoflagellate *Amylax triacantha* with Plastids of the Cryptophyte Origin: Phylogeny, Feeding Mechanism, and Growth and Grazing Responses. *J. Eukaryot. Microbiol.* **60**(4), 363–376.

Paerl, H.W., Rudek, J. & Mallin, M.A. (1990). Stimulation of phytoplankton production in coastal waters by natural rainfall inputs: nutritional and trophic implications. *Mari. Biol.* **107**(2), 247-254.

Platt, T., Fuentes-Yaco, C. & Frank, K.T. (2003). Marine ecology: spring algal bloom and larval fish survival. *Nature* **423**(6938), 398-399.

Redfield, A.C. (1958). The biological control of chemical factors in the environment. *American Scientist* **46**, 205-221.

Phlips, E.J., Hendrickson, J., Quinlan, E.L. & Cichra, M. (2007). Meteorological influences on algal bloom potential in a nutrient-rich blackwater river. *Freshwater Biol.* **52**(11), 2141-2155.

Reichwaldt, E.S. & Ghadouani, A. (2012). Effects of rainfall patterns on toxic cyanobacterial blooms in a changing climate: between simplistic scenarios and complex dynamics. *Water research* **46**(5), 1372-1393.

Richardson, A.J. & Schoeman, D.S. (2004). Climate impact on plankton ecosystems in the Northeast Atlantic. *Science* **305**(5690), 1609-1612.

Rogato, A., D' Apuzzo, E., Barbulova, A., Omrane, S., Parlati, A., Carfagna, S., Costa, A., Schiavo, F.L., Esposito, S. & Chiurazzi, M. (2010). Characterization of a Developmental Root Response Caused by External Ammonium Supply in Lotus japonicus. *Plant Physiology* **154**(2), 784-795.

Smayda, T.J. (1997). Harmful algal blooms: their ecophysiology and general relevance to phytoplankton blooms in the sea. *Limnol. Oceanogr.* **42**, 1137–1153.

Smayda, T.J. & Reynolds, C.S. (2001). Community assembly in marine phytoplankton: application of recent models to harmful dinoflagellate blooms. *J. Plankton Res.* **23**(5), 447–461.

Sampedro, N., Franco, J.M., Zapata, M., Riobó, P., Garcés, E., Penna, A., Caillaud, A., Diogéne, J., Cacho, E. & Camp, J. (2013). The toxicity and intraspecific variability of *Alexandrium andersonii* Balech. *Harmful algae* **25**, 26–38.

Samson, J.C., Shumway, S.E. & Weis, J.S. (2008). Effects of the toxic dinoflagellate, *Alexandrium fundyense* on three species of larval fish: a food-chain approach. *J. Fish Biol.* **72**(1), 168–188.

Sarmiento, J.L., Slater, R., Barber, Bopp, R.L. Doney, S.C., Hirst, A.C. Kleypas, J., Matear, R., Mikolajewicz, U., Monfray, P., Soldatov, V., Spall, S.A. & Stouffer, R. (2004). Response of ocean ecosystems to climate warming. *Global Biogeochem. Cy.* **18**(3), GB3003.

Seong, K.A., Jeong, H.J., Kim, S., Kim, G.H. & Kang, J.H. (2006). Bacterivory by co-occurring red-tide algae, heterotrophic nanoflagellates, and ciliates on marine bacteria. *Mar. Ecol. Prog. Ser.* **322**, 85–97.

Seuthe, L., Iversen, K.R. & Narcy, F. (2011). Microbial processes in a high-latitude fjord (Kongsfjorden, Svalbard): II. Ciliates and dinoflagellates. *Polar Boil.* **34**, 751-766.

Sherr, E.B. & Sherr, B.F. (2002). Significance of predation by protists in aquatic microbial food webs. *Ant. van Leeuwenh.* **81**, 293-308.

Shumway, S.E., Allen, S.M. & Boersma, P.D. (2003). Marine birds and harmful algal blooms: sporadic victims or under-reported events? *Harmful Algae* **2**, 1-17.

Smayda, T.J. (2002). Turbulence, watermass stratification and harmful algal blooms: an alternative view and frontal zones as "pelagic seed banks". *Harmful Algae* **1**, 95-112.

Sommer, U., Lengfellner, K. (2008). Climate change and the timing, magnitude, and composition of the phytoplankton spring bloom. *Global Change Biology*, **14**, 1199-1208.

Sommer, U., Lewandowska, A. (2011). Climate change and the phytoplankton spring bloom: warming and overwintering zooplankton have similar effects on phytoplankton. *Global Change Biol.* **17**, 154-162.

Sournia, A., Chrdtiennot-Dinet, M.J. & Ricard, M. (1991). Marine phytoplankton: how many species in the world ocean? *J. Plankton Res,* **13**(5), 1093-1099.

Steinacher, M., Joos, F., Frolicher, T.L., Boop, L., Cadule, P., Cocco, V., Doney, S., Gehlen, M., Lindsay, K., Moore, J.K., Schneider, B. & Segschneider, J. (2010). Projected 21st century decrease in marine productivity: a multi-model analysis. *Biogeosciences*, **7**, 979-1005.

Stoecker, D.K. & Capuzzo, J.M. (1990). Predation on protozoa: its importance to zooplankton. *J. Plankton Res.*, **12**, 891-908.

Strickland, J.D. & Parsons, T.R. (1972). A practical handbook of seawater analysis, 2nd ed. Bull. Fish. Res. Board. Can. p. 167.

Strom, S.L. & Buskey, E.J. (1993). Feeding, growth, and behavior of the thecate heterotrophic dinoflagellate *Oblea rotunda. Limnol. Oceanogr*. **38**, 965-977.

Thompson, P.A., O'Brien, T.D., Paerl, H.W., Peierls, B.L., Harrison, P.J. & Robb, M. (2015a). Precipitation as a driver of phytoplankton ecology in coastal waters: A climatic perspective. *Estuar. Coast. Shelf S.* **162**, 119-129.

Thompson, P.A., Bonham, P., Thomson, P., Rochester, W., Doblin, M.A., Waite, A.M., Richardson, A. & Rousseaux, C.S. (2015b). Climate variability drives plankton community composition changes: the 2010-2011 El Ni›o to La Ni›a transition around Australia. *J. Plankton Res.* **37**(5), 966-984.

Tillmann, U. (2004). Interactions between planktonic microalgae and protozoan grazers. *J. Eukaryot. Microbiol.* **51**, 156-168.

Turner, R.E., Rabalais, N.N., Justic, D. & Dortch, Q. (2003) Global patterns of dissolved N, P and Si in large rivers. *Biogeochemistry*, **64**, 297-317.

Turner, J.T. (2006). Harmful algae interactions with marine planktonic grapers. In: Grane´ li, E., Turner, J.T. (Eds.), Ecology of Harmful Algae. Springer-Verlag, Berlin, pp. 259-270.

Uchida, T., Kamiyama, T. & Matsuyama, Y. (1997). Predation by a photosynthetic dinoflagellate Gyrodinium instriatum on loricated ciliates. *J. Plankton Res.* **19**(5), 603-608.

Weyhenmeyer, G.A., Willén, E. & Sonesten, L. (2004). Effects of an extreme precipitation event on water chemistry and phytoplankton in the Swedish Lake Mälaren. *Boreal Environ. Res.* **9**(5), 409-420.

Westberry, T.K., Schultz, P., Behrenfeld, M.J. Dunne, J.P., Hiscock, M.R., Maritorena, S., Sarmiento, J.L. & Siegel, D.A. (2016). Annual cycles of phytoplankton biomass in the subarctic Atlantic and Pacific Ocean. *Global Biogeochem. Cy.* **30**, 175-190.

Weisse, T., Gröschl, B. & Bergkemper, V. (2016). Phytoplankton response to short-term temperature and nutrient changes. *Limnologica-Ecology and Management of Inland Waters* **59**, 78-89.

Williams, J.A. (1996). Blooms of *Mesodinium rubrum* in Southampton Water—do they shape mesozooplankton distribution? J. Plankton Res. 18:1685-1697.

Wong, G.T.F., Gong, G.C., Liu, K.K. & Pai, S.C. (1998). 'Excess Nitrate' in the East China Sea. *Estuar. Coast. Shelf S.* **46**(3), 411-418.

Woodworth-Jefcoats, P.A., Polovina, J.J., Dunne, J.P. & Blanchard, J.L. (2013) Ecosystem size structure response to 21st century climate projection: large fish abundance decreases in the central North Pacific and increases in the California Current. *Global Change Biol.* **19**, 724–733.

Yih, W., Kim, H.S., Jeong, H.J., Myung, G. & Kim, Y.G. (2004). Ingestion of cryptophyte cells by the marine photosynthetic ciliate *Mesodinium rubrum*. *Aquat. Microb. Ecol.* **36**, 165–170.

Yih, W., Kim, H.S., Myung, G., Park, J.W., Yoo, Y.D. & Jeong, H.J. (2013). The red-tide ciliate *Mesodinium rubrum* in Korean coastal waters. *Harmful Algae* **30**, S53–S61.

Yoo, Y.D., Jeong, H.J., Kim, M.S., Kang, N.S., Song, J.Y., Shin, W.G., Kim, K.Y. & Lee, K.T. (2009). Feeding by phototrophic red-tide dinoflagellates on the ubiquitous marine diatom *Skeletonema costatum*. *J. Eukaryot. Microbiol.* **56**, 413–420.

Yoo, Y.D., Jeong, H.J., Kang, N.S., Kim, J.S., Kim, T.H. & Yoon, E.Y. (2010a). Ecology of *Gymnodinium aureolum*. II. Predation by common heterotrophic dinoflagellates and a ciliate. *Aquat. Microb. Ecol.* **59**, 257–272.

Yoo, Y.D., Jeong, H.J., Kang, N.S., Song, J.Y., Kim, K.Y., Lee, K.T. & Kim, J.H. (2010b). Feeding by the newly described mixotrophic dinoflagellate *Paragymnodinium shiwhaense*: feeding mechanism, prey species, and effect of prey concentration. *J. Eukaryot. Microbiol.* **57**, 145–158.

Yoo, Y. D., Jeong, H. J., Kim, J. S., Kim, T. H., Kim, J. H., Seong, K. A., Lee, S. H., Kang, N. S., Park, J. W., Park, J. Y., Yoon, E. Y. & Yih, W. H. (2013a). Red tides in Masan Bay, Korea in 2004–2005: II. Daily variations in the abundance of heterotrophic protists and their grazing impact on red-tide organisms. *Harmful Algae* **30**, S89-S101.

Yoo, Y.D., Yoon, E.Y., Lee, K.H., Kang, N.S. & Jeong, H.J. (2013b). Growth and ingestion rates of heterotrophic dinoflagellates and a ciliate on the mixotrophic dinoflagellate *Biecheleria cincta*. *Algae* **28**, 343-354.

Yoo, Y.D., Yoon, E.Y., Jeong, H.J., Lee, K.H., Hwang, Y.J., Seong, K.A., Kim, J.S. & Park, J.Y. (2013c). The newly described heterotrophic dinoflagellate *Gyrodinium moestrupii*, an effective protistan grazer of toxic dinoflagellates. *J. Eukaryot. Microbiol*. **60**, 13-24

Zhou, M.J., Shen, Z.L. & Yu, R.C. (2008). Responses of a coastal phytoplankton community to increased nutrient input from the Changjiang (Yangtze) River. *Cont. Shelf Res.* **28**, 1483-1489.

국문초록

한국 연안에서 기상학적, 수리학적, 생물학적 요인들이 적조 유발 생물의 생태생리에 미치는 영향에 대한 연구

이 경 하

해양학 전공

지구환경과학부

자연과학대학

서울대학교 대학원

해양플랑크톤의 생태, 생리학적 특성은 기상학에서 주요하게 고려되는 두 가지 요소인 온도와 강수량에 쉽게 영향을 받는다. 이들 해양플랑크톤은 수많은 포식자-피식자간 연결 경로를 구성하고 있는 근본적인 해양 먹이망을 구성하는 요소이며, 해양 내의 다양한 원소들의 순환에 기여한다. 아울러, 지난 수십 년간 지구온난화와 부영양화는 해양생태계를 변화시키는 가장 심각한 환경 문제로 부각되고 있다. 그러나 이러한 기상학적, 수리학적, 생물학적 요인들이 통합적으로 플랑크톤 군집에 미치는 영향에 대한 이해는 많이 부족한 현실이다. 따라서 본 논문에서는 기상학적, 수리학적, 생물학적 요인들의 영향이 적조 유발 해양 플랑크톤의 생태생리에 미치는 영향에 대한 연구를 진행하였고, 실내 배양실험과 현장 조사 결과를 병행하여 통합적 연구를 진행하였다.

제 1 장에서는 전반적으로 본 연구를 시작하게 된 배경에 대해 기술하였다. 제 2장에서는 한국 연안에서 강우, 염분, 영양염류의 상관관계가 식물플랑크톤 군집에 미치는 영향에 대해 조사하기 위해서, 광양만에서 2011년부터 2013년 까지 그리고, 시화호에서 2009년부터 2011년까지 매월 시료 채집을 진행하였다. 광양만에서는 7, 10, 12, 14, 16, 18, 20일간의 강우량 합이 염분과 큰 상관관계를 보였다 ($p<0.001$). 특히 여름철 자료를 분석한 결과, 2011년과 2012년도에 염분과 질산염 (NO_3^-)의 농도가 강한 음의 선형 관계를 나타내었고 그 시기에 규조류가 우점하였다. 그러나 염분과 질산염의 농도가 상관관계를 보이지 않은 2013년도에는 ($p>0.05$) 와편모류가 우점하였다. 시화호에서도 7, 10, 14, 20일 강수량 합이 염분과 큰 상관관계를 보였다 ($p<0.05$). 각 년도별 자료를 분석한 결과, 2009년과 2010년도에 염분과 질산염(NO_3^-)의 농도가 상관관계를 나타내지 않았고, 그 시기에 와편모류가 우점하였다. 그러나 염분과 질산염의 농도가 강한 음의 선형상관관계를 보인 2011년에는 규조류와 소형 편모류에 속하는 은편모류가 우점하였다. 따라서 이러한 강우, 염분, 영양염류의 농도간의 순차적인 상관관계는 우점 식물플랑크톤 그룹을 결정하는데 주요 요소임을 확인하였다.

제 3장에서는 시화호에서 신종으로 발견된 *Gymnodinium smaydae* 의 혼합영양 메커니즘과 섭식 가능한 먹이에 대한 연구를 진행하였다. 19종의 먹이종이 제공되었을 때, *G. smaydae*는 유각 (thecate) 와편모류인 *Heterocapsa rotundata, Heterocapsa triquetra*, *Heterocapsa* sp., *Scrippsiella trochoidea* 를 잘 섭식하는 것으로 나타났다. G. smaydae는 tow filament로 먹이를 고정한 후에 섭식관(peduncle)을 이용하여 먹이를 섭식하였다. 실험에서 제공된 모든 *Heterocapsa* spp. 종에 대해 *G. smaydae*의 성장이 일어나는 것이 확인되었으나, *S. trochoidea*는 거의 성장이 유지되는 것으로 나타났다. *G.*

smaydae 가 20 ℃ 온도 유지, 20 μE m^{-2} s^{-1} 의 광도로 14:10 h 광-암 cycle 의 조건에서 광합성만으로 성장할 경우에 성장률은 were 0.005 d^{-1}이었으나, *H. rotundata*와 *H. triquetra*를 먹이로 하였을 때의 최대 혼합영양 성장률은 각각 0.226 d^{-1}와 1.053 d^{-1}이었다. 더불어 *G. smaydae* 가 *H. rotundata*와 *H. triquetra*를 먹이로 하였을 때의 최대 섭식률은 각각 1.59 ng C grazer^{-1}d^{-1} 와 0.24 ng C grazer^{-1}d^{-1} 이었다. 현장에서 *H. rotundata* 나 *H. triquetra* 와 동시에 출현하였을 때 *G. smaydae*의 먹이 제거 능력은 각각 0.23 h^{-1} 와 0.02 h^{-1} 이었다. 이러한 연구 결과는 *G. smaydae*가 순수 광합성만으로 성장은 어려우나, 다른 다양한 혼합영양성 와편모류들을 섭식함으로서 생존이 가능하며, 혼합영양을 이용하여 적조를 유발할 수 있는 잠재적인 종임을 밝혔다.

제 4장에서는 우리나라 연안에서 발견된 유해성 *Alexandrium* 속에 속하는 세 종들 (*A. andersonii*, *A. affine*, and *A. fraterculus*)의 혼합영양 능력 여부에 대한 연구를 진행하였다. 박테리아 크기의 micro-beads를 포함하여 광합성세균 (cyanobacteria)와 다양한 먹이 종에 대해 섭식여부를 관찰한 결과 *A. andersonii*는 먹이종인 prasinophyte 그룹에 속하는 *Pyramimonas* sp., cryptophyte 그룹에 속하는 *Teleaulax* sp., dinoflagellate 그룹에 속하는 *Heterocapsa rotundata*를 마비(immobilize)를 시키며 먹이로 섭식하는 혼합영양 능력을 가진 것으로 확인한 반면, *A. affine* 나*A. fraterculus* 는 먹이섭식을 하지 않는 것으로 나타났다. 그러나 혼합영양 능력이 결핍된 두 종들 역시 다른 먹이종들을 마비 시키거나 용해 (lysis) 시키는 현상이 관찰되었다. 더불어 혼합영양은 *A. andersonii* 의 성장을 증가시켰다. *A. andersonii* 가 광합성만으로 성장했을 때의 성장률은 0.243d^{-1}인 반면, 먹이종 *Pyramimons* sp.으로 배양하여 20 μE m^{-2} s^{-1} 의 광도로 12시간 광

/10시간 암조건 cycle에서 배양하였을 때, 최대 성장률은 0.432 d^{-1}이었다. *A. andersonii* 의 먹이종 *Pyramimons* sp.에 대한 최대 섭식률은 1.03 ng C $predator^{-1}d^{-1}$ 이었다. 따라서 *A. andersonii* 역시 영양염류만 흡수하지 않고 다른 종들을 섭식하는 성장 및 생존전략을 가지고 있으며, 더불어 혼합영양을 하지 않는 두 *Alexnadirum* 종들과 더불어 화학 물질을 분비하여 다른 원생생물들을 마비시키거나 용해시켜 다른 먹이종이나 영양염류 흡수에 이득을 얻을 것으로 판단된다. 이러한 연구결과는 *A. andersonii*의 혼합영양 능력이 적조 발생, 유지, 소멸에 관한 예측에 반드시 고려되어야 한다고 판단된다.

제 5 장에서는 적조 유발 생물인 *Mesodinium rubrum*의 원생동물 포식자에 대한 연구를 진행하였다. *M. rubrum*을 포식하는 원생동물을 탐색하기 위해 10종의 종속영양성 와편모류와 1종의 무각 섬모류에 대한 섭식 여부를 관찰하였다. 그 결과, *Gyrodinium dominans*, *Luciella masanensis*, *Oblea rotunda*, *Polykrikos kofoidii*, *Strombidium* sp. 이 *M. rubrum*을 섭식하는 것으로 나타났다. 그러나 그 중에서도 *G. dominans* 만 *M. rubrum*을 섭식하여 성장률이 증가되었다. 이때 최대 성장률은 0.48 d^{-1} 인 반면, 최대 섭식률은 0.55 ng C $predator^{-1}\,d^{-1}$이었다. 현장에서 함께 출현한 자료를 분석한 결과, *G. dominans*의 *M. rubrum*에 대한 제거율은 최대 0.236 h^{-1}이었다. 따라서 *G. dominans*의 출현 여부는 *M. rubrum* 의 현장 분포 농도 조절 및 적조 발생에 영향을 미칠 것으로 판단된다.

제 6 장 에서는 지구 온난화와 부영양화가 복합적으로 식물플랑크톤의 생산력에 미치는 영향을 연구하기 위해 매월 연안 현장물을 채집한 후 4개의 온도구간 (현장온도+2, +4, and +6 °C)과 2개의 영양염류 처리 방식 (현장농도유지, 부영양화)을 결합하여 총 64개의 서로 다른 초기조건 에서 시작된 실험을 진행하였다. 먼저 영양염류를 추가하지 않

은 영양염류 현장농도유지 구간에서는 수온상승에 따른 식물플랑크톤의 생산량이 일정하지 않았다 (증가, 감소, 혹은 변화 없음). 그러나, 부영양화 시킨 구간에서는 식물플랑크톤의 생산량이 모두 증가하는 추세를 보였다. 이러한 변화 양상을 분석한 결과, 영양염류 중 질산염 대비 클로로필의 양 [nitrate concentration to Chl-a concentration, NCCA, μM $(\mu g\ L^{-1})^{-1}$] 이 수온 영향에 결정적인 방향성을 제시하는 요인인 것으로 나타났다. 일부 예외적인 부분을 제외하고 NCCA가 1.5 이상일 경우 수온이 증가할수록 식물플랑크톤의 생산량은 증가되었다. 본 연구결과는 NCCA 수치가 지구온난화가 연안 식물플랑크톤 생산력의 증가 혹은 감소의 방향성을 결정해주는 주요 요인임을 처음으로 밝혔다. 제 7장에서는 본 논문의 5개 소 주제에 대한 통합적인 고찰에 대해 기술하였다.

본 연구는 플랑크톤 군집 변화와 적조 유발 생물의 변동에 영향을 주는 기상학적, 수리학적, 생물학적인 다양한 요인들에 대해 다방면에서 접근하여 융합적이고 복합적인 연구 결과물로서 매우 중요하다. 가속화되고 있는 지구온난화와 부영양화 영향은 식물플랑크톤 생산력과 원생생물 군집 조성을 변화시킬 것으로 예측되며, 이는 어장을 통해 인류의 먹이망까지 영향을 주는 요인으로 직결된다. 그렇기 때문에 해양 생태계에 대한 깊이 있는 이해와 유용자원으로 활용가치가 높아질 해양적조생물자원에 대한 관리가 절실한 현재 시점에서 본 연구 결과는 해양환경의 건강성에 대한 과거와 현재 상태를 정확하게 이해하여 향후 환경변화에 대한 해양생태계 반응 및 예측에 대한 기반자료로 중요하게 활용 될 것으로 사료된다.

Keyword: 연안 환경, 부영양화, 지구온난화, 유해 조류 대번성, 식물플랑크톤, 원생생물, 적조

Student Number: 2012-30095